MECHANISMS OF ANOXIA TOLERANCE

IN

THE TURTLE CORTEX

by

CHRISTOPHER JOSEPH DOLL
B.A., The University of Hawaii, 1986

A THESIS SUBMITTED IN PARTIAL FULFILLMENT OF

THE REQUIREMENTS FOR THE DEGREE OF

DOCTOR OF PHILOSOPHY

in

The faculty of Graduate Studies
(Department of Zoology)

We accept this thesis as conforming
to the required standard

The University of British Columbia

October 1993

© Christopher Joseph Doll, 1993

In presenting this thesis in partial fulfilment of the requirements for an advanced degree at the University of British Columbia, I agree that the Library shall make it freely available for reference and study. I further agree that permission for extensive copying of this thesis for scholarly purposes may be granted by the head of my department or by his or her representatives. It is understood that copying or publication of this thesis for financial gain shall not be allowed without my written permission.

(Signature)

Department of Zoology

The University of British Columbia
Vancouver, Canada

Date October, 1993

DE-6 (2/88)

ABSTRACT

The high sensitivity of the mammalian brain and the insensitivity of the turtle brain to O_2 deprivation led to the use of cortical slice preparations in both species being utilized for a comparative study of anoxia tolerance. To assess anoxic survival, intracellular recording techniques were employed. Turtle neurons survived both anoxia (aCSF equilibrated with 95% N2 / 5 % CO_2) and pharmacological anoxia (anoxia + 1mM NaCN) for 180 min. with no measurable degradation. Rat pyramidal neurons responded with a decrease in whole cell resistance followed by transient hyperpolarization and a subsequent depolarization to a zero membrane potential (41.3 ± 6.5 min., anoxia; 25.8 ± 12.6 min., pharmacological anoxia). Pharmacological ischemia (pharmacological anoxia + iodoacetate 10 mM) caused a rapid decrease in whole cell resistance, transient hyperpolarization, and a rapid depolarization in both turtle (4.6 ± 1.1 min.) and rat (3.1 + 0.5 min.) neurons. Ouabain perfusion caused a rapid depolarization in the rat cortical neuron (8.6 ± 1.1 min.), but no initial decrease in whole cell resistance or a hyperpolarization.

Calorimetric measures converted to ATP utilization rate indicated that the turtle cortical slice has an initial ATP utilization of 1.72 μmoles ATP/g/min. which agrees closely to *in vivo* whole brain metabolic measures. This value supports a 9 fold lower metabolic rate compared to analogous guinea pig cortical slice preparations. Based on heat depression measures, resulting ATP utilization estimates indicated a metabolic depression of 30 % (nitrogen) and 42% (pharmacological anoxia). Heat flux changes over pharmacological anoxia, support a large initial Pasteur effect which gradually declines over the 120 min. insult interval. Activities of hexokinase and lactate dehydrogenase were similar between the rat and turtle cortical slice (25 ^{o}C), but the turtle cortex only expressed 80 % of the activity of the rat cortex for citrate synthase. Surprisingly, the turtle cortical slice did not exhibit a change in any measured adenylate parameter up to 120 min. of anoxia or pharmacological anoxia. Significant changes did occur in [ADP], ATP/ADP ratio, and energy charge at 240 min.

In order to assess difference in ion leakage in both the turtle and rat pyramidal neurons, intracellular recording techniques for short term anoxia (120 min.) and whole cell patch clamp techniques (on cell populations) for long term anoxia (6 - 9 hrs.) were utilized. Both techniques indicated that turtle cortical pyramidal cells did not change in conductance (whole cell conductance or specific membrane conductance) with anoxia. Whole cell patch clamp techniques supported a 4.2 fold higher specific membrane conductance in rat pyramidal neurons compared to turtle neurons at the same temperature (25 ^{o}C) which was accentuated by temperature so that rat pyramidal neurons at 37 ^{o}C were 22 times more conductive than turtle neurons at 15 ^{o}C. A conductance Q_{10} of 1.9 was measured for both turtle (15 - 25 ^{o}C) and rat (25 - 35 ^{o}C) pyramidal neurons. To asses pumping activity capacity, Na^{+}-K^{+}-ATPase activity was measured in cortical slices of both species. At the same temperature (25 ^{o}C) a 2.3 fold higher activity was measured in the rat cortex compared to the turtle supporting the patch clamp results of a lower normoxic specific membrane conductance in the turtle cortex.

Taken together these results support that the turtle brain is able to survive anoxia through an enhanced glycolytic capability, a low normoxic brain metabolism with the ability to further depress metabolism during anoxia. Electrophysiological techniques support reduced ion pumping through reduced ion leakage as one mechanism for a depressed normoxic metabolic rate in the turtle cortical slice but do not support further down regulation of channel activity with anoxia.

TABLE OF CONTENTS

LIST OF TABLES

LIST OF FIGURES

ABBREVIATIONS

aCSF	artificial cerebrospinal fluid
ATP	adenosine triphosphate
[ATP]	adenosine triphosphate concentration
$[ATP]_i$	intercellular adenosine triphosphate concentration
ADP	adenosine diphosphate
AMP	adenosine monophosphate
A_o	offset
A_1	maximum voltage
Ca^{+2}	calcium
$[Ca^{+2}]_o$	calcium concentration extracellular
$[Ca^{+2}]_i$	calcium concentration intracellular
$CaCl_2$	calcium chloride
^oC	degrees Celsius
cm	centimeter
C_m	specific membrane capacitance
CO_2	carbon dioxide
CN	cyanide
CNS	central nervous system
e	natural logarithm
DTT	5 dithiothreitol
EGTA	ethylene glycol bis(ß-aminoethyl) ether
EPSP	excitatory post synaptic potential
EEG	electroencephalograph
GABA	γ-aminobutyric acid
GAP	Glyceraldehyde 3-phosphate
GΩ	gigaohm
G_m	specific membrane conductance
GTP	guanosine 5'-triphosphate
G_w	whole cell conductance
H_2O	water
H^+	hydrogen proton
HCl	hydrochloric acid
HPLC	high pressure liquid chromatography
I	current
K^+	potassium
K_{ATP}	ATP sensitive potassium channels
K_{Ca}	Ca sensitive potassium channels
$[K^+]_i$	potassium concentration intracellular
$[K^+]_o$	potassium concentration extracellular
KCl	potassium chloride
kHz	kilohertz
KOH	potassium hydroxide
IAA	iodoacetic acid
I_{AHP}	after hyperpolarization current
mA	milliampere(s)
$MgCl_2$	magnesium chloride
min.	minute(s)
mM	millimolar

mS	millisecond(s)
mV	millivolt(s)
MYA	million years ago
MΩ	megaohm(s)
N_2	nitrogen
Na^+	sodium
$[Na^+]$	sodium concentration
$[Na^+]_i$	sodium concentration intracellular
$[Na^+]_o$	sodium concentration extracellular
nA	nanoamperes
NaCN	sodium cyanide
NaCl	sodium chloride
NAD^+	oxidized nicotinamide adenine dinucleotide
NADH	reduced nicotinamide adenine dinucleotide
Na^+-K^+-ATPase	sodium, potassium - ATPase
$NADP^+$	oxidized nicotinamide adenine dinucleotide phosphate
NADPH	reduced nicotinamide adenine dinucleotide phosphate
$NaHCO_3$	Sodium bicarbonate
NaH_2PO_4	monosodium phosphate
NaOH	sodium hydroxide
nS	nanosecond(s)
nm	nanometer(s)
O_2	oxygen
pA	picoampere(s)
pH	inverse log of percent hydrogen ion concentration
Pi	inorganic phosphate
P_{O_2}	partial pressure of oxygen
Q_{10}	effect of a 10 ^oC temperature change
R	least squares residual
R_m	specific membrane resistance
R_w	whole cell resistance
T_c	time constant
Tris · Cl	tris (hydroxymethyl) aminomethane
V	voltage
$\dot{V}_{O_2}$	oxygen consumption

Nonalphabetical abbreviations

μF	microfarad(s)
μmole	micromole(s)
μm	micrometer(s)
μM	micromolar
μS	microsemin(s)
ΔS	entropy
Ω	ohm(s)
1,3DPG	1,3-Diphosphoglycerate

ACKNOWLEDGMENTS

I would like to thank both of my supervisors, Peter Hochachka and Peter Reiner, in general, for their support, encouragement, constant enthusiasm, and patience. In particular, I would like to thank Peter Hochachka for teaching me how to identify fundamental problems, and Peter Reiner for teaching me conciseness both in experimental design and writing techniques. Special thanks go to Andy Laycock who's duct tape and wire nuts kept the electrophysiology laboratory running, and Raul Suarez who was a constant source of productive agitation. Special thanks also go to the Medical Research Council of Canada who's support made this project possible. Finally, I would like to thank my first undergraduate biology professor, James Kanz, (Texas A & M University) who taught me that biology was not a science but a philosophy.

CHAPTER 1: ANIMAL ANOXIA TOLERANCE - AN INTRODUCTION

Preface

This chapter is intended to give the reader an overview and orientation to the subject of anoxia in vertebrates, and how, based on this information, the focus of this thesis evolved. Parts of this chapter were excerpted form C. J. Doll (In *Surviving Hypoxia*, CRC Press, pgs. 389-400, 1993).

A Species Overview

The graceful glide of a marine mammal beneath the ocean surface is a reflection of the extreme evolutionary morphological change which has occurred to this group of mammals. Though not sharing a common ancestor with whales, seals have also forgone a terrestrial mode of life in exchange for the sea. Whales and dolphins abandoned terrestrial life about 45 m.y.a. (Gingerich and Russell, 1991) compared to seals who abandoned the land about 23 m.y.a. (Berta *et al.*, 1989). Both groups have undergone considerable morphological change; yet, with respect to cellular adaptations to anoxia these animals are remarkably similar to nondiving mammals of today (Castellini *et al.*, 1980).

Both terrestrial and marine mammals have tissues such as skeletal muscle which are tolerant to both anoxia and ischemia, however, they both also possess oxygen sensitive tissues such as the brain. Mammalian skeletal muscle is known to survive ischemia for several hours (Beyersdorf *et al.*, 1991) while the brain function is noted to fail within a minute for a similar insult (Hansen, 1985). In terms of asphyxia duration, the champion vertebrate homeotherm is the elephant seals reported to dive to depths of 1.5 Km. (DeLong, 1991) and for times up to 120 min. (Hindell *et al.*, 1991). Yet, no diving mammal or bird has been recorded with a zero blood P_{O_2} (Kooyman, 1989). Rather, these animals rely on mechanisms which conserve and carry more oxygen to their tissues. These adaptations include: (i) a large body size to minimize oxygen consumption ; (ii) the diving reflex to conserve oxygen for critical tissues; (iii) increased hematocrit/volume of blood, as well as more hemoglobin/cell to increase blood oxygen stores; (iv) large stores of myoglobin in the

skeletal muscle to increase cellular oxygen stores; and (v) the release of oxygenated red blood cells from the spleen during a dive to provide additional oxygen to critical areas, [for reviews see (Elsner and Gooden, 1983; Hochachka, 1980; Kooyman, 1989)].

That brain is considered the most sensitive tissue to hypoxia and anoxia in the vertebrate has been the topic of investigation for a considerable time (Boyle, 1670). Even though marine mammals live the majority of their lives in an anoxic environment experiencing hypoxia daily, their central nervous system (CNS) appears to be only slightly better adapted to living without oxygen as compared to the canine brain. Studies have shown CNS failure occurring at a P_{O_2} of 10 torr (Kerem and Elsner, 1973b) for the seal brain compared to 14 torr for the canine brain (Kerem and Elsner, 1973a). This difference is not very significant when considering: (i) the scaling effect of brain size vs. metabolic rate which gives the larger seal brain a lower metabolism (Mink *et al.*, 1981) and (ii) the increased capillary density of the seal brain allowing a greater extraction of oxygen from the blood (Elsner and Gooden, 1983). Through millions of years of selective pressure for hypoxia tolerance, marine mammals do not appear to be significantly better adapted to cerebral anoxia tolerance than a typical terrestrial counter part. This observation suggests that the CNS of homeotherms may operate under certain limitations which disallow anoxic tolerance.

The CNS in most vertebrates is highly sensitive to oxygen deprivation. The only notable exceptions are the crucian carp (*Carassius carassius*), the goldfish (*Carassius auratus*), and a few reptiles of which the most notable is the painted turtle (*Chrysemys picta*) (Ultsch, 1985). This species can survive 6 months in anoxic water at 3 ^{o}C (Ultsch, 1985) and 48 hours at 25 ^{o}C (Musacchia, 1959). In the fall, *C. picta* submerges into the anoxic sediments of ponds and river bottoms and overwinters until spring (Ultsch, 1989). The turtle's anoxic resistance has presumably evolved as a survival mechanism to overwintering in anoxic water and mud. This hypothesis is supported by the observation that long hibernators (northern species) exhibit greater tolerances to anoxia compared to southern species (Ultsch, 1985).

Turtle Whole Body Anoxic Adaptations

Perhaps the most striking adaptation of the turtle is its ability to control whole body metabolism. As indicated above, the turtle is an excellent oxygen conformer suggesting that it has the ability to regulate metabolism during hypoxia. Jackson (1968) demonstrated that the turtle was able to depress its metabolism (heat production) during anoxia to 1/5 its normoxic rate within a few hours of submergence (Jackson, 1968). Regulation of whole body metabolism aids the survival of the turtle in several ways: i) it allows the stores of on board fuel (glucose and glycogen) to last longer; ii) it lessens the cellular energy (ATP) demand allowing glycolytic machinery to match cellular demand; and iii) it decreases the build-up of harmful toxic products.

With decreasing metabolism, the second problem facing the anoxic organism is supplying critical tissues like the brain with enough substrate (glucose). Adaptations in this category can be broadly defined into two areas. First, the shunting of blood to critical areas (diving reflex), and second, the regulation of substrate utilization.

Blood flow studies have indicated that the turtle (*C. scripta*) increases blood flow up to 250% (compared to normoxia) to the brain during an anoxic insult while other organs such as liver, intestines, pancreas, and kidneys all receive large (50 - 100%) reductions (Bickler, 1992b; Daves, 1989). This shunting to the brain clearly demonstrates the importance of maintaining a large glucose supply to this critical organ.

Another adaptation in conjunction with blood shunting is the ability to regulate blood [glucose] through the mobilization of liver glycogen. Studies have shown that turtles are able to increase blood [glucose] by up to 11 fold (compared to control) during anoxia (Clark and Miller, 1973; Daw *et al.*, 1967; Keiver *et al.*, 1992; Penney, 1974). This increase is reflected by a dramatic drop in liver glycogen (Clark and Rothman, 1987; Penney, 1974). The glucose rise can be prevented by the administration of propranolol (a ß-adrenergic receptor antagonist) supporting the role of hepatic mobilization of glycogen in this increase (Keiver

and Hochachka, 1991). Turtles also appear to have large reserves of liver glycogen compared to non-anoxia tolerant species (Hochachka and Somero, 1984).

One of the most detrimental effects of anoxia on the turtle is the accumulation of harmful end products. Numerous studies have documented a decrease in blood pH and subsequent rise in [lactate] (up to 200 mM) occurring during anaerobiosis in the turtle (Gatten, 1981; Herbert and Jackson, 1985; Robin *et al.*, 1981; Ultsch and Jackson, 1982). Additionally, studies have shown that if blood pH drops below 1 pH unit of resting, the animal is not likely to fully recover (Herbert and Jackson, 1985). Long term anoxic survival necessitates the need for the accumulation of lactate, but the organism can only tolerate limited amounts of either lactate or the accompanying drop in pH. One solution as discussed above is to minimize metabolism, and thus minimize the accumulation of these end products. In part, the turtle can remove some protons and lactate through the urine (Ultsch, 1989). However, this is a wasteful strategy since upon recovery, the turtle could no longer utilize the large remaining energy reserve of lactate for re-establishment of glycogen stores or further oxidation. Another mechanism would be to increase buffering capacity of both blood and intracellular fluid, but the evidence does not support enhanced buffering capacity in either compartment (Ultsch, 1989; Ultsch and Jackson, 1982). What the turtle does appear to utilize is the mobilization of counter positive strong ions (Ca^{+2} and Mg^{+2}) to ionically balance the formation of lactate anions (Herbert and Jackson, 1985; Jackson, 1982b). This balance depresses the drop in pH of the blood significantly (Herbert and Jackson, 1985). The concentrations of both of these ions increase greatly with submergence, with calcium reaching 100 mequiv/l (3X control) and magnesium about 30 mequiv/l (2X control).(Jackson, 1982a) The close correlation in the rise of these two ions with lactate suggests that this is a controlled response (Ultsch, 1989). The unphysiologicially high blood [Ca^{+2}] appears to be achievable through the formation of Ca^{+2}-lactate complexes which are believed to bind 2/3 of the Ca^{+2} formed (Jackson, 1982b). High blood [Ca^{+2}] has been observed in several reptiles. The highest recorded concentrations are in the ovulating snake (*Thamnophis*

sauritus) which can achieve a 90 mM blood [Ca^{+2}] (Dessauer and Fox, 1959). The high blood Ca^{+2} solubility is achieved through the use of phosphoprotein (Dessauer, 1970). Thus, the turtle may use a similar mechanisms along with lactate complexes to aid in dissolving blood Ca^{+2} (Jackson, 1982a).

Tissue Hypoxic Response

Both animals and individual organs can be classified broadly into two groups with respect to their response to varying oxygen tension (P_{O_2}) (oxygen conformers or oxygen regulators). Oxygen conformers decrease their oxygen consumption ($\dot{V}_{O_2}$) as the oxygen partial pressure (P_{O_2}) is decreased where as oxygen regulators retain a relatively constant $\dot{V}_{O_2}$ with decreasing P_{O_2} (Prosser, 1986; Schmidt-Nielsen, 1979; Fig. 1). Mammalian skeletal muscle which survives long term anoxia and ischemia is classified as an oxygen conformer (Whalen *et al.*, 1973), but the mammalian brain (including the seal brain), which has little or no tolerance to oxygen deprivation is a stringent oxygen regulator (Jones and Trystman, 1984; Kerem and Elsner, 1973a; Kerem and Elsner, 1973b; Kitner *et al.*, 1984). Interestingly, anoxia tolerant invertebrates (Herreid, 1980; Mangum and Van Winkle, 1973)and vertebrates (Fry and Hart, 1948; Glass *et al.*, 1983; Jackson and Schmidt-Neilsen, 1966; Processer *et al.*, 1957) tend to exhibit oxygen conformity suggesting that anoxia tolerance, in part, is related to the ability to regulate metabolic rate (Hochachka, 1980; Hochachka, 1986). Regulation of brain metabolic rate will be discussed in further detail in Chapters 4 and 5.

Energy And Anaerobiosis

Under normal aerobic circumstances, brain tissue consumes exogenous glucose as an energy supply (Hawkins, 1985; Macmillan and Siesjö, 1972), and the turtle brain appears to be no exception (Pérez-Pinzón *et al.*, 1992b; Robin *et al.*, 1979). Aerobically catabolized glucose (per mole) yields approximately 36 moles of ATP:

$$\text{Glucose} + 36\,P_i + 36\,ADP + 6\,O_2 \longrightarrow 6CO_2 + 36\,ATP + 44H_2O$$

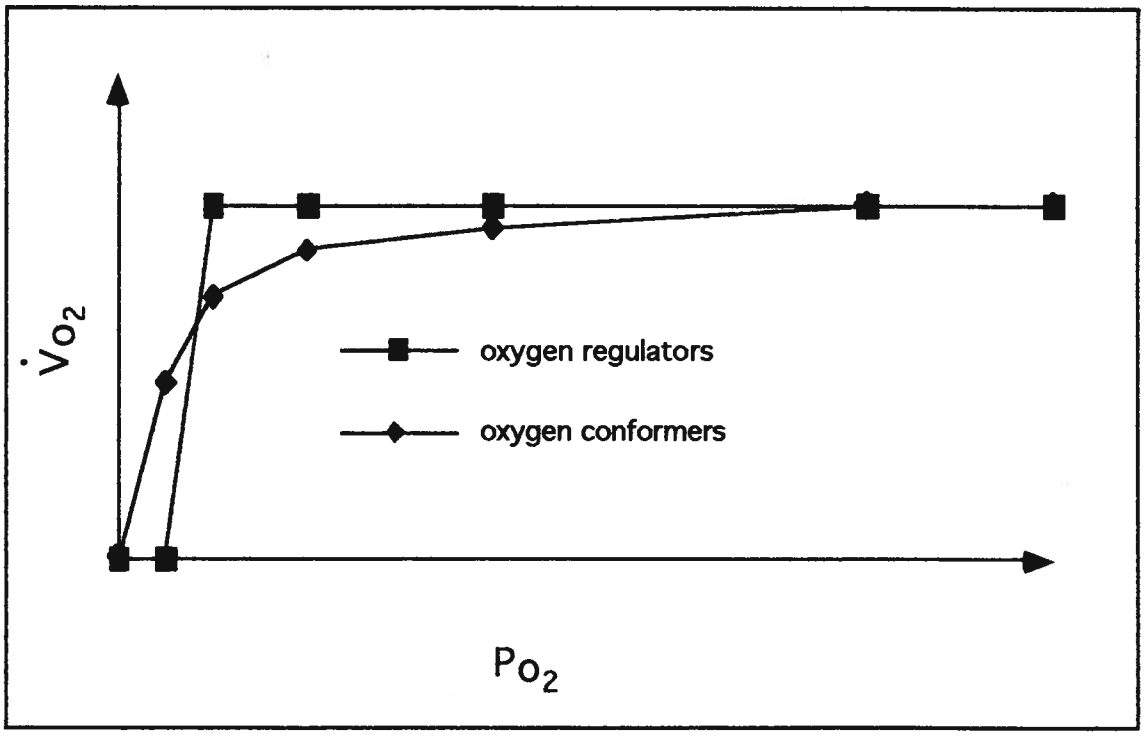

Figure 1. Theoretical response of an oxygen conformer and an oxygen regulator to varying oxygen partial pressures.

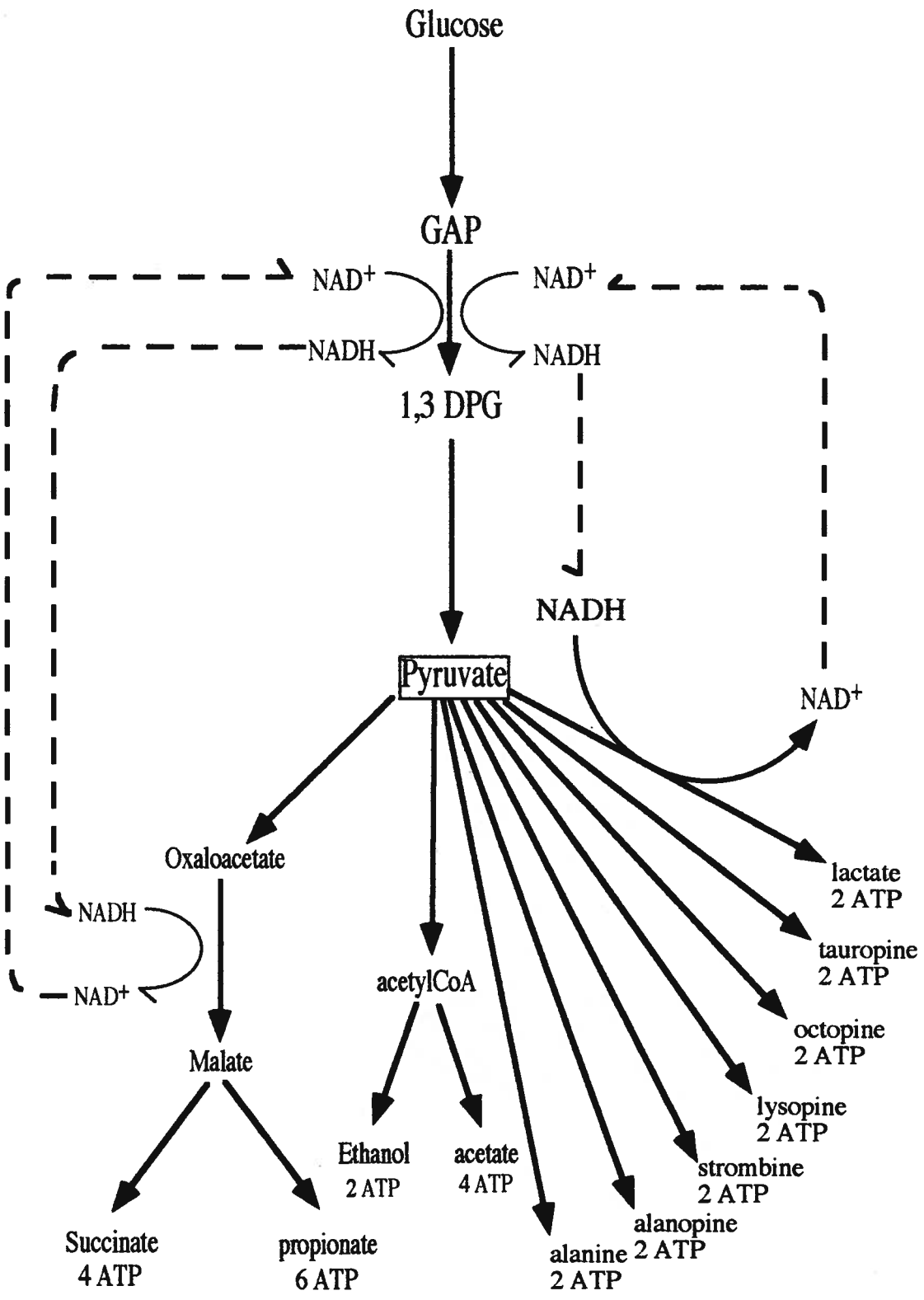

Figure 2. Fermentation pathways identified in vertebrates and invertebrates. Modified from Hochachka and Guppy, 1987.

However, when a tissue becomes anoxic, it no longer has oxygen as an electron acceptor and therefore can no longer use the Krebs cycle and electron transport system and still maintain mitochondria redox balance (Hochachka, 1980). However, glycolysis can still function because cytosolic redox balance can be maintained through the lactate dehydrogenase (LDH) reaction:

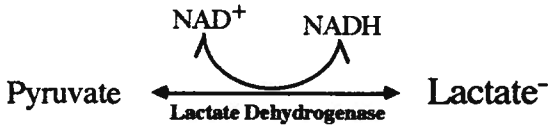

However, various invertebrates (helminths and bivalves being particularly inventive) have developed several different fermentative reactions allowing for increased yields of ATP (Fig. 2) (Hochachka and Guppy, 1987). Surprisingly, the only two pathways which appear to be utilized by vertebrates to any extent is the ethanol pathway (found in carp) (Shoubridge and Hochachka, 1981) and the lactate pathway (found in all vertebrates), both yielding a net of 2 ATP (Fig. 2). Turtles do not appear to use any of the other fermentative pathways besides lactate (Buck and Hochachka, In Press; Hochachka *et al.*, 1975; Robin, et al., 1979). The advantage of these fermentative pathways is that despite oxygen lack the cytosol can remain in redox balance, a small amount of ATP can be produced (Fig. 2), and relatively nontoxic end products are formed. However, the tissue has gone from a condition of producing 36 ATP/glucose to 2 ATP/glucose (in the case of glycogen, there are 3 ATP/glucosyl unit):

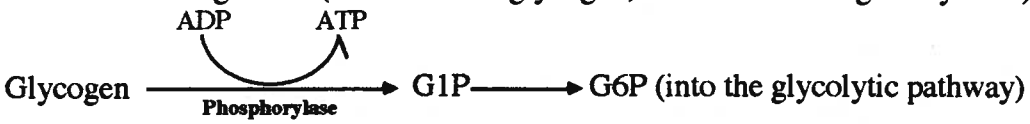

The turtle brain appears to use glycogen only as a last resort (Clark and Miller, 1973). The loss of significant ATP production suggests two possibilities for the turtle brain if ATP supply is to meet anoxic demands: (i) glycolytic flux must increase (Pasteur effect), (ii) the ATP tissue demand must be decreased (metabolic arrest).

Pasteur Effect

The Pasteur effect was named after its discoverer (Louis Pasteur) who first noticed an inhibition of carbohydrate (glucose) consumption when oxygen concentrations were high and

an increase in glucose consumption when oxygen concentrations were low (Pasteur, 1861). Given that the ATP production from 1 mole of glucose under anoxic conditions is 1/18 that of normoxic conditions, one would expect that glycolysis would be increased 18 fold if ATP supply is to meet demand (12 fold if glycogen were used). However, this does not appear to be the case with most tissues (specifics for brain tissue will be discussed in chapter 3). One of the largest observed Pasteur effects (15 fold) is found in bull sperm (Hammerstedt and Lardy, 1983). There are two basic reasons that a tissue may not exhibit a full Pasteur effect and yet still maintain energy (ATP) balance. First, the tissue may depress its metabolic rate as it enters into the anoxic state, thus ATP demand has diminished and a lower glycolytic flux will meet cellular ATP consumption. Secondly, the assumption that all of the glucose under normoxic conditions is fully oxidized may not be correct (Lynch and Paul, 1983) which may result in a substantial overestimation of energy utilization.

Insights into Brain Anoxia Tolerance

Based on the above information three mechanisms can be hypothesized to play a central role in turtle neuronal anoxia tolerance: (i) a Pasteur effect; (ii) a low normoxic metabolic rate; (iii) further down regulation of metabolism with anoxia (metabolic arrest).

The presence of a Pasteur effect would appear to be crucial if energy balance is to remain constant. Maintenance of energy balance is most critical in the transition phase where the cell must switch from a highly aerobic state to anaerobiosis. This rapid transition causes a nonequilibrium with regards to cellular function and energy balance (especially with respect to pharmacological anoxia, see Appendix B). Thus, the Pasteur effect would serve as a temporary buffer allowing the neuron to make necessary metabolic adjustments. As discussed above, if metabolism can be lowered significantly (12 - 18 fold depending on the anoxic substrate), then the presence of a Pasteur effect may be transitory. The initial Pasteur effect may be subsequently down regulated to allow normal or reversed glycolytic flux (a reversed Pasteur effect).

With regards to a reduced metabolic rate, several critical points can be made for anoxic survival: (i) a low ATP demand would aid the cell in maintaining cellular energy supply for a given glycolytic flux; (ii) a low metabolism would decrease the build-up of toxic endproducts such as lactate anions and protons; (iii) a low ATP demand would allow a given amount of on board substrate (glucose or glycogen) to last longer; and (iv) since the turtle brain relies on exogenous glucose for its substrate (Clark and Miller, 1973; Pérez-Pinzón, et al., 1992b), a lower metabolic demand would better enable membrane glucose transporters to meet the glycolytic demand. Membrane glucose transport rate has been proposed as a rate limiting step in the catabolism of glucose in the rat brain (Furler *et al.*, 1991).

Anoxic Membrane Coupled Function

The mechanisms proposed above all share one common goal: the coupling of energy production to meet energy demand. If supply can meet demand, then an energy deficit will be avoided and normal neuronal function can continue. However, not all systems maintain energy balance during anoxia. Both *Artemia* embryos and locusts are known to lose energy balance during anoxia (Hand and Gniager, 1988; Wegener, 1987; Wegener *et al.*, 1987), and thus, completely shut down their systems. The turtle, on the other hand, maintains some degree of alertness during anoxia (Ultsch, 1989) and thus, must maintain some degree of brain function.

The neuron is an electrical cell. Thus, the maintenance of ion gradients is crucial if electrical function is to continue throughout an anoxic bout. The disadvantage to maintenance of ion gradients is the energy cost. It has been estimated that in the normal conscious mammalian brain, maintenance of ion gradients may consume as much as 50 - 60% of metabolism (Hawkins, 1985). Ion homeostasis is maintained through the use of ATP utilizing ion pumps (Na^+-K^+-ATPase and the Ca^{+2} -ATPase). One possible scenario is the down regulation of ion channels during anoxia 'channel arrest' (Hochachka, 1986; Hochachka, 1987; Hochachka and Guppy, 1987; Lutz *et al.*, 1985). Down regulation of ion channels (leakage or voltage-gated channels) would indirectly conserve energy through the

reduction of ion pumping. This mechanism of energy reduction would allow anoxic brain function and still conserve energy. Such a channel arrest hypothesis will be explored in Chapter 4.

Thesis Overview

The extreme anoxia tolerance exhibited by *C. picta* and the high sensitivity of the mammalian brain to O_2 depletion led to the use of the turtle and rat as comparative models. The lack of literature in regards to anoxia and hypoxia in the cortex and the easy dissection of these tissues in both species suggested an ideal model for comparative studies. Earlier studies (Connors and Kreigstein, 1986) had identified similar neurons (pyramidal and stellate) in both the turtle and rat cortex again suggesting the appropriateness of this tissue for a comparative study. As a result, this thesis will focus on turtle and rat cortical tissue in order to understand some of the mechanisms which *C picta* utilizes to cope with both energy and oxygen depletion.

Chapter 2 examines turtle and rat neuronal function during anoxia. Prior to the publication of this study, nothing was known with respect to how individual turtle neurons were responding to anoxia. This study was made possible through the use of intracellular recording techniques (see Appendix A) which allows the measurement of individual neuronal parameters such as membrane potential, cell resistance, and action potential parameters.

Chapter 3 focuses on the brain biochemistry (energy balance and glycolytic enzymes) and the metabolism of the turtle cortical slice preparation. This chapter will examine whether the cortical slice possesses a low resting metabolic rate and whether this metabolic rate is further reduced with anoxia.

Chapter 4 will investigate the role of 'channel arrest' in the turtle slice again using electrophysiological techniques, intracellular recording and patch clamping techniques (see Appendix A) to measure whether the turtle pyramidal neuron exhibits a lower resting ion leakage compared to the rat counter part and whether this leakage is further down regulated with anoxia as a possible explanation for metabolic arrest.

The thesis concludes in Chapter 5. This chapter presents two hypotheses. First, a unified theory is presented which explains how the turtle neuron maintains membrane integrity during anoxia in contrast to the rat neuron. This theory, in part, is based on the observed differences in brain metabolic rates of the turtle and the rat. A second hypothesis is then presented which explains why there is a metabolic difference between these two species brain preparations.

CHAPTER 2: EFFECTS OF ANOXIA AND PHARMACOLOGICAL ISCHEMIA ON TURTLE AND RAT CORTICAL NEURONS

Preface

This chapter is excerpted (in part) from a paper published by C. J. Doll, P. W. Hochachka, and P. B. Reiner (*Am. J. Physiol.* 260: R747-R755, 1991). This chapter examines how the cortical pyramidal cell responds to anoxia and similar insults using intracellular recording techniques. Prior to the publication of this paper, no intracellular recording had been done on the anoxic turtle brain. The results obtained in this study were the foundation for the chapters to follow.

Introduction

Mammalian brains are very sensitive to lack of O_2. When blood P_{O_2} reaches critical levels, brain function ceases (Hansen, 1985). Of particular interest is the mechanism by which this rapid failure occurs because of the brain's importance to survival. Due to the considerable amount of literature in this field, this chapter will begin with a review of some of the relevant observations that have been made in this area. This broad overview will aid in the interpretation of the results and discussion to follow.

Mammalian CNS Response

When mammalian brain tissue becomes ischemic/anoxic, it typically responds with a large Pasteur effect (Drewes and Gilboe, 1973; Kauppinen and Nichols, 1986; Lowry *et al.*, 1964). Unfortunately, energy supply does not appear to meet demand resulting in [ATP] declining to $\approx$ 25% of control within the first minute in the rat brain (Lowry, et al., 1964; Ridge, 1972). The initial response of the mammalian brain appears to be a flat EEG followed by changes in the extracellular environment beginning with a slight increase in $[K^+]_o$ followed by a massive decrease of $[Na^+]_o$ and $[Ca^{+2}]_o$ and increases in $[K^+]_o$ (Hansen, 1978; Hansen, 1982; Hansen, 1985; Sick *et al.*, 1987; Suzuki *et al.*, 1985). These events occur within the first minute of the ischemic insult and cause brain dysfunction ultimately leading to the death of the neuron. These initial events resemble those observed in spreading

depression which is brought about when the brain receives a severe trauma (Hansen and Zeuthen, 1981; Kraig and Nicholson, 1978). Accompanying these changes in the intracellular and extracellular environment is the sudden loss of neuronal membrane resistance (R_m) and membrane potential (M.P.) (Hansen, 1982).

With regards to anoxia/hypoxia, there has been considerable work done with the hippocampus. Interestingly, anoxia/hypoxia appears to cause similar changes in the neuron that ischemia does, but over a much longer time frame (Fujiwara *et al.*, 1987; Higashi *et al.*, 1988). The slower time frame to complete membrane depolarization of the neuron during this insult has allowed the study of individual events taking part in the cell depolarization. Currently clamp methods have revealed 3 basic conductance and current changes when a hippocampal cell is held at -70 mV with KCl electrodes. An initial inward current flow corresponding to a slight or no depolarization of the neuron (phase 1) followed by a much larger outward flow of current and increase in membrane conductance (G_m) (phase 2) corresponding to a hyperpolarization, and (phase 3) a variable net inward flow corresponding to the final depolarization of the membrane to a 0 mV resting potential (Krnjevic and Leblond, 1989; Leblond and Krnjevic, 1989). Efforts to try and unravel this complexity of currents is still being sought. Current evidence suggests that in the CA1 region of the hippocampus, the second phase (the outward flow corresponding to a hyperpolarization), is most likely carried by Ca^{+2} dependent K^+ current (I_{AHP}) due to its blockade by carbachol and CsCl (Cummins *et al.*, 1991; Krnjevic, 1993; Krnjevic and Xu, 1990). However, whether the I_{AHP} is fully responsible for the hyperpolarization in all neurons is still speculative. Recently, glibenclamide was shown to prevent the anoxic hyperpolarization in the CA3 region. However, this blockage of the hypoxic hyperpolarization by glibenclamide appears to be an indirect action related to the suppression of hypoxic glutamate release (Ben-Ari, 1990). Recent unpublished data suggests that talbutamide but not glibenclamide may suppress the outward current in CA1 (J. M. Godfraind and K. Krnjevic, unpublished). Thus, no definitive conclusions can be made at this time.

Phases one and three correspond to a net inward flow of current leading to neuronal depolarization. Phase 2 can also be identified with this inward flow if the outward current flow (I_{K^+}) is blocked with CsCl or carbachol (Krnjevic and Leblond, 1989). The reversal potential of this current is around -40 - 0 mV suggesting the contribution of a nonselective cation channel (Partridge and Swandulla, 1988; Yellen, 1982). However, phase 3 has been associated with complex events such as neurotoxicity (Benveniste *et al.*, 1984; Choi, 1988a; Clark and Rothman, 1987) and uncoupling of the Na^+-K^+-ATPase pump (Fujiwara, et al., 1987; Krnjevic, 1993) making this phase exceptionally complex and far from understood at this time

Turtle CNS Anoxic Response

In marked contrast to the rat brain, the turtle brain responds to anoxia with only a slight increase in $[K^+]_O$ with concentrations rising less than 2.5 fold over a 48 hour period *in vivo* (Lutz, et al., 1985; Sick *et al.*, 1982) In addition, there is evidence for an initial Pasteur effect possible decreasing with time (Kelly and Storey, 1988). With ischemia(Sick *et al.*, 1985) or the addition of iodoacetic acid (Pérez-Pinzón, et al., 1992b) (glycolytic inhibitor), the turtle brain responds with an increase in extracellular $[K^+]_O$ similar to the anoxic/hypoxic rat brain. Most importantly, the turtle brain retains the ability to maintain [ATP]. Both cerebellum (Pérez-Pinzón, et al., 1992b), cortex (Bickler, 1992b) and whole brain (Lutz *et al.*, 1984) *in vivo* have been shown to maintain [ATP] during anoxic insults.

The goals of this chapter are two fold. First, to examine the response of the rat cortical pyramidal neurons to the anoxic / ischemic insult. Secondly, to examine intracellularly, the changes which occur to the turtle pyramidal neuron during anoxia and ischemia.

Methods

Tissue Preparation

Young male Wistar rats 50-100 g were anesthetized with halothane, decapitated, the brain rapidly dissected free and immersed in precooled oxygenated artificial cerebrospinal fluid (aCSF). After a few minutes precooling, the brain was bisected along the midline. A

block containing frontal - parietal cortex was dissected free, glued with cyanoacrylate to a mounting block and sliced (400 μm thickness) on a vibratome. Slices were stored at room temperature $\approx$ 22 ^{o}C in a holding chamber for at least 1 hr. until their use in the recording chamber at 25 ^{o}C or 35 ^{o}C. The recording chamber was a modification of a previous design (Haas *et al.*, 1979) (refer to appendix A for more detail) in which slices were continuously superfused with aCSF at a flow rate of 1.5 to 2.0 ml/min. Turtles (*Chrysemys picta*) ranged in weight from 250 to 600g. The dissection has been previously discussed in (Connors and Kreigstein, 1986). In brief, turtles were cold anesthetized prior to decapitation. The brain was dissected free and immediately placed in precooled aCSF . After cooling ($\approx$ 2 min.) the turtle brain was bisected along the midline. The cortex (whole) was then dissected free in an intact sheet. The cortical sheet was then used whole or divided in half depending on the size. Subsequent storage of slices was identical to that discussed above for the rat brain.

Data Acquisition

For a more general discussion of intracellular recording techniques, the reader is referred to Appendix A and B). Intracellular recordings were carried out using 1.2 mm o.d. micropipettes filled with 2 M-KCl with resistance ranging from 40 - 90 MΩ connected to an Axoclamp 2A amplifier. Data were acquired using the Pclamp suite of programs and an Axolab 1100 interface, which also served to generate current commands. Data were also independently digitized at 49 kHz and stored on videotape for off-line analysis.

Pyramidal neurons in the turtle were identified by location, action potential size and duration, as well as input resistance and time constant as previously discussed (Connors and Kreigstein, 1986). Pyramidal neurons in the rat were identified by location as well as action potential duration and size as discussed elsewhere (McCormick *et al.*, 1985). Criteria for a healthy neuron included positive going action potentials, a minimum of 40 MΩ resistance for rat neurons and 100 MΩ resistance for turtle neurons, and stable membrane potential for 15 minutes.

Fluid Composition

The rat aCSF consisted of NaCl 126 mM, KCl 2.5 mM, $MgCl_2$ 1.2 mM, $CaCl_2$ 2.5 mM, NaH_2PO_4 1.2 mM, Glucose 2 mM, $NaHCO_3$ 25 mM and phenol red .03 mM as a pH indicator. The aCSF for the turtle was a modification of (Connors and Kreigstein, 1986) and consisted of NaCl 96.5 mM, KCl 2.6 mM, $CaCl_2$ 2.5 mM, $MgCl_2$ 2.0 mM, NaH_2P0_4 2.0 mM, Glucose 10 mM, $NaHCO_3$ 26.5 mM, and phenol red .03 mM as a pH indicator. Final pH of both solutions was 7.4 when saturated with 95% O_2/5% CO_2. To mimic anoxia, the solution was switched to a presaturated aCSF solution of 95%N_2/5%CO_2. For pharmacological anoxia, the aCSF solution was the same as anoxia and contained 1 mM NaCN. For pharmacological ischemia, the solution was the same as pharmacological anoxia and also contained 10 mM iodoacetic acid (IAA) titrated to a pH of 7.4 with concentrated NaOH. For the ouabain and IAA experiments the aCSF contained 100 μM ouabain and 10 mM iodoacetic acid respectively, equilibrated with 95% O_2/5%CO_2

Results

The results for various pharmacological treatments are illustrated in Fig. 3. This figure represents the mean times for cell survivability which for the purpose of this paper is the time it takes for a cell to depolarize from its resting membrane potential to 0 mV once a drug was applied. These measurements are corrected for the lag time for the drug to reach the slice and equilibrate in the slice chamber ($\approx$ 30 sec). All turtle cells were recorded at 25 ^oC due to problems associated with survivability of ectothermic cells at unphysiologicially high temperatures. All treatments were significantly different ($P \leq 0.05$; Newman-Keuls multiple comparison test) from each other except IAA vs. ouabain. All values within a group were significantly different ($P \leq 0.05$; independent *t* test), except rat pharmacological anoxia 35 vs. 25 ^oC and rat vs. turtle pharmacological ischemia 25 ^oC . Rat neurons were recorded at 25 ^oC as a comparison to the turtle. In addition, some insults were repeated at 35 ^oC in the rat in order to demonstrate the repeatability of the low temperature results at a more physiological temperature. The average whole cell resistance were as follows: turtle 25 ^oC

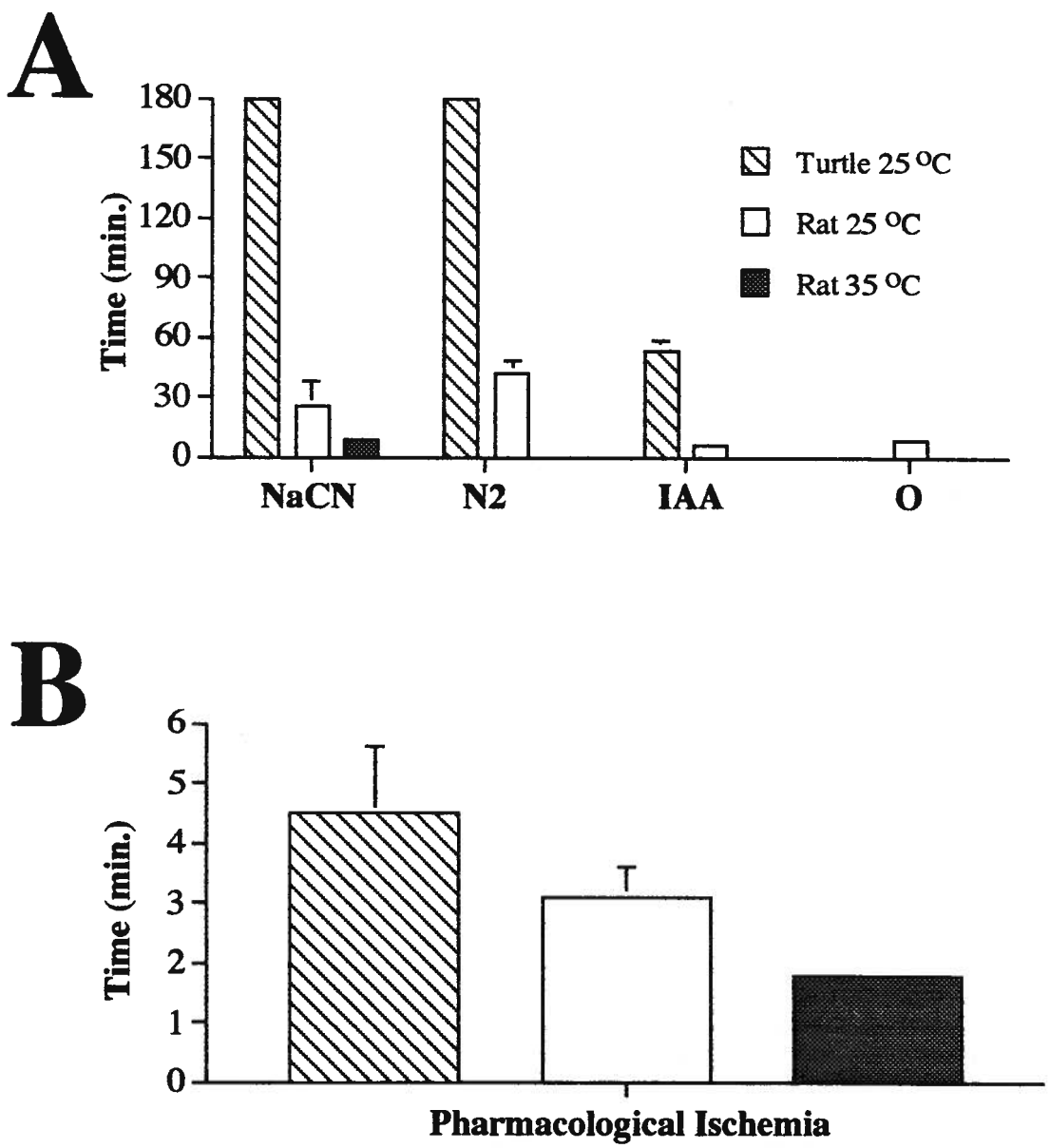

Figure 3. Time to depolarization for turtle and rat pyramidal cortical neurons in response to various pharmacological treatments: pharmacological anoxia (NaCN), anoxia (N_2), iodoacetate (IAA), and ouabain (O), (A) and pharmacological ischemia, (B). All treatments have an *n* of 6 except rat 35 °C ($n = 3$), turtle 25 °C NaCN ($n = 5$), and turtle N_2 ($n = 5$). Data are presented ± SE bars. Treatments without SE bars do not represent survival times. Note different time scales on ordinate.

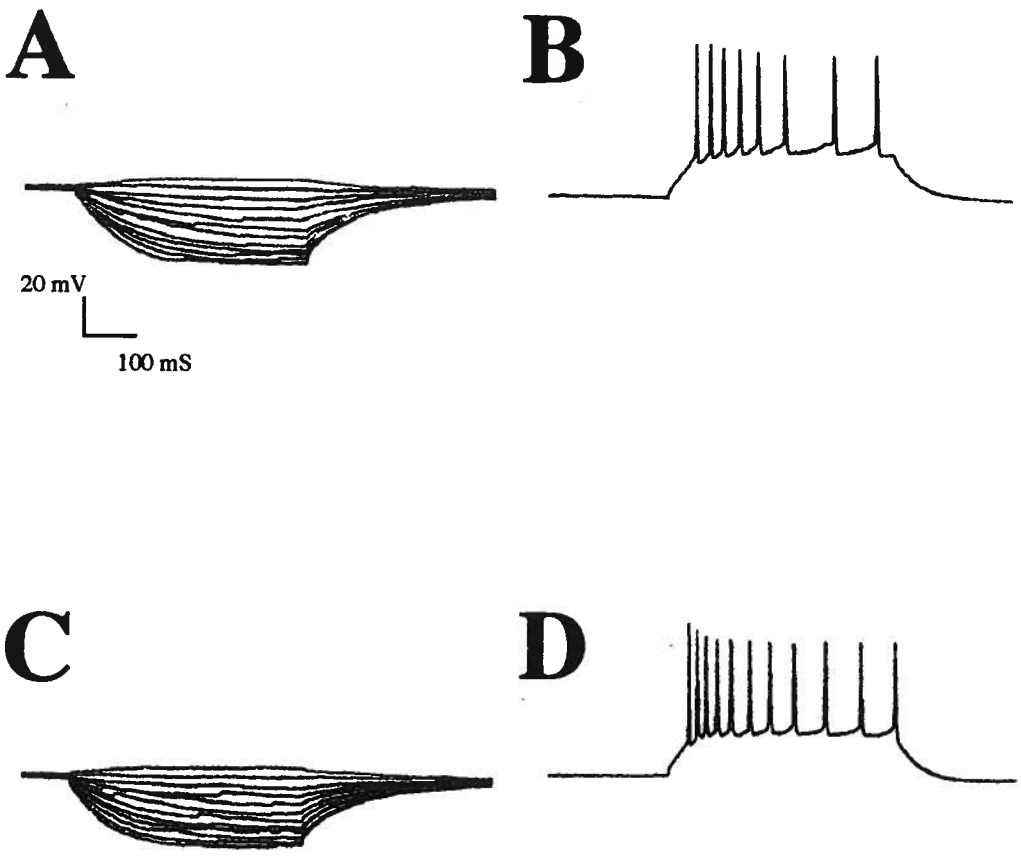

Figure 4. Effect of 180 mins. of anoxia on a continuously impaled turtle cortical pyramidal cell. Cell initially was impaled and recorded from using oxygenated aCSF (A and B) and then was subjected to 180 mins.. of anoxia while measurements were repeated (C and D). Membrane potential in both cases was -65 mV. Current steps were from -0.5 nA by 50 pA in A and C. A stimulating pulse of 0.5 nA was used in B and D.

Table 1. Effect of anoxia and pharmacological anoxia on membrane potential and action potentials of turtle neurons

Treatment	Parameter	*n*	Control	180 min
		Membrane parameter		
N_2	MP, mV	4	-67.8 ± 3.8	-70.0 ± 6.4
NaCN	MP, mV	4	-74.0 ± 4.2	-74.5 ± 3.6
		Action potential parameters		
N_2	Spike Rise, mV/mS	4	92.6 ± 4.7	91.9 ± 5.5
	Spike fall, mV/mS	4	28.4 ± 0.9	33.9 ± 3.7
	Threshold, mV	4	-36.0 ± 1.5	-43.0 ± 2.5
	Spike amplitude, mV	4	62.7 ± 1.1	63.4 ± 1.6
	Spike width, mS	4	4.8 ± 0.4	4.7 ± 0.4

Values are means ± SE; *n*, no. of turtles at 25 °C. Values given are an average from a set of continuously impaled cells. There were no statistical differences between any data sets ($P > 0.05$; paired t test). N_2 , anoxia; NaCN pharmacological anoxia; MP, membrane potential.

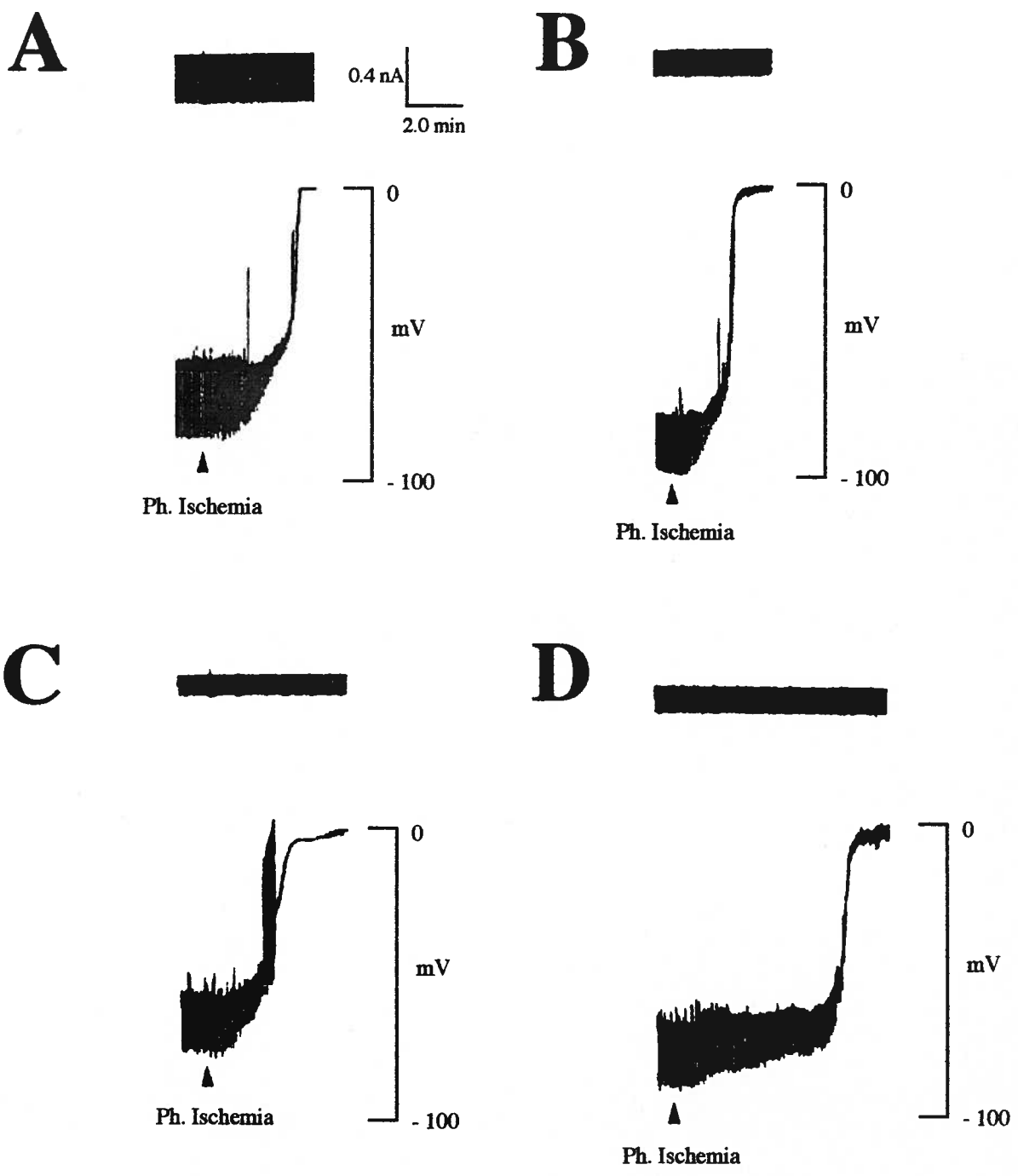

Figure 5. Response of rat and turtle pyramidal cortical neurons to pharmacological ischemia (Ph. Ischemia). Treatment was applied to a rat cortical cell at 25 (A) and 35 °C (B). Treatment was applied to a turtle cortical pyramidal neuron at 25 °C and iodoacetate was applied after cell had been subjected to pharmacological anoxia for 180 mins. at 25 °C (D). Time scale in (A) is representative for (A - D)

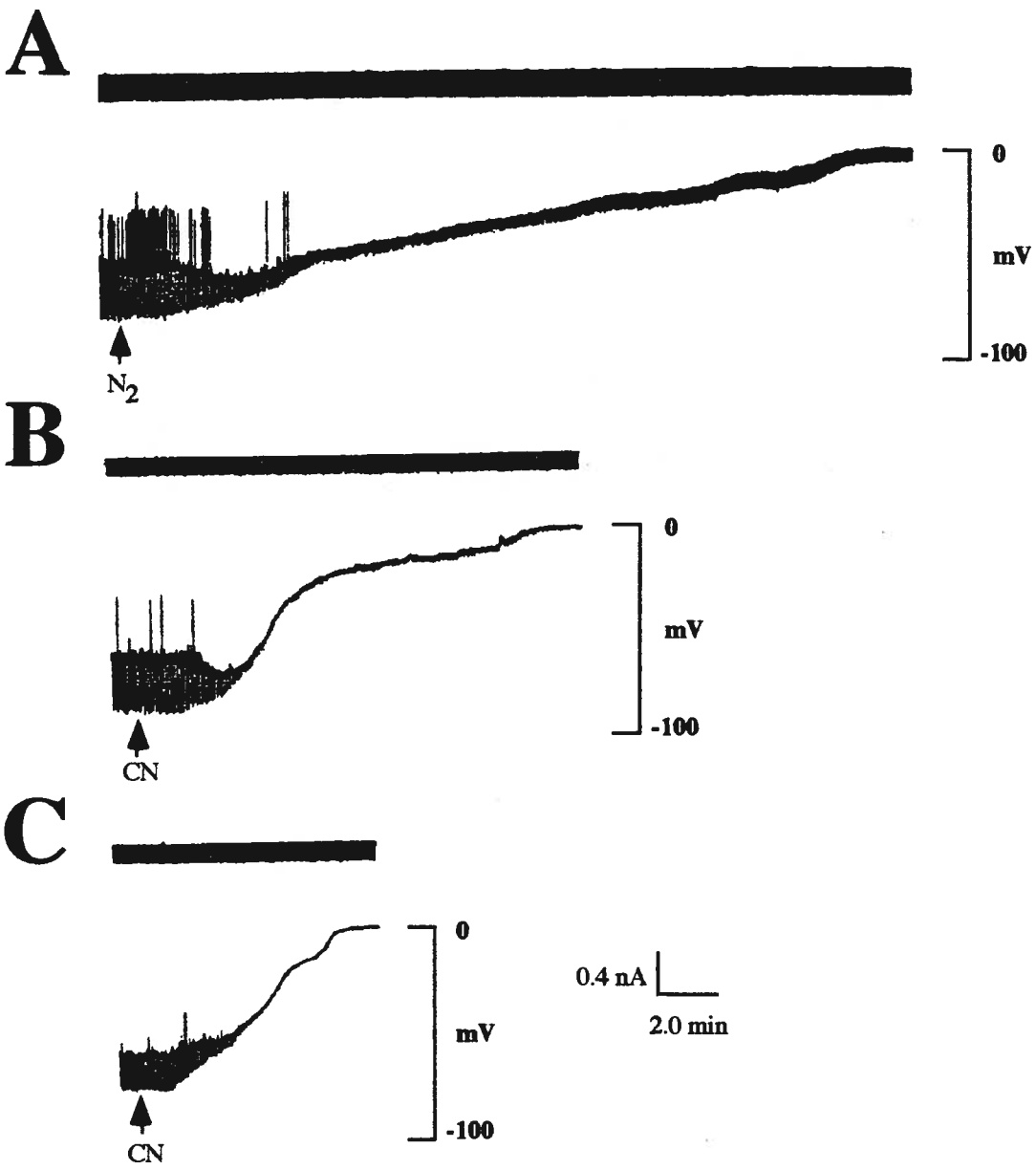

Figure 6. Effect of perfusing solutions of anoxia and pharmacological anoxia on rat pyramidal neurons. In (A), the perfusing solution was anoxic (25 ^{o}C) compared to pharmacological anoxia in (B) and pharmacological anoxia at 35 ^{o}C in (C).

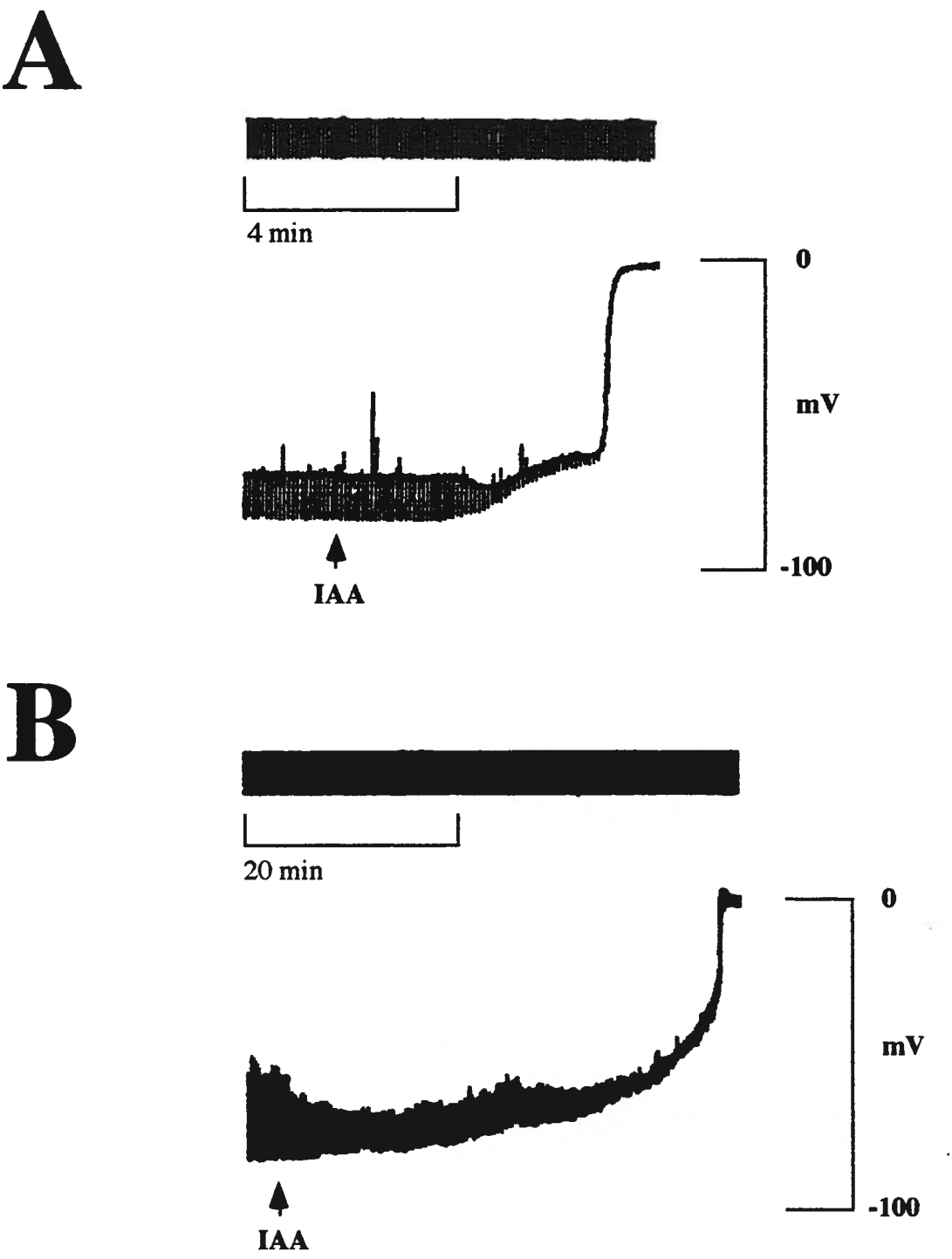

Figure 7. Effect of perfusing iodoacetate on turtle and rat pyramidal cells (rat, A; turtle, B) at 25 °C.

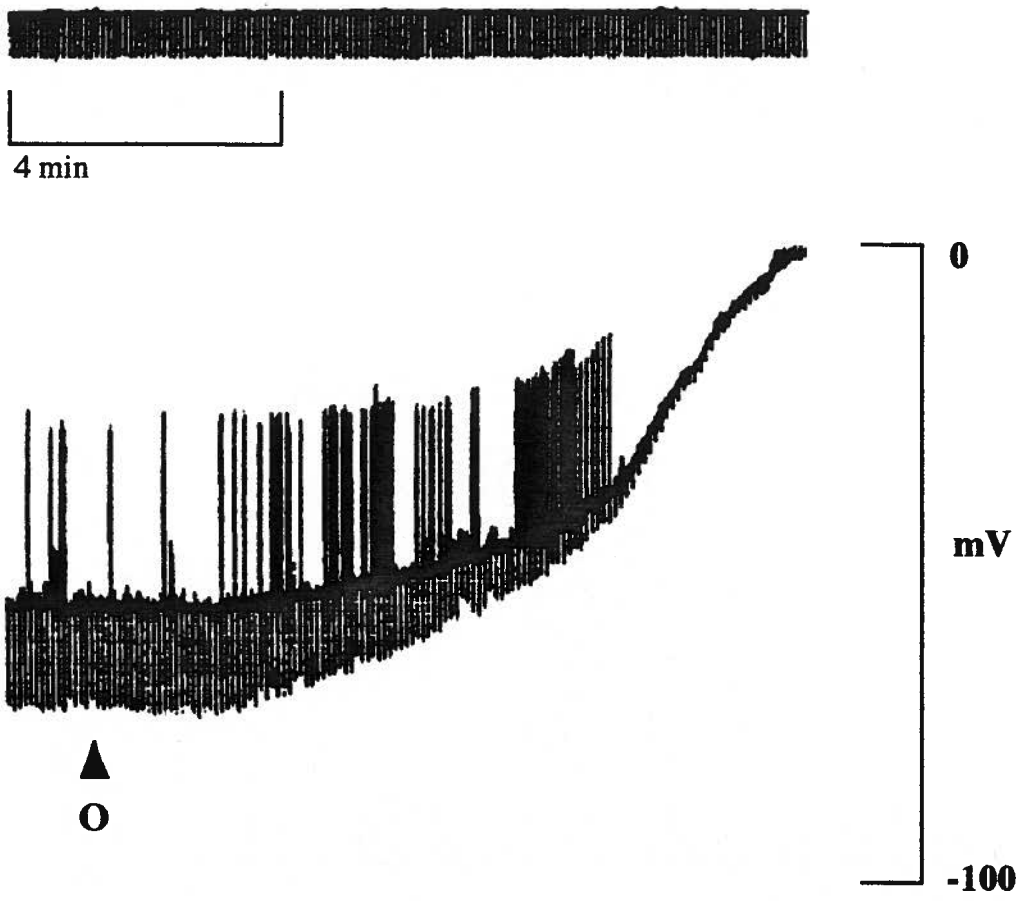

Figure 8. Effect of perfusing ouabain on rat pyramidal neurons (100 μM at 25 ^{o}C).

151 ± 12 MΩ (n = 23), rat 25 °C 86 ± 5 MΩ (n = 30), and rat 35 °C 66 ± 13 MΩ (n = 6). These values are similar to those reported for both turtle and rat using whole cell patch clamping (Blanton *et al.*, 1989).

The turtle neurons maintained a healthy whole cell resistance throughout the anoxic and pharmacological anoxic insults, and were able to fire action potentials for the duration of the experiment (180 minutes) (Fig. 4). Individual turtle cells impaled under normoxic conditions were held up to five hours under anoxia. In addition, slices were held in a holding chamber bathed with nitrogen equilibrated aCSF for up to 18 hours. These cells qualitatively showed no effect of the treatment. In order to quantitatively study the effect of anoxia on certain cellular parameters, turtle neurons were impaled under control conditions (oxygenated aCSF) and held for 180 minutes under anoxic conditions (Table 1). Cells were tested for changes in resting membrane potential (M.P.), action potential rate of rise and fall, threshold, spike amplitude and width following various treatments. Spike amplitudes were measured from threshold, and the rates of spike rise and fall were measured at the maximum slopes. The results indicate that there were no significant changes in any of the measured parameters.

When the turtle cells were exposed to pharmacological ischemia, the neurons quickly depolarized (4.6 ± 1.1 min.) (Fig. 3). This experiment was carried out under oxygenated conditions (Fig. 5c) as well as anoxic conditions (Fig. 5d). In both instances, the turtle cortical neurons exhibited a slight hyperpolarization (4.6 ± 1.8 mV) preceded by or concurrent with a loss in whole cell input resistance followed by a rapid depolarization to a zero membrane potential.

Rat cortical neurons responded to pharmacological ischemia similarly to the turtle, also exhibiting a slight hyperpolarization (8.0 ± 2.7 mV, 25 °C; 1.0 ± 0.6 mV, 35 °C) preceded by or concurrent with a loss in apparent whole cell input resistance leading again to a rapid depolarization (3.1 ± 0.5 min., 25 °C; 1.8 ± 0.2 min., 35 °C) (Figs. 3 & 5a,b). There was a significant temperature effect for both the loss of membrane potential (Q_{10}, 0.56) and hyperpolarization (Q_{10}, 0.13) ($P \leq 0.05$; independent *t*-test).

The results of anoxia and pharmacological anoxia show that in both instances the rat responded with slight hyperpolarization (anoxia 3.2 ± 0.1 mV, 25 °C; pharmacological anoxia 5.5 ± 1.7 mV, 25 °C; 1.3 ± 0.3 mV, 35 °C) preceded by or concurrent with a loss in whole cell input resistance and a slow and gradual depolarization (anoxia 41.8 ± 6.6 min., 25 °C; pharmacological anoxia 25.8 ± 12.6 min., 25 °C, 9.3 ± 1.8 min., 35 °C) (Figs. 3 & 6). Again, there was a significant effect of temperature on both the loss of the membrane potential (Q_{10}, 0.36) and the hyperpolarization (Q_{10}, 0.24) for pharmacological anoxia ($P \leq 0.05$; independent *t*-test).

The addition of IAA by itself was applied in order to test the cell's ability to rely on other sources of substrate besides glucose from intracellular reserves. Since IAA blocks the glycolytic enzyme, glyceraldehyde-3-phosphate dehydrogenase, the cell can no longer utilize glucose and glycogen as a glycolytic substrate. Under these conditions, rat cells depolarized to 0 mV in an average of 6.5 ± 0.8 min. compared to 53.5 ± 4.6 min. for turtle cells (Figs. 3 & 7). This treatment also caused a hyperpolarization (3.0 ± 1.2 mV, turtle; 4.0 ± 1.7 mV, rat).

To test whether pharmacological ischemia or anoxia may simply reflect an inability of the Na^+-K^+-ATPase to function, ouabain (100 μM) was perfused onto the rat cortical slice at 25 °C. The average time to depolarization was 8.7 ± 1.1 min. (Fig. 8). The cells never showed a hyperpolarization, and there was no loss in membrane resistance until there was a loss in membrane potential. The time to depolarization was faster than anoxia or pharmacological anoxia, but less than total metabolic inhibition

Additional Statistics

In addition to testing the significance of these pharmacological treatments to each other, each treatment was individually tested (Pearson Correlation Matrix) to see if there were any correlations within treatments corresponding to membrane potential, whole cell resistance, degree of hyperpolarization, and the time to depolarization. Although there were a few correlations, there were no consistent trends throughout all of the treatments. The most

consistent correlation was with the membrane potential versus the time to depolarization with the treatments of nitrogen and pharmacological anoxia in the rat, and with IAA in the turtle ($P \leq 0.05$).

Discussion

The evidence presented in this chapter strongly supports the supposition that the mechanism responsible for the rapid failure of the brain during anoxia (rat brain) and ischemia (rat and turtle brain) involves the breakdown of ion gradients across the neuron. This observation is not surprising in view of the evidence discussed earlier. However, the question further explored here is why cortical neurons lose apparent input resistance under these treatments.

One hypothesis for the loss of membrane resistance observed here and elsewhere concerns the loss of metabolism, and hence, the energy state of the cell (Hansen, 1982; Hochachka, 1986; Lipton and Whittingham, 1982). This hypothesis centers around the idea that high energy phosphates are directly or indirectly responsible for maintaining ion gradients through pumping and regulation of ion channels. Brain tissue is metabolically very active compared to other tissues. A reliance on the low ATP producing glycolytic pathway during anoxia/ischemia results in the inability to maintain intracellular [ATP] as discussed in the Introduction. The loss of [ATP] would cause energy consuming processes to cease, including the ion pumping action of Na^+,K^+-ATPase and Ca^{+2}-ATPase. The increasing $[Ca^{+2}]_i$ and decreasing [ATP] could potentially activate a host of ion channels sensitive to low [ATP] and Ca^{+2} including non selective ion channels (Ashford *et al.*, 1988; Partridge and Swandulla, 1988) as well as voltage gated ion channels (Hille, 1992). The ultimate apex of these events would be the observed anoxic/ischemic massive release of neurotransmitters (Beal, 1992; Benveniste, et al., 1984; Choi, 1988a; Choi, 1988b; Globus *et al.*, 1988; Sánchez-Prieto and González, 1988) which would only serve to perpetuate the membrane and cell degeneration. This hypothesis will be discussed in further detail in chapter 5.

Current support for this 'ATP' hypothesis is indirect, but includes such observations as bathing the slice with creatine leading to prolonged anoxic and ischemic survival (Leblond and Krnjevic, 1989), the extracellular addition of high energy compounds to neurons after cyanide exposure leading to a partial re-establishment of the membrane ion gradient (Caldwell *et al.*, 1960), hypothermia protecting the neuron (Okada *et al.*, 1988b), and correlating low [ATP] concentration with the loss of electrical activity (Lipton and Whittingham, 1982).

Our data support the concept that metabolic inhibition, and hence, limiting ATP, plays a major role in the loss of neuronal membrane resistance. First, the cell's ability to maintain resistance and membrane potential is inversely related to the degree of metabolic inhibition. Thus, the use of nitrogen gave the longest degree of survival followed by pharmacological anoxia, IAA, and finally, the most inhibitory regime used, pharmacological ischemia (Fig. 3). The use of nitrogen presumably allows the cell to exist longer due to the fact that the cytochrome system is not immediately inhibited; in contrast, sodium cyanide leads to an almost immediate and total inhibition of the system aided by the fact that the aCSF was equilibrated with nitrogen. The use of IAA alone is the most severe single drug treatment. The inhibition of glycolysis by IAA leaves only the low levels of endogenous fatty acids, lactate, Krebs cycle intermediates, and the reserves of high energy phosphates to fuel metabolism. The most severe was the use of pharmacological ischemia which inhibited all energy production and allowed the cell to use only its reserve of high energy phosphates.

Secondly, the observation that the turtle lasted 10 times longer during treatment of IAA compared to the rat also supports this statement. In an earlier paper (Suarez *et al.*, 1989), we showed that in the turtle brain resting metabolic rates were approximately 1/10 to 1/20 resting metabolic rate in a rat brain *in vivo*. Assuming a Q_{10} of 2 for turtle metabolism (Funk and Milsom, 1987), the expected difference between the turtle and the rat neuronal depolarization would be 5 - 10 fold since in the turtle ATP would be consumed 5 - 10 times

more slowly assuming usable energy stores were similar between the two tissues (McDougal *et al.*, 1968).

Although there have been some suggestions that cyanide does not provide a good mimic of anoxia (Aw and Jones, 1989), our data suggest the opposite. Pharmacological anoxia and anoxia provided qualitatively similar results (Figs. 3 & 6). The turtle responded well with the treatment and illustrated no difference to either treatment suggesting that pharmacological anoxia is not alternately inhibiting other processes which are necessary for survival under these circumstances.

The pharmacological mimic of ischemia appears to reflect the observed extracellular observations well (Hansen, 1982; Reiner *et al.*, 1990). The initial slow gradual rise in $[K^+]$, as observed in the extracellular space, could be caused by an evoked K^+ current resulting in the initial loss of membrane resistance and concurrent neuronal hyperpolarization (Krnjevic and Xu, 1989). The sequential sudden and massive loss in membrane resistance resulting in the depolarization of the neuron would correspond to the sudden drop of $[Na^+]$ and $[Ca^{+2}]$ in the extracellular compartment since these ions would be entering the neuron flowing down their electrochemical gradient. Further confirmation that pharmacological ischemia provides a plausible *in vitro* mimic of the *in vivo* response awaits simultaneous recording of changes in membrane potential and extracellular ion concentrations.

There is currently considerable evidence that one mechanism which aids the turtle brain in surviving anoxia is the ability to depress brain metabolic rate (Kelly and Storey, 1988; Lutz, et al., 1984; Robin, et al., 1979). Two biochemical mechanisms are actively being studied for the mechanism of this depression. The first involves the down regulation of ion channels responsible for the normal ion fluxes in a resting state and is termed 'channel arrest'. The metabolic depression is the result of reduced ion pump activity due to the reduced ion leakage. The prediction which is forwarded is that anoxia tolerant species will have cell membranes which are less conductive than non anoxia tolerant species. This hypothesis will be discussed in detail in chapter 4. The second hypothesis for the reduction of turtle brain

metabolic rate is a reduction in brain electrical activity (Lutz, et al., 1985; Suarez, 1987) aptly termed 'spike arrest' (Sick *et al.*, 1993). Three general mechanisms could alter brain electrical activity in the turtle brain during anoxia: i) increasing the release of inhibitory neurotransmitters such as γ-aminobutyric acid (GABA) and decreasing the release of excitatory neurotransmitters such as glutamate; ii) altering the physical properties of neurons such as the membrane potential (hyperpolarize) or a resistance (decrease) to make the neurons less excitable; and iii) directly regulating ion channels such as voltage gated Ca^{+2} and Na^{+} channels.

With regards to the first proposed mechanism, studies support that the anoxic turtle brain increases substantially in [glycine], [taurine], and [GABA] inhibitory neurotransmitters (Hitzig *et al.*, 1985; Lutz and McMahon, 1985; Nilsson *et al.*, 1990). Additionally, there is evidence for the increased release of these neurotransmitters during anoxia while the release of the excitatory neurotransmitter glutamate remains relatively constant (Nilsson and Lutz, 1991). However, increase in brain concentrations as well as release does not occur until about 120 minutes into the anoxic insult (Lutz and McMahon, 1985; Nilsson, et al., 1990; Nilsson and Lutz, 1991) where as reduction in electrical activity has been implicated to occur very rapidly (≤ 30 mins) (Feng *et al.*, 1988; Feng *et al.*, 1990; Feng *et al.*, 1988; Sick, et al., 1982). Additionally, increases in these neurotransmitters occur to both reptiles and mammals during anoxia (Nilsson *et al.*, 1991) suggesting that this may not be an adaptation but a byproduct of the insult. These data suggest that at least on the short term basis, we must examine different mechanisms. The data reported here can neither support nor refute this mechanism as playing a role during anoxia in the cortex.

With regards to changes in physical properties of the neuron, we have tested threshold, MP, and resistance (discussed in chapter 4). There were no significant changes in any of these parameters (Table 1). Interestingly, studies from the cerebellum of the anoxic turtle suggest that anoxic cells in this area of the brain lose resistance, and MP during anoxia. In

addition, spike thresholds appear more depolarized(Pérez-Pinzón *et al.*, 1992a) suggesting that the cerebellum may have different anoxic control mechanisms compared to the cortex.

The third set of alterations involves the direct regulation of ion channels which are voltage gated. By removing or blocking these channels, action potential generation would be inhibited. Evidence in the anoxic turtle cerebellum suggests that voltage gated sodium channels are inhibited or possibly even physically removed from the membrane as reported from binding studies(Pérez-Pinzón *et al.*, 1992c). However, our evidences in the cortex shows no change in the threshold or the rate of spike rise which would be expected if there were fewer active voltage gated Na^+ channels in this area of the brain. This observation again suggests that regulation in the cerebellum may be different than in the cortex. One side mechanism to this hypothesis would be to make receptors less sensitive to excitatory neurotransmitters, (such as glutamate activation of Ca^{+2} channels on the postsynaptic membrane). Cortical studies using fura-2 suggest that the Ca^{+2} influx is 75% reduced for a given application of glutamate during anoxia compared to normoxia (Bickler and Gallego, 1993). However, the turtle brain increases its $[Ca^{+2}]_o$ by 6 fold during an anoxic bout (Cserr *et al.*, 1988). Under these conditions, if Ca^{+2} channels were not down regulated in response to neurotransmitter application, there would be a state of hyperexcitivity. Thus, whether this down regulation is simple a response to the 6 fold increase in the cerebral spinal fluid $[Ca^{+2}]$ or an attempt to decrease electrical activity is unknown.

The emphasis throughout this chapter has been on the importance of supplying cells with an adequate amount of energy (ATP) in order to maintain ion homeostasis during anoxia. If this theory is correct, then the turtle cell in the absence of any energy production should rapidly lose its membrane potential. The results of pharmacological ischemia on the turtle neuron are illustrated in Fig. 5c,d. Although this is the first study to observe turtle neuronal response directly to total metabolic inhibition, an extracellular rise in $[K^+]$ has been reported with both the addition of IAA plus nitrogen (Sick, et al., 1982) as well as with clamping the arterial supply to the turtle brain (Sick, et al., 1985). The results in all cases clearly

demonstrate the importance of glycolysis for maintaining ion homeostasis across the neuronal membrane. Statistically, the turtle neuron maintains a membrane potential no longer than the rat neuron which suggests that the turtle cell is not designed to survive on low amounts of ATP but is designed to maintain ATP concentrations during anoxia. This hypothesis is further strengthened by the observation of the turtle brain has been shown to exhibit a Pasteur effect (Kelly and Storey, 1988) as well as the comparatively large amounts of key glycolytic control enzymes compared to the rat at physiological temperatures (see chapter 3)

Our data support metabolism playing a direct role in the maintenance of ion homeostasis, but it is unclear if the rapid failure of the neuron which accompanies anoxia and ischemia and their pharmacological mimics is due to a lack of energy dependent pumping, channel opening, or the release of excitatory neurotransmitters. It is conceivable that the mechanisms of failure between the two insults may not be the same. To look at one facet of this model, ouabain was used to block Na^+-K^+-ATPase and observe the resulting time to depolarization. The results indicate that the ouabain treatment (Figs. 3 & 8) did not adequately mimic any of the previous times of survival. In addition, there was no initial hyperpolarization in any of the cortical cells. This observation is in contrast to hippocampus in which a slight hyperpolarization has been observed using lower concentrations of ouabain (Fujiwara, et al., 1987). In addition, there was no initial loss in whole cell resistance until there was a change in the membrane potential of the cell. This data suggests that although the anoxic failure could be explained by the inhibition of the pump system, it seems unlikely that the rapid membrane degeneration observed in pharmacological ischemia could be explained fully by ion pump inhibition.

CHAPTER 3: A BIOCHEMICAL AND MICROCALORMETRIC STUDY OF THE TURTLE CORTEX

Preface

This chapter explores metabolic and biochemical mechanisms which allow the turtle brain to survive extended bouts of anoxia. This chapter is excerpted (in part) from C. J.. Doll, P. W. Hochachka, and S. H. Hand (submitted, *J.E.B.*). The enzymatic measures were adapted from R. K. Suarez, C. J. Doll, A. E. Buie, T. G. West, G. D. Funk, and P. W. Hochachka (*Am. J. Physiol.* 257: R1083-R1088, 1991).

Introduction

Long term anoxic survival of the freshwater turtle (*Chrysemys picta*) is well documented in the literature with individuals having survived forced submergence for up to 6 months at 3 ^{o}C (Ultsch, 1985). The high sensitivity of the mammalian brain to anoxia and ischemia (Hansen, 1985), has lead to the turtle brain being used as a comparative model for anoxic studies. However, only recently have healthy *in vitro* preparations of turtle brain become available. Three such preparations are the turtle brain stem slice preparation (Jiang *et al.*, 1992), whole cerebellum preparation (Pérez-Pinzón, et al., 1992b), and the cortical slice preparation (Connors and Kreigstein, 1986; Chapter 2).

In the previous chapter, we demonstrated that the turtle cortical neurons can survive anoxia and still maintain a healthy membrane resistance, potential, and ability to fire action potentials. Several biochemical mechanisms are currently believed to aid the turtle brain in surviving anoxia, [for review see (Lutz, 1992)]. However, we believe that two adaptations are central to helping maintain energy stability in the turtle brain: (i) an enhanced ability to produce ATP (glycolytic capacity) coupled with the ability to increase glycolytic flux during anoxia (Pasteur effect); (ii) a low metabolic rate with the ability to further depress metabolism with anoxia.

As discussed in Chapter 1, the Pasteur effect serves to replace some of the lost ATP production (2 vs. 36 ATP for glucose) resulting form the exclusive use of glycolysis during

anoxia. However, the Pasteur effect appears to be only temporary and never achieves the predicted 18 fold increase which is necessary to replace all of the lost ATP production. Mammalian brain studies (*in vivo* and *in vitro*) have indicated glycolytic activation between 2 and 10 fold during hypoxia/anoxia/ischemia or simulated conditions (Borgström *et al.*, 1976; Drewes and Gilboe, 1973; Kauppinen and Nicholls, 1986; Kauppinen and Nichols, 1986; Ksiezak and Gibson, 1981; Lowry, et al., 1964; Rolleston and Newsholme, 1967a) which (in part) could explain the inability of the rat brain to maintain [ATP] (Lowry, et al., 1964; Ridge, 1972)during these insults (maintenance of energy balance will be discussed in further detail in Chapter 5). Although *in vivo* turtle brain studies indicate glycolytic activation with anoxia (Kelly and Storey, 1988; Lutz, et al., 1984), none have indicated a full 18 fold activation, and the one study which examined turtle brain slices in detail for glycolytic activation failed to measure any Pasteur effect (Robin, et al., 1979). The ability of the turtle brain to maintain [ATP] during anoxia (Kelly and Storey, 1988; Lutz, et al., 1984) combined with the low or non existent Pasteur effects suggests that the turtle brain is experiencing some degree of metabolic depression with anoxia.

Metabolic depression was first measured in the turtle using calorimetry. The initial experiments indicated that turtle whole body heat dissipation decreased 85% (Jackson, 1968). Whole body calorimetry has also been used to measure metabolic depression in other anoxia tolerant vertebrates with similar results. For ectotherms, for example, the goldfish (*Carassius auratus*) depresses heat production 70% (van Waversveld *et al.*, 1988), and the marine toad (*Bufo bufo*) has also been observed to reduce heat production by 80% with submersion (Leivestad, 1960). Current *in vivo* studies on the turtle brain based on lactate accumulation over the duration of anoxic insult suggests a severe (> 80%) metabolic depression with anoxia (Kelly and Storey, 1988; Lutz, et al., 1984). However, these numbers may be misleading due to lactate not being trapped in the brain tissue compartment (Drewes and Gilboe, 1973; Hawkins, 1985; Schurr *et al.*, 1988). As a result, the lactate pool measured

may not include the lactate washed out of the tissue compartment and therefore, may not reflect the anoxic metabolic rate.

In vitro turtle brain preparations are able to survive extended periods of anoxia compared to rat counterparts as observed in Chapter 2 and other studies (Jiang, et al., 1992; Pérez-Pinzón, et al., 1992b). However, whether metabolic depression occurs in the *in vitro* preparation as suggested by the above the *in vivo* studies has not been established. In this chapter, three areas of metabolic adaptation in the turtle cortical slice will be explored with respect to anoxia: (i) metabolic rate, (ii) changes in adenylates and energy balance, (iii) glycolytic capability and activation.

Methods

Slice Preparation

Turtles (*C. picta*), 150 - 300 g were cold anesthetized before decapitation. The brain was rapidly dissected free and immersed in artificial cerebrospinal fluid (aCSF) which had been precooled and equilibrated with 95% O_2 /5% CO_2. The cortical tissue was then dissected free as previously described (Connors and Kreigstein, 1986). Blocks of whole cortex ($\approx$ 500 μM thickness) were stored at room temperature 22 ^{o}C in a recirculating holding chamber until their use in the calorimeter or incubation chamber.

For the enzymatic assays, the brains (turtle and rat) were rapidly dissected free after cervical dislocation or decapitation. The brains were dissected over ice and the cortex was removed. The cortex was then placed in 9 Volumes of 50 mM tris (hydroxmethyl) aminomethane (Tris)-Cl (pH 7.4 at 4 ^{o}C), 2 mM EDTA and 0.5% Triton X-100. Rat cortex was homogenized with and UltraTurrax homogenizer 3 times 10 sec. each time. Turtle brains were homogenized with a hand glass homogenizer and sonicated for 10 sec twice. Homogenates were the spun at 12,000 g for 5 mins. The resulting supernatant was then used for enzyme assays.

Artificial Cerebrospinal Fluid

The aCSF for the turtle was a modification(Connors and Kreigstein, 1986) which consisted of (in mM) 96.5 NaCl, 2.6 KCl, 2.5 $CaCl_2$, 2.0 $MgCl_2$, 2.0 NaH_2PO_4, 10 glucose, 26.5 $NaHCO_3$, and 0.03 phenol red as a pH indicator. Final pH of the solution was 7.4 when saturated with 95% 0_2 / 5% CO_2. To mimic anoxia, the aCSF was equilibrated with 95% N_2 / 5% $C0_2$. Pharmacological anoxia was the same solution as anoxia, but in addition contained 1 mM NaCN.

Adenylates

Slices used in the adenylate measurements were incubated (in a recirculating slice chamber) for two hours in oxygenated aCSF before the experiment was commenced. This incubation period allowed slices to stabilize after dissection and was done for all experiments including the calorimetry studies. After incubation, the slices were transferred to 60 ml recirculating semiclosed chambers. The chambers were sealed at the top with an O ring and bolted shut. All gases flowed through gas impermeable Viton tubing. Gas at positive pressure inside the chamber was allowed to escape via a variable flow escape valve. By adjusting the opening of the valve, a slight but constant positive pressure could be maintained on the liquid above the slice maximizing saturation of the gas used and minimizing contamination from the atmosphere. For anoxic experiments, chambers were tested for oxygen contamination using a Radiometer gas analyzer and O_2 electrode. No O_2 contamination was detected compared to a sodium dithionate solution. Upon completion of the experiment, the tissue was removed from the chamber with a pair of forceps and blotted dry. Slices were immediately immersed in precooled (-5 ^{o}C), preweighed vials of 5% perchlorate acid (PCA) and weighed. The procedure from removal to PCA immersion took less than 20 seconds. The tissue was then sonicated 3 times (10 sec. duration) with 30 seconds in between each burst. The vials were kept on a rock salt/ice slurry ($\approx$ -5 ^{o}C). The homogenate was then spun at 15000 rpm for 20 minutes (-5 ^{o}C). The resulting supernatant was removed and adjusted to a pH of $\approx$ 2.5 with 3M K_2CO_3 (potassium bicarbonate). The

partially neutralized supernatant was respun at 15000 rpm for 20 minutes (-5 ^{o}C) to remove precipitated perchlorate salts. The resulting supernatant was removed and frozen in liquid N_2. Samples were stored at -70 ^{o}C until analysis (within one week).

Chromatography

All adenylates in this paper were measured using high performance liquid chromatography (HPLC) on an LKB 2152 HPLC controller and 2150 titanium pump coupled to a 2220 recording integrator as previously described (Schulte *et al.*, 1992). In brief, sample separation was performed on an Aquapore AX-300 7 μm weak anion exchanger (Brownlee labs). Elution off the column was performed by running an isocratic solution of 60 mmol/l KH_2PO_4 (pH 3.2) for the first five minutes followed by a linear increasing concentration to 750 mmol/l KH_2PO_4 (pH 3.5) for the next 10 min. This concentration and pH was maintained for the next 12 min. The column was re-equilibrated for 5 min with the starting buffer for the next run. Adenylates were detected using a BIO-RAD flow through UV detector at 254 nm. Standard curves were done for all adenylates to assure linearity over relevant concentrations. Analytical reagent grade KH_2PO_4 was purified before use in the HPLC by running a stock 1M solution through a BIO RAD Econo column packed with anion exchange resin (AG1 X8, chloride form, a cation exchanger (chelex 100, sodium form) and activated charcoal (14-60 mesh). The solution was kept at 4 ^{o}C and constantly recirculated through the column by a peristaltic pump ($\approx$ 3 ml/min) for 24 hrs. Before use, the stock 1M buffer was diluted, pH adjusted, and vacuum filtered (0.22 μm filter).

Microcalorimetry

Calorimetry was used in this study because it allowed the continuous measurement of heat dissipation over reversible bouts of oxygen limitation with tissue from a single turtle. The only other method giving this advantage is NMR spectroscopy. However, preliminary experiments with NMR indicated that sufficient cortical tissue was not attainable from a single turtle to permit adenylate concentrations to be measured during a reasonable time frame. Additionally, the low normoxic metabolic rate of the turtle brain gave an extremely

slow spin-lattice relaxation time (T_{1M}) making saturation transfer measurements impossible (Shoubridge *et al.*, 1982).

Heat dissipation measurements on turtle cortical slices were performed with an LKB 2277 thermal activity monitor equipped with a 3.5 ml perfusion chamber. The perfusion aCSF was identical to that described above for normoxia, anoxia, and pharmacological anoxia. Perfusion aCSF was held in semiclosed glass bottles that were kept at 25 ^{o}C with a circulating water bath. Flow lines for gases and aqueous media were made of Viton and stainless steel, respectively. Flow rate of the perfusion media through the slice and chamber was set at 15.0 ml/hr, and the temperature was maintained at 25 ^{o}C for all experiments. Heat dissipation in microwatts was time corrected by the calibration unit of the calorimeter; typical time constants were t_1 = 600s and t_2 = 17100s. Heat measurements were taken every 60 s and stored on an IBM XT personal computer. For all experiments, blanks (no slices) were run in parallel and subtracted from the measurements obtained with slices.

Two cortical slices from a single turtle were prepared as described above. After calibration of the instrument, the slices were placed in the perfusion chamber and lowered into the calorimeter. Heat dissipation was then monitored for a minimum of 1 hr before data collection was begun. Total time from dissection to collection of data was approximately 2 hrs. The normoxic solution was switched over to nitrogen perfusion or pharmacological anoxia once heat dissipation of the slices had stabilized to less than 0.2 μW/min change. During perfusion with nitrogen saturated medium, previous measurements indicated a period of 60 - 90 min. was needed at similar flow rates to reduce oxygen content below 0.5% air saturation in the excurrent flow (Hand and Gniager, 1988). For nitrogen perfusion experiments, nitrogen equilibrated aCSF was switched to normoxic aCSF to monitor recovery. The experiment was terminated once heat dissipation had returned to predicted levels of heat dissipation or stabilized.

Enzymatic Methods

For hexokinase, the following recipe was used: 5 mM glucose (omitted for control), 5 mM ATP, 5 mM MgCl2, 0.5 mM $NADP^+$, 5 mM dithiothreitol (DTT), and 50 mM imidazole-Cl (pH 7.5). For lactate dehydrogenase, the recipe was as follows: 1 mM pyruvate (omitted for control), 0.15 mM NADH, 5 mM DTT, and 50 mM imidazole-Cl (pH 7.0). For Citrate Synthase the recipe contained 0.5 mM oxaloacetate (omitted for control), 0.3 acetyl-CoA, 0.1 mM dithiobisnitrobenzoic acid, and 50 mM Tris-Cl (pH 8.0). Total volume of assay was 1.0 ml. Measurements were done at 25 ^oC turtle, and 37 ^oC rat and started by the addition of 10 - 20 μl of crude supernatant. All Enzymatic assays were done using a Pye-Unicam SP-1800 spectrophotometer with water jacketed cuvette holders and a chart recorder for data acquisition.

Calorimetric Data Analysis

Data collected with IBM XT was imported into CA-Cricket Graph III for the Macintosh. Based on blank runs after the removal of slices, any baseline drift or signal from bacterial contamination (due to high glucose in the aCSF) was apportioned linearly over the entire experiment using CA - Cricket Graph III.

The heat depression data was then graphed similar to Fig. 9a and b. These data were then curve fit by hand to estimate aerobic values over the nitrogen perfusion period. Data (control and treatment) over the anoxic period were then digitized using Sigmascan. Percentage heat depression was then calculated. ATP turnover estimates were derived by a conversion factor of .76 μmoles ATP/g/min/mW for aerobic heat dissipation and .86 μmoles ATP/g/min/mW for anaerobic heat dissipation with the following assumptions and conversion factors:

Aerobic Conditions

1) The turtle slice is using only (glucose or glycogen) as a fuel (Clark and Miller, 1973; Pérez-Pinzón, et al., 1992b).
2) The aerobic catabolism of glucose to CO_2 and H_2O yields -469 - 476 kJ/mole O_2 (Gnaiger and Kemp, 1990).
3) For glucose, 6 moles of ATP are produced for every mole of O_2 consumed.

Anaerobic Conditions

1) The turtle slice is using only glucose as a fuel (see ref. to 1 above).
2) Lactate is the only anaerobic end product produced (Robin, et al., 1979)
3) The catabolism of glucose to lactate yields -70 kJ/mole lactate (Gnaiger and Kemp, 1990).
4) Production of one mole of lactate from glucose provides one mole of ATP.

Results

Calorimetry

Typical calorimetry recordings are illustrated in Figs. 9a,b. Results demonstrated that cortical cells depress heat flow under both treatments (Fig. 10a,b). Both nitrogen perfusion and pharmacological anoxia produced rapid declines in heat dissipation, but pharmacological anoxia produced a significantly ($P \leq 0.05$) more rapid effect (32.8 ± 1.8^{SE}% vs. 8.6 ± 1.8^{SE}% by 20 minutes; Fig 14a), due to the slow washout of oxygen. By 60 minutes into the insult, treatments had decreased the rate of change to 6.3 ± 0.8^{SE} %/hr (nitrogen perfusion) vs. 3.1 ± 0.8^{SE} (pharmacological anoxia). Nitrogen perfusion followed by normoxia reestablishes heat flow to predicted control level in all trials similar to Fig. 9a. Average heat depression (percentage of control) by the termination of the insult was significantly less in the nitrogen perfusion group compared to the pharmacological group (36.3 ± 2.6^{SE} vs. 49.3 ± 1.6^{SE}; Fig. 11b).

Observations of heat flow depression indicated highly significant differences between the control heat dissipation and both treatment groups by 120 mins (Fig. 12a). Similarly, the ATP utilization rates based on these heat dissipation values indicated large differences between control and treatment groups by the end of the insult (nitrogen perfusion control, 1.36 ± 0.05^{SD} vs. 120 min., 0.97 ± 0.09^{SD}; pharmacological anoxia control, 1.42 ± 0.05^{SD} vs. 120 min., 0.82 ± 0.07^{SD} μmoles ATP/g/min; Fig 12b). The ATP metabolism was based on a conversion factor of .76 μmoles ATP/g/min./mW for normoxia and .86 μmoles ATP/g/min./mW for anoxia (see Methods). Because heat output under aerobic conditions

A

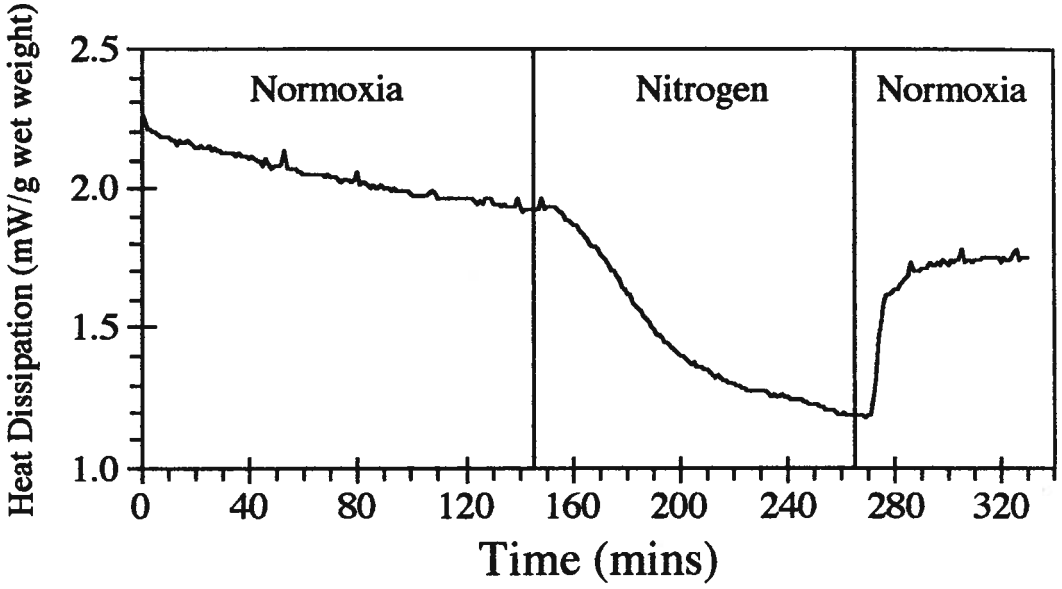

B

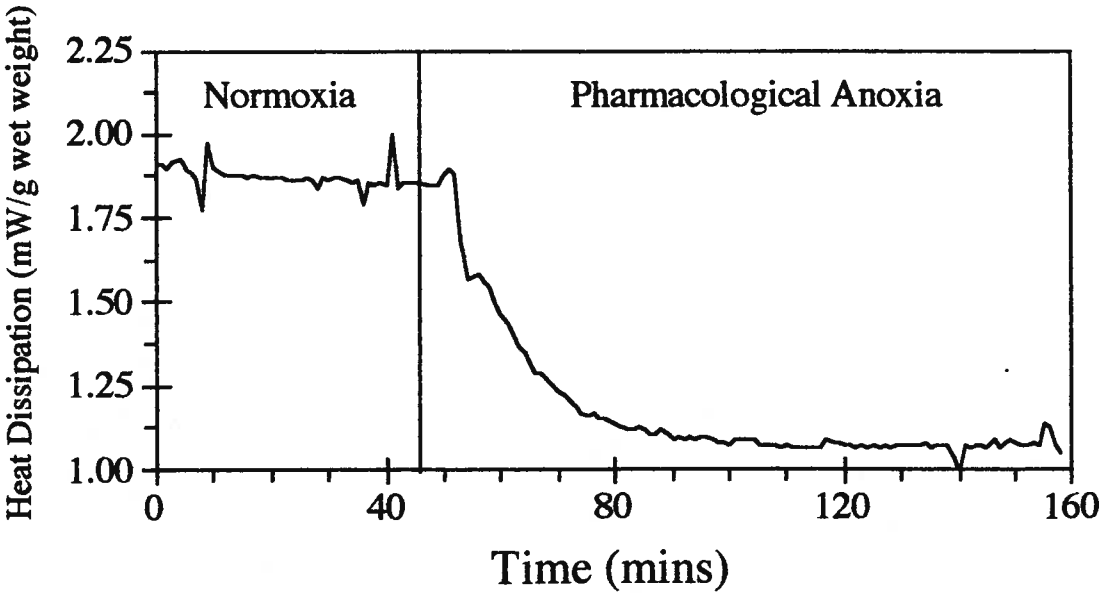

Figure 9. Representative chart recordings of heat dissipationover nitrogen perfusion (A) and pharmacological anoxia (B) for turtle cortical slices (25 ^{o}C). Vertical lines across chart tracings indicate the time at which the indicated solution entered the calorimeter chamber.

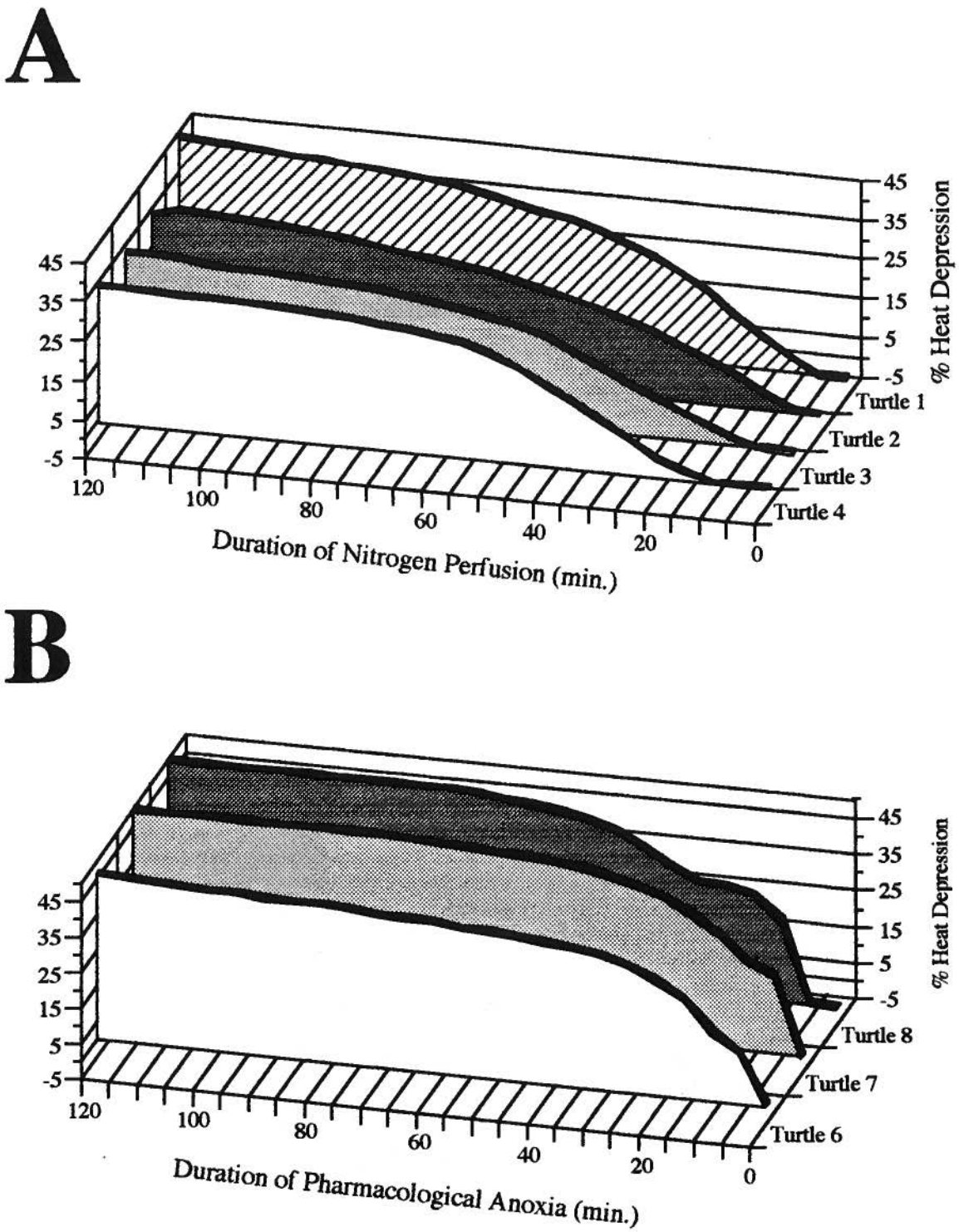

Figure 10. The individual percent heat depression from the predicted corresponding control value over nitrogen perfusion (A) and pharmacological anoxia (B) for all tested slices. Time 0 indicates the point at which the test solution first entered the calorimeter slice chamber.

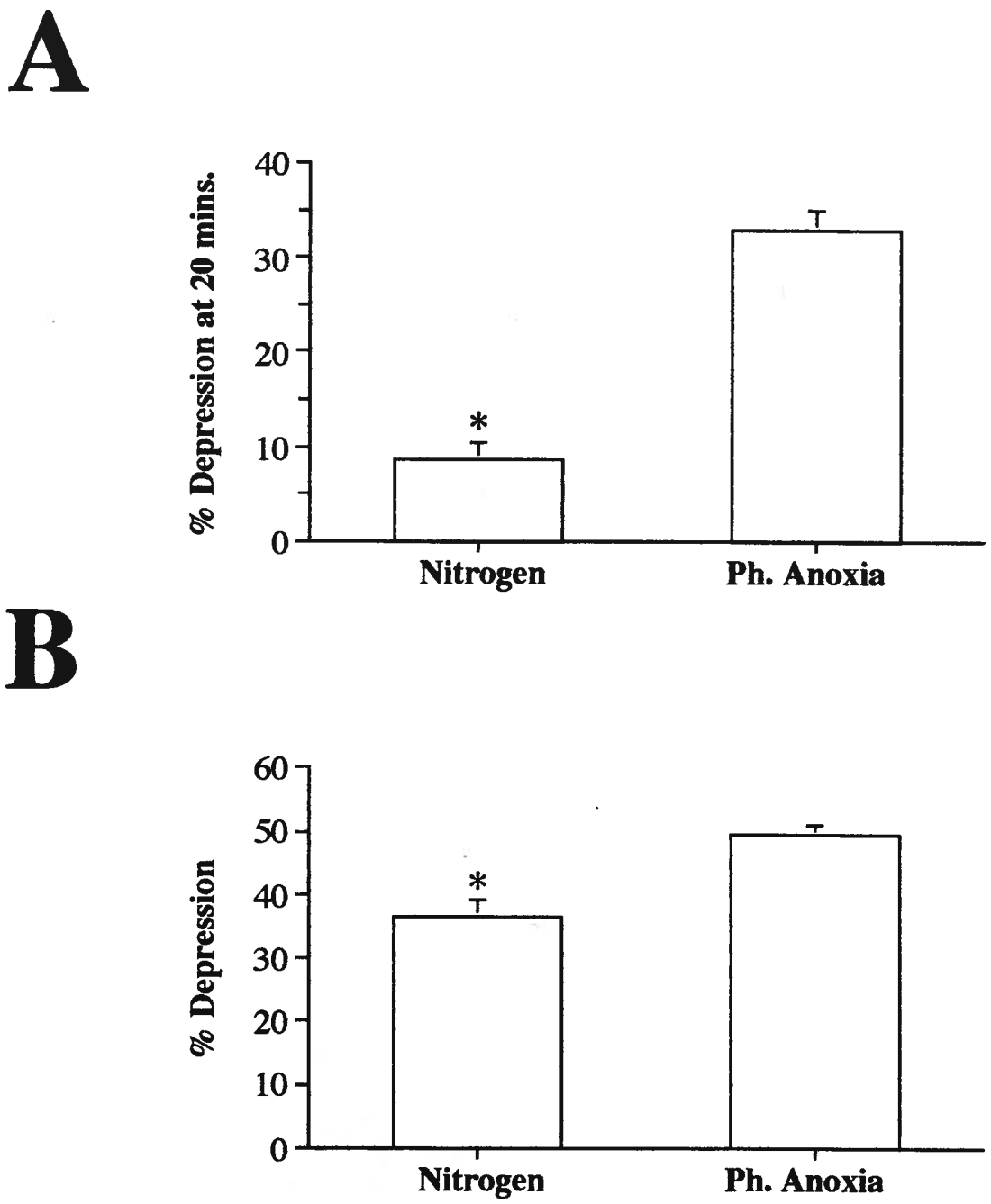

Figure 11. The average heat depression (percentage) relative to the predicted corresponding control value. (A) The heat depression at 20 minutes into the nitrogen perfusion or pharmacological (ph. anoxia) insult. (B) The average percentage of heat depression from the corresponding predicted control value at the end of the insult (120 mins). For both (A and B), values are derived from Fig. 10. An asterisk denotes a significant difference ($P \leq 0.05$, unpaired *t*- Test) from the corresponding treatment. See results for exact numbers. Data (nitrogen perfusion, n=4; pharmacological anoxia, n=3) are mean values ± SE.

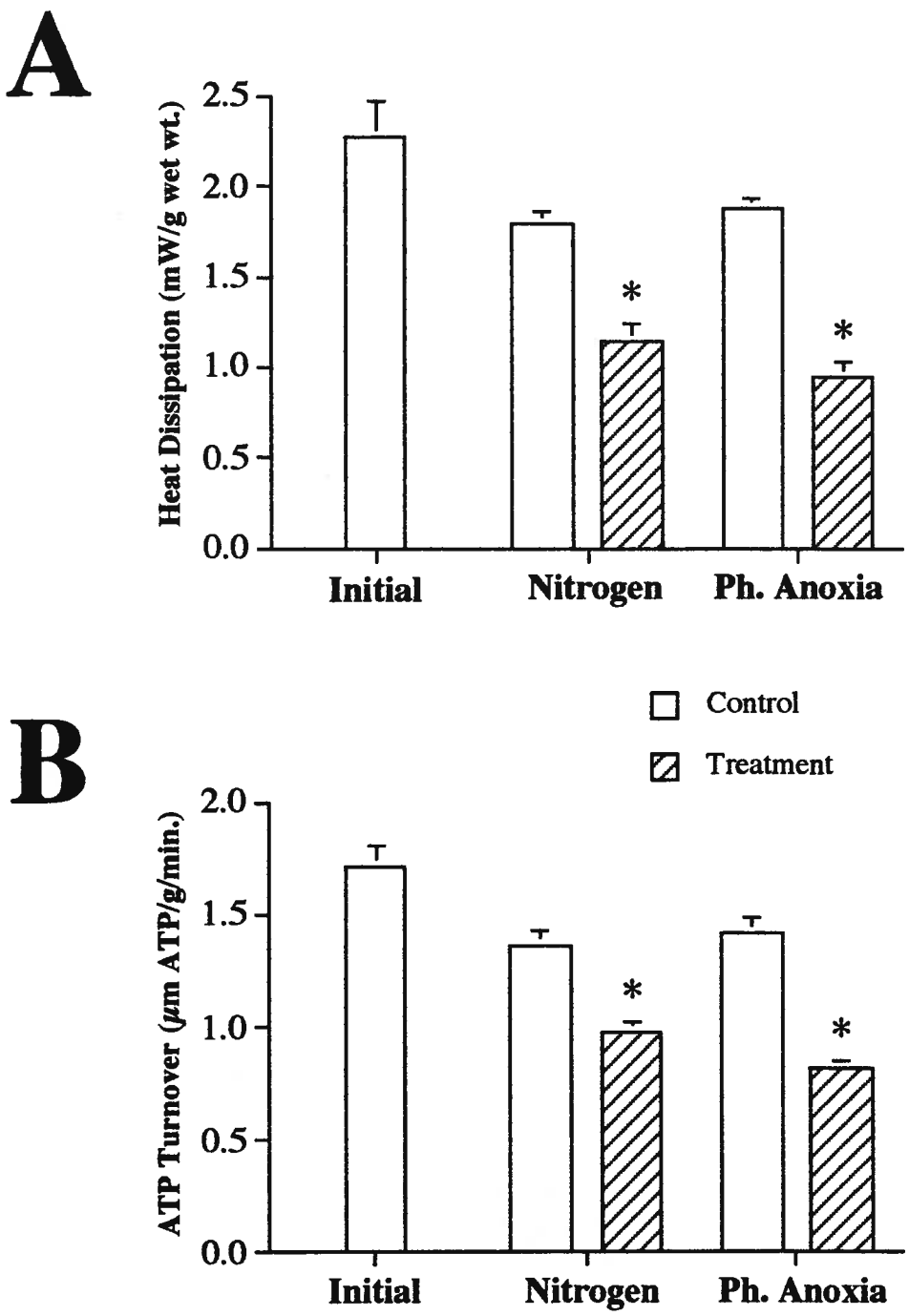

Figure 12. Effects of nitrogen perfusion and pharmacological anoxia on heat dissipation and metabolism (A and B respectively) compared to the corresponding predicted control value. The initial value in both (A and B) denotes the condition of the slice at the beginning of the experiment. In both figures, an asterisk denotes a significant difference from the corresponding control ($P \leq 0.001$; paired *t*-Test). The ATP turnover is calculated from A (see methods for further detail). Data (anoxia, n=4; pharmacological anoxia, n=3) are mean values ± SD.

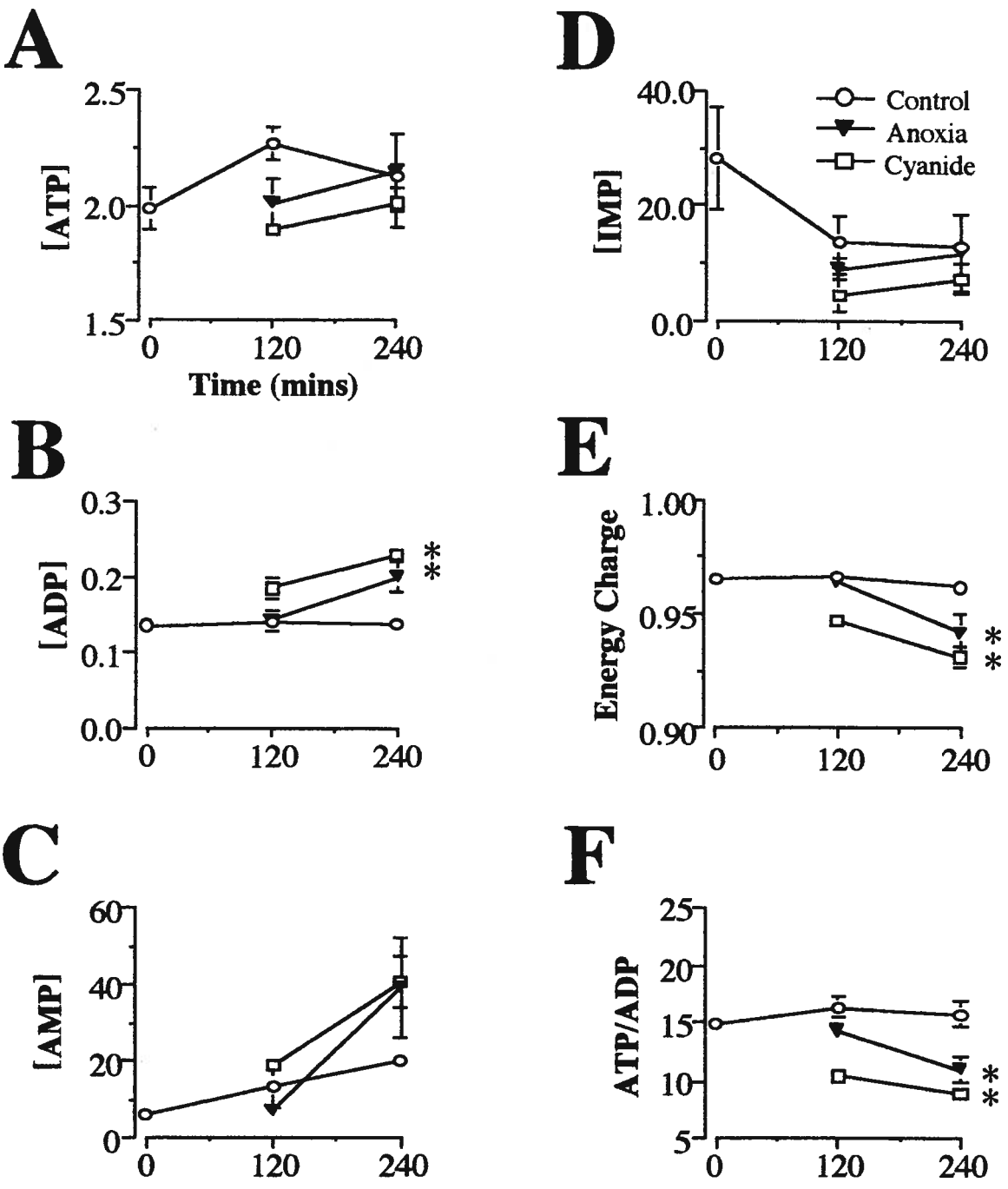

Figure 13. The effect of anoxia and pharmacological anoxia on adenylates, energy charge, and adenylate ratios for turtle cortical slices (25 ^{o}C). Time sequence in (A) and symbol definitions in (D) are the same for all graphs. An asterisk denotes a significant difference for that particular mean value compared to the corresponding control mean value ($P \leq 0.05$; Tukey HSD test). Data (n=4) are mean values ± SE. Concentrations are expressed as μmoles/g wet wt. (ATP; ADP) and pmoles /g wet wt (AMP; IMP).

Table 2. Enzyme activities in the cortex of the rat and turtle

Enzymes	Rat (37 °C)[a]	Turtle (25 °C)[a]	Turtle (37 °C)[b]
Hexokinase	25.7 ± 1.9	21.7 ± 1.2	43.4
Lactate Dehydrogenase	217.1 ± 14.6	177.2 ± 7.5	354.4
Citrate Synthase	60.9 ± 2.8	17.2 ± 0.4	34.4

[a]Values are means ± SE expressed in units of activity; $n = 6$.

[b]Values are mathmatically obtained from turtle (25 °C) values, assuming a Q_{10} of 2.

tended to drop slowly over the experiment, an initial control ATP turnover rate (1.72 ± 0.06^{SE} μmoles ATP/g/min; n = 7) was calculated for comparison to other experimental preparations.

Adenylates were measured in this experiment for two reasons. First, although some studies have been done on the whole turtle brain with respect to these metabolites, very little is known on individual tissue compartments in the brain and their changes with anoxia. Secondly, one assumption made in calculating ATP turnover directly from heat dissipation was that energy intermediates remain in steady state (Shick *et al.*, 1983). This information is important not only for the metabolic rate determination, but also as an indicator of the health of the tissue. ATP, ADP, and AMP showed no significant changes over the control data points ($P \leq 0.05$; Fig. 13a,b,c). The 240 minute [ADP] levels for both treatment groups were significantly higher compared to the corresponding control time point ($P \leq 0.05$; Fig 13b). IMP did not change significantly under control or treatment conditions ($P > 0.05$; Fig. 13d). Differences among adenylates exhibited higher statistical significance when expressed as energy charge (E.C.) or adenylate (ATP/ADP) ratios. Both anoxia and pharmacological anoxia produced significant differences in E.C. and ATP/ADP ratios at time 240 minutes compared to equivalent control values ($P \leq 0.05$ Fig. 13e,f).

Enzymatic Analysis

The results of the enzymatic study of turtle and rat cortical slices are illustrated in Table 2. At physiological temperatures, turtle (25 ^{o}C) and rat (37 ^{o}C), both species expressed approximately the same amount of enzyme activity for lactate dehydrogenase and hexokinase, but the turtle cortex expressed approximately 30% of the acitivity of the rat cortex for Citrate Synthase. When the results were normalized for temperature ($Q_{10} \approx 2$) the turtle brain expressed twice the activity of hexokinase and lactate dehydrogenase and only about 60 % of the activity for citrate synthase found in the rat cortex.

Discussion

There were four goals to this study: i) to measure adenylate pools during anoxia, ii) to establish a metabolic rate for the turtle cortical slice, iii) to establish whether the turtle cortical slice further depresses metabolism with simulated anoxia, and iv) to examine turtle cortical slices using both enzymology and calorimetry for evidence and capacity of a Pasteur effect.

Adenylates

The control concentrations reported here for all adenylates are similar to those reported in slices and whole brain *in vivo* (Kelly and Storey, 1988; Lutz, et al., 1984). Kelly and Storey (1988) reported that ATP tended to rise in the whole brain with anoxia, but our results in the cortical slice are similar to those of Bickler which reported no increase (Bickler, 1992a). Significant differences with anoxia did occur with respect to [ADP], adenylate ratios, and energy charge compared to the corresponding control time; however, these changes do not occur until 240 min. into the insult which is beyond the time course of the calorimetry experiments.

Normoxic Metabolic Rates

The higher metabolic rate for cortical slices (1.72 μmoles ATP/g/min; Fig. 12b), calculated from heat values of normoxic controls, was obtained at the beginning of each run, because heat dissipation tended to drop over the course of the experiment (Fig. 9a,b). The reason for this decrease is unknown, but presumable is due to degeneration of unhealthy cells. Interestingly, our initial value is very close to the turtle whole brain ATP utilization (assuming 36 ATP/glucose catabolized) of 1.9 μmoles ATP/g/min (Suarez, et al., 1989) based on deoxyglucose measures. The close agreement between the two independent studies suggests that the initial ATP utilization is an accurate assessment. Glucose consumption (initial) in guinea - pig cortex slices (37 ^{o}C) yields a value of 16 μmoles ATP/g/min when glucose consumption values are corrected for glycogen breakdown and lactate production (Rolleston and Newsholme, 1967b). This estimate indicates a 9.3 fold difference in

metabolic rate between the turtle and mammalian slice preparation consistent with our earlier whole brain deoxyglucose observation of a 12 fold difference (Suarez, et al., 1989). Additional support for the difference in metabolic rates between the turtle and the rat cortex can be seen in the measurement of citrate synthase (Table 2). The rat cortex (37 ^{o}C) expressed 3.5 times the activity compared to the turtle cortex (25 ^{o}C) supporting a larger aerobic flux rate in the rat cortex.

Anoxic Metabolic Rates

The nitrogen perfusion experiments indicate a reduction in heat dissipation in the turtle cortex during O_2 deprivation. The resulting ATP utilization estimates indicate that the turtle cortex depresses metabolism between 30% (nitrogen) and 42% (pharmacological anoxia) during O_2 limitations. Estimates from lactate accumulation studies with whole brain as well as whole brain slices suggest a larger (> 80%) metabolic depression (Kelly and Storey, 1988; Lutz, et al., 1984; Robin, et al., 1979). While our estimates do not support this degree of depression in the cortex, the data clearly show a significant metabolic reduction.

The discrepancies between previous *in situ* studies and the current *in vitro* study may be partially explained by the absence of spontaneous electrical activity in the bran slice preparation. Current evidence suggests that one mechanism for turtle brain metabolic depression in the *in vitro* is reduction of spontaneous electrical activity (Lutz, 1992). Brain slices consume approximately 50% less oxygen than the intact tissue (Lipton and Whittingham, 1984). This discrepancy has been attributed to the loss of spontaneous electrical activity in the tissue slice (McIlwain and Bachelard, 1971). This hypothesis is supported by the observations that tetrodotoxin (voltage-gated Na^{+}- channel blocker) causes only a 5% reduction in oxygen consumption *in vitro*(Okamoto and Quastel, 1972), but barbiturate anesthetics (electrical activity depressants) do inhibit oxygen consumption by 50% in the intact brain (Siesjo, 1978). The absence of significant amounts of spontaneous electrical activity in the turtle cortical slice may cause a reduced metabolic depression compared to the *in vivo*. The lack of electrical activity in the slice combined with the large

metabolic depression observed in the present study would suggest that other metabolic processes are being depressed besides electrical activity.

Anoxic Gap

In some organisms, the anoxic heat dissipation does not match indirect measures of metabolism (heat dissipation can exceed measured end product formation by as much as 50%) (Gnaiger, 1980; Shick, et al., 1983). Several reasons suggest a negligible "anoxic gap" for our turtle cortical slice preparation (Hardewig *et al.*, 1991; Shick, et al., 1983): i) adenylate levels were fairly constant, ii) all experiments were short duration, iii) use of cyanide + N_2 minimized any oxidative metabolism, and iv) the 1:2 matching of glucose consumption and lactate production in whole brain slices of anoxic turtles indicating no other glucose catabolic pathways during anoxia (Robin, et al., 1979). Based on glucose consumption and lactate production, turtle whole brain slices yield an anoxic ATP utilization rate of 0.88 μmoles ATP/g/min (Robin, et al., 1979) which is almost identical to the .82 μmoles ATP/g/min reported in this study suggesting that our estimation of the anaerobic cortical slice metabolic rate is accurate assessment. It is important to note, however, that if such a gap does exists in our preparation, this discrepancy would increase the difference between control and anoxic ATP utilization.

Glycolysis

In the calculation of ATP turnover, we have assumed that the slices are fully aerobic or fully anaerobic. Aerobic brain tissue generally has an anaerobic component (Robin, et al., 1979; Rolleston and Newsholme, 1967b). Additionally, as a tissue enters an anoxic transition, there is a shift from aerobic to anaerobic metabolism making metabolic calculations difficult (Gnaiger and Kemp, 1990). However, for our tissue, because the theoretical amount of heat dissipated per mole of ATP consumed is similar between aerobic and anoxic conditions (0.76 and 0.86, respectively; see methods), the error associated with assuming the tissue is totally aerobic or anaerobic is small ($\approx$ 12%). Consequently, we

conclude that heat dissipation along the experimental curves (Fig 9a or b) approximates changes in ATP turnover fairly closely.

Under conditions of pharmacological anoxia, the insult is rapid. The mixture of N_2 + cyanide minimizes any oxidative metabolism in the transition phase giving an accurate anaerobic metabolic picture. As a result, the percent depression by 20 minutes for pharmacological anoxia is significantly greater than for nitrogen perfusion (Fig 11a). Because adenylates through pharmacological anoxia are reasonably constant (indicating glycolytic ATP supply is matching cellular ATP demands; Fig 13) and because the total inhibition of oxidative metabolism, the heat dissipation curve reflects both metabolic rate changes and glycolytic changes. Hence, changes in heat flux during pharmacological anoxia represent changes in both the metabolic rate and the glycolytic rate. Four possible anoxic transition scenarios are illustrated in Fig. 14. A 12% drop in heat dissipation with the insult would be indicative of no metabolic depression in the slice due to the difference between aerobic and anaerobic ATP/mW heat production (see methods), and also would be indicative of a large Pasteur effect (Fig. 14a). Note that this 12% would be a theoretical maximum and assumes that the control heat measure is 100% oxidative. A more likely scenario is the gradual decline of heat dissipation, and thus, metabolic rate indicating a gradually declining Pasteur effect (Fig 14b). A biphasic transition into pharmacological anoxia would be an indicator of both a sustained, but depressed metabolic rate and Pasteur effect during the biphasic plateau of the curve (Fig. 14c). A rapid transition into a large heat flux depression would be indicative of a large metabolic depression which is most likely accompanied by a slight or reversed Pasteur effect. Note that due to the catabolic heat production from glucose (140 kJ/mole, anoxia vs. 2820 kJ/mole, aerobic), heat flux would have to drop to $\approx$ 5% of control measures before a reversed Pasteur effect would occur. However, this measure again represents a theoretical value which assumes that the control heat production is 100% aerobic. Kelly and Storey have suggested that the turtle brain goes through a biphasic transition into anoxia (Kelly and Storey, 1988). In the first phase, the glycolytic activation

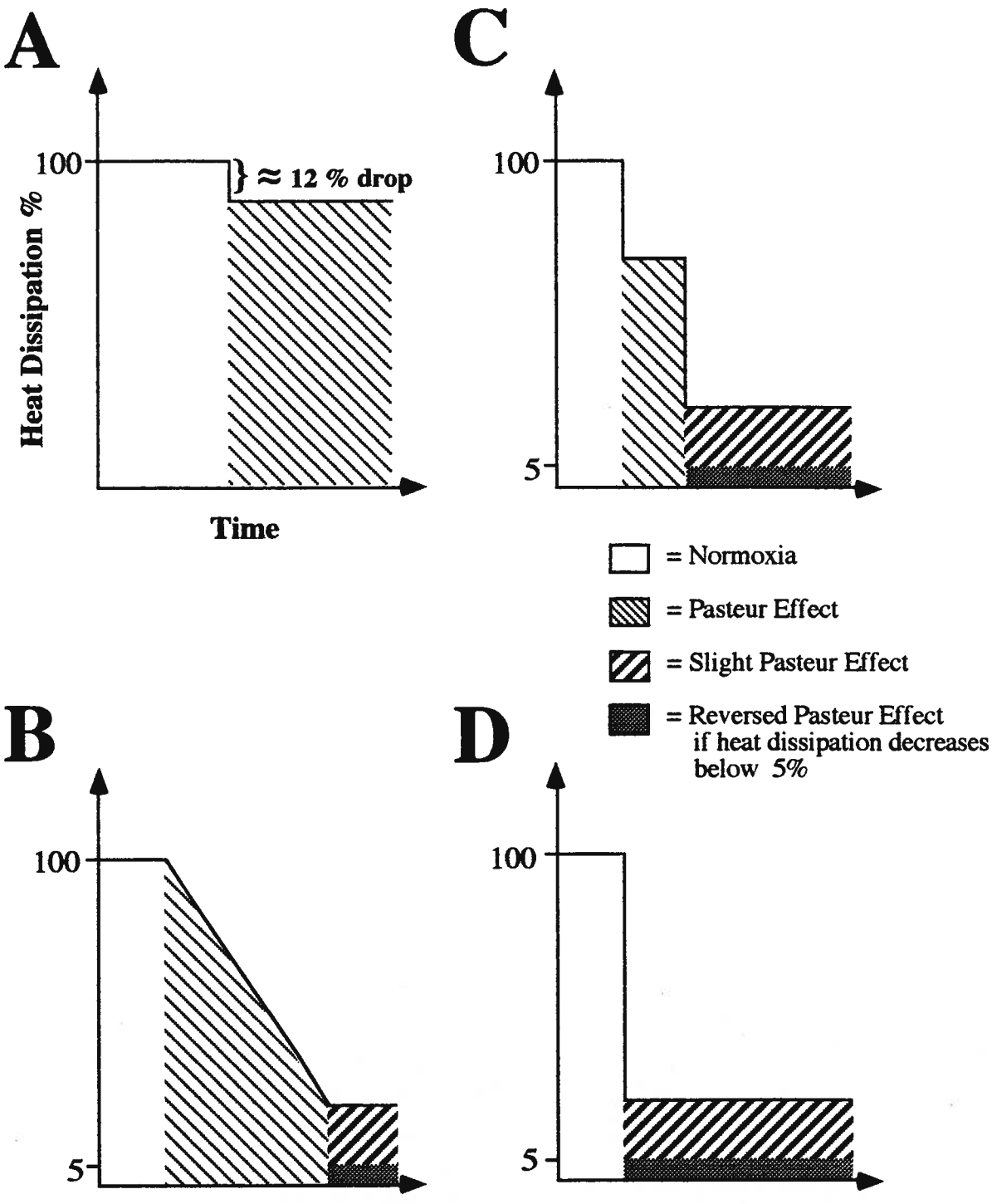

Figure 14. Four possible scenarios for the response of cortical brain slices to pharmacological anoxia(see text for further details).

occurs to maintain ATP concentrations. As the brain reduces its metabolism, glycolysis can return to normal or reduced rate (reversed Pasteur effect). All pharmacological cases appear to conform to a combination of 3 of these scenarios. There is initially a very rapid drop in heat dissipation similar to Fig. 14d which plateaus for ≈ 10 minutes similar to Fig. 14c. At this plateau point, the average heat dissipation for all three cells was ≈ 77% of control indicating a 15.5 fold Pasteur effect which gradually dropped similar to Fig. 14b. Based on the final heat dissipation measures for all three pharmacological anoxia cases (49 % of control) the final Pasteur effect would be 10.3 fold at 120 minutes of anoxia. Thus, the anoxic data support an initial large Pasteur effect which is gradually declining over the insult..

Enzymatic Analysis

The correlation of both hexokinase and lactate dehydrogenase with glycolytic flux rates has been documented (Hochachka and Somero, 1984). One reason why maximal enzyme activity can be compared usefully *in vitro* is because there is a potent conservation of catalytic turnover of substrate for homologous enzymes in vertebrates (Hochachka and Somero, 1984). The enzyme activities reported in Table 2 indicates that the turtle cortex at 25 ^{o}C has an equal activity as the rat cortex at 37 ^{o}C. When activities are corrected for temperature (Q10 ≈ 2), the turtle brain exhibits twice the glycolytic capacity which supports a relatively enhanced glycolytic capacity in the turtle cortex compared to the rat cortex.

Two additional mechanisms deserve mention with regards to glycolytic capacity in the turtle. Recent studies have indicated covalent modification of glycolytic enzymes during anoxia through reversible incorporation of phosphate into proteins. This modification can produce rapid changes in the expressed activity of cellular enzymes and possible influence there association with certain cellular or subcellular components (Brooks and Storey, 1989). Glycogen phosphorylase, phosphofructokinase, and pyruvate kinase were shown to be modulated during anoxia in the turtle such as to increase activity. Additionally, in brain, hexokinase, phosphofructokinase, and phosphoglycerate kinase were all shown to bind to

subcellular components(Duncan and Storey, 1992). The resulting positioning is believed to channel ATP to critical areas such as ion pumps.

Conclusion

Data presented give strong evidence for the maintenance of adenylates during anoxia in the turtle brain. The low metabolic rate combined with the ability to further suppress metabolism during anoxia undoubtedly plays a critical role in allowing the cell to maintain energy balance during anoxia. However, at least on the short interim, the ability to increase glycolytic flux (Pasteur effect) combined with increased glycolytic machinery appears also to play an important role. The end result of all of these adaptations is that cellular ATP supply can meet demands even when ATP production is substantially inhibited by an anoxic episode. The reader is refereed to chapter 5 where a more complete discussion of these issues are presented.

CHAPTER 4: A CRITICAL TEST OF CHANNEL ARREST

Preface

In the previous chapter, calorimetric measures supported both a low normoxic metabolic rate and the ability to further depress metabolism during anoxia in the turtle cortical slice. This chapter explores the concept of reduced ion leakage as a mechanism for metabolic depression in the turtle cortex during both normoxia and anoxia. This chapter is excerpted (in part) from the papers C. J. Doll, P. W. Hochachka, and P. B. Reiner (*Am. J. Physiol.* 261: R1321-R1324, 1991) and C. J. Doll, P. W. Hochachka, and P. B. Reiner (*Am. J. Physiol.*, In Press). The enzymatic measures were adapted from R. K. Suarez, C. J. Doll, A. E. Buie, T. G. West, G. D. Funk, and P. W. Hochachka (*Am. J. Physiol.* 257: R1083-R1088, 1989).

Introduction

If energy status is to be sustained in the turtle brain during anoxia, supply must meet demand. Three basic mechanisms in principle could aid in the maintenance of energy balance during anoxia assuming the tissue is not substrate limited: (i) enhanced glycolytic capability to aid in the supply of ATP to the cell, (ii) low normoxic metabolic rate to lessen the initial ATP demand of the brain (Chapter 3), (iii) metabolic depression during anoxia to further accentuate a low normoxic metabolic rate.

With respect to (i) and (ii) above, we have demonstrated that the turtle brain expresses twice the glycolytic capability of the rat brain while consuming only 1/9 to 1/12 the glucose under control (normoxic) conditions (Suarez, et al., 1989; Chapter 3). Additionally, earlier indirect estimates implied that the metabolic rate of the turtle brain appears low compared to other ectotherms (McDougal, et al., 1968). With regards to (iii), significant anoxic metabolic depression has been estimated in both whole brain preparations (Kelly and Storey, 1988; Lutz, et al., 1984), as well as in slices (Robin, et al., 1979; Chapter 3).

Two of the three protective mechanisms outlined above concern a reduced cellular metabolic rate. However, the question remains as to what ATP requiring processes are being suppressed in both normoxia and anoxia to account for lowered ATP turnover. It has been

hypothesized that one mechanism which could reduce energy expenditure in turtle brain would be to decrease ATP-dependent ion pump activity by reducing ion leakage (Hochachka, 1986).

All cell membranes leak ions. Leakage is the result of both intracellular and extracellular ions flowing down their electrochemical gradients. Several cellular processes contribute to this phenomena in neurons including activation of voltage- and ligand- gated channels, neurotransmitter release and uptake, co- and counter- transport systems, and leakage channels (voltage independent ion channels) (Hille, 1992). Maintenance of a homeostatic intracellular environment requires the redistribution of these ions through the use of energy demanding pumping systems such as the Na^{+}-K^{+}-ATPase which may consume as much as 50% of the cell's resting metabolic rate (McBride and Milligan, 1985). One mechanism by which the turtle brain could reduce its metabolism would be to reduce ion leakage (Hochachka, 1986; Lutz, et al., 1985), which could conceivable occur through the reduction of any of the above leakage processes.

The concept of regulating cell metabolism through regulation of ATP-dependent ion pump activity is not new (Whittam and Blond, 1964) and has been forwarded as a possible mechanism for the action of thyroid hormone in controlling thermogenesis (Ismail-Beigi and Edelman, 1970). This idea was later expanded as a mechanism contributing to the origin of endothermy (Edelman, 1976). The hypothesis predicts that endotherms have leakier membranes, and thus increased ATP dependent ion pump activity serving as an indirect mechanism of heat production. A similar concept involving regulation of ion pumping by the Ca^{+2} -ATPase is believed to account for thermogenesis in marlin heater tissue, a modified muscle which displays an expanded sarcoplasmic reticulum but has little contractile protein (Block, 1987). Taken together, this evidence provides strong support for the idea that regulation of leakiness, and hence, ion pump activity, could regulate ATP turnover in the cell.

This paper tests two predictions of such a 'channel arrest' hypothesis (Hochachka, 1986; Hochachka, 1987). First, do turtle cortical pyramidal neurons display lower passive ion leakage (conductance) compared to the rat cortical pyramidal neurons during normoxia, and second, are leakage channels in the turtle pyramidal neuron further down regulated during both long and short term anoxia as a potential survival strategy.

Methods

General

Methods for data acquisition, tissue preparation, and fluid composition for intracellular recording techniques were identical to those described in chapter 2, pgs. 3-4. Notable exceptions of patch clamping techniques and data analysis in general are described below. The reader is referred to Appendix A and B for a more general discussion of these techniques and terminology.

Patch Clamp Tissue Preparation

Young Wistar rats (25 - 40 g) were anesthetized with halothane decapitated and the brain rapidly removed and immersed in precooled oxygenated aCSF. After a few minutes of precooling, a block containing frontal - parietal cortex was dissected free, glued with cyanoacrylate to a mounting block and sliced (400 μM thickness) on a vibratome. Slices were stored at $\approx$ 22 ^{o}C for at least 60 min. prior to use.

Patch Clamping Techniques

Methods for the formation of whole cell seals in slices of both turtles and rats have been described in detail elsewhere (Blanton, et al., 1989). A general discussion can be found in appendix A. In brief, whole cell patch recordings were carried out using sutter 1.5 O.D. X 1.10 I.D. boro silicate non filament glass. Electrodes were pulled on Sutter model P-15 horizontal puller. Patch solution contained (in mM) 15 NaCl, 110 KOH (pHed to 7.4 , titrated with Methanesulphonic Acid), 10 Na^{+} Hepes, 11 EGTA (dissolved in 29 mM KOH), 1 $CaCl_2$, 2Mg-ATP, 0.3 GTP, final pH = 7.4, for the rat. Turtle patch solution was the rat

patch solution diluted by 10%. The osmolarity of the patch solution was 320 - 330 mosmol / Kg rat; 290 - 300 mosmol / Kg turtle.

Data were acquired using an Axoclamp 2A amplifier connected to an Axolab 1100 interface, which also served to generate current commands using the Pclamp suite of programs. Data were also independently digitized at 49 kHz and stored on videotape for off-line analysis. Criteria for using a patched cell included the GΩ seal, positive going action potentials, and electrode impedance ≤ 45 MΩ (most were less than 20 MΩ) at the completion of the experiment. Although some cells were held for up to 3 hours, changes in cell conductance generally occurred within 30 to 45 minutes after breaking into the cell. All measurements were made within 10 minutes of obtaining the whole cell configuration.

Data analysis

Whole cell conductance (G_W) and time constant (T_C) were calculated using depolarizing current pulses of 500 mS duration (turtle) or 200 mS duration (rat) sufficient to elicit 6.2 ± $0.9^{(SE)}$ mV change in membrane potential from the resting potential of the cell. All measures were done on cells in a quiescent state to minimize leakage due to electrical activity. In brief, G_W was calculated from Ohm's law:

$$V_m = I / G_W$$

where V_m is the change in membrane potential and I is the current. T_C was calculated by fitting the membrane charging curve to the equation:

$$Y = A_0 + A_1 e^{-t/T_C}$$

where Y is the voltage at any given time t, A_O is the offset, and A_1 is the maximum voltage, using the Clampfit feature of Pclamp. Specific membrane conductance (G_m) was calculated from the equation:

$$T_C = C_m / G_m$$

where C_m is the capacitance of the membrane per unit area which is assumed to be 1 μF / cm^2. All computer fits of membrane charging curves showed a 0.9900 least squares residual (R) value or they were rejected.

The term Q_{10} is used to refer to the effect of a 10 ^{o}C temperature change on the values being measured, and for the purpose of this paper, it is defined as:

$$\mathbf{Q_{10} = Value\ (x + 10\ ^{o}C)\ /\ Value\ (x\ ^{o}C)}$$

where x is the variable being tested.

Na^{+}-K^{+}-ATPase Activity

Methods for tissue dissection were identical to those described in Chapter 3 for the enzymatic analysis. Once the brain was dissected free, the cortex was removed and placed in 9 volumes of 50 mM Tris-Cl (pH 7.4 at 4 ^{o}C) which contained 0.1 mM phenylmethylsulfonylfluoride. Tissue was homogenized 3 times, 10 sec. each interval with 30 sec. in between each interval. Crude homogenates were then assayed for Na^{+}-K^{+}-ATPase activity without further processing.

In brief, K^{+} dependent *p* nitrophenylphosphate hydrolysis is an expression of Na^{+}-K^{+}-ATPase activity (Swann and Albers, 1975). This indicator is used to circumvent problems associated with competition of ATP utilization characteristic of crude tissue homogenates containing mitochondria. Final incubation mixture contained 0.05 M Tris-HCl, pH 7.5, 5 mM $MgCl_2$ 10 mM Tris-*p*-nitrophenylphosphate, about 20 μg of brain homogenate. Reactions were conducted in duplicate in a final volume of 0.2 ml at 25 ^{o}C. Assays were done in the presence of either 25 mM KCl or 1 mM ouabain (control). Reactions were terminated by the addition of 0.8 ml of 0.1 N NaOH. Final concentration (*p*-nitrophenol) after incubation period (10 min.) was determined spectrophotometrically by absorption at 410 nm.

Results

Data presented (intracellular and patch clamp methods) are based upon recordings of (n = 38) turtle and (n = 20) rat pyramidal neurons resulting in a total of 58 cells being tested. Each patch clamp group represents an n of 10 recordings and the intracellular group represents an n of 8 repeatedly measured cells. No neurons were repeatedly used for any

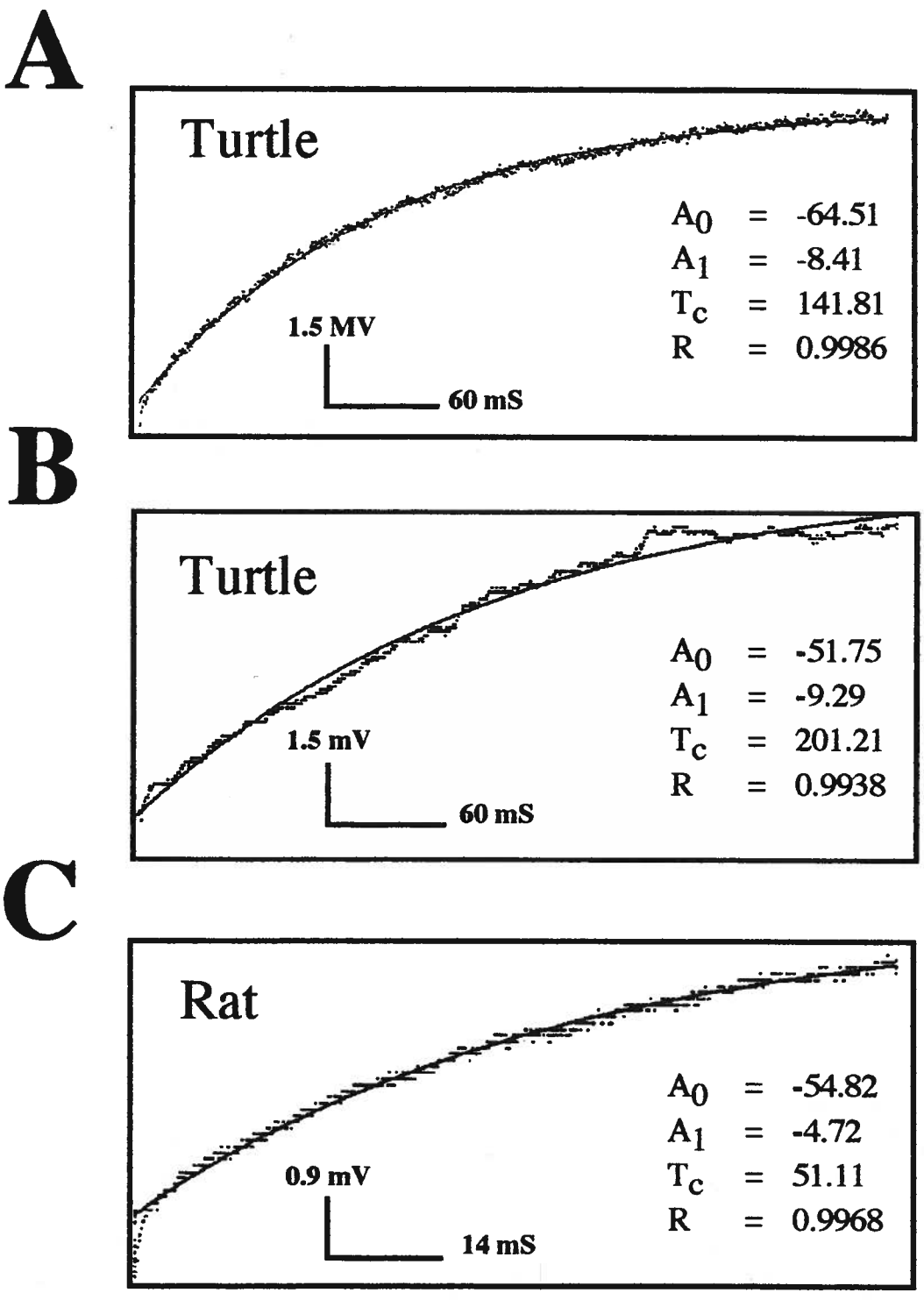

Figure 15. Examples of membrane charging curves for turtle and rat pyramidal neurons. Turtle neurons (25 ^{o}C)are represented in (A), intracellular recording techniques and (B), patch clamp techniques. A rat pyramidal neruon (25 ^{o}C)is represented in (C) using patch clamping techniques. Refer to methods for a complete discussion of the fitting procedures and analysis.

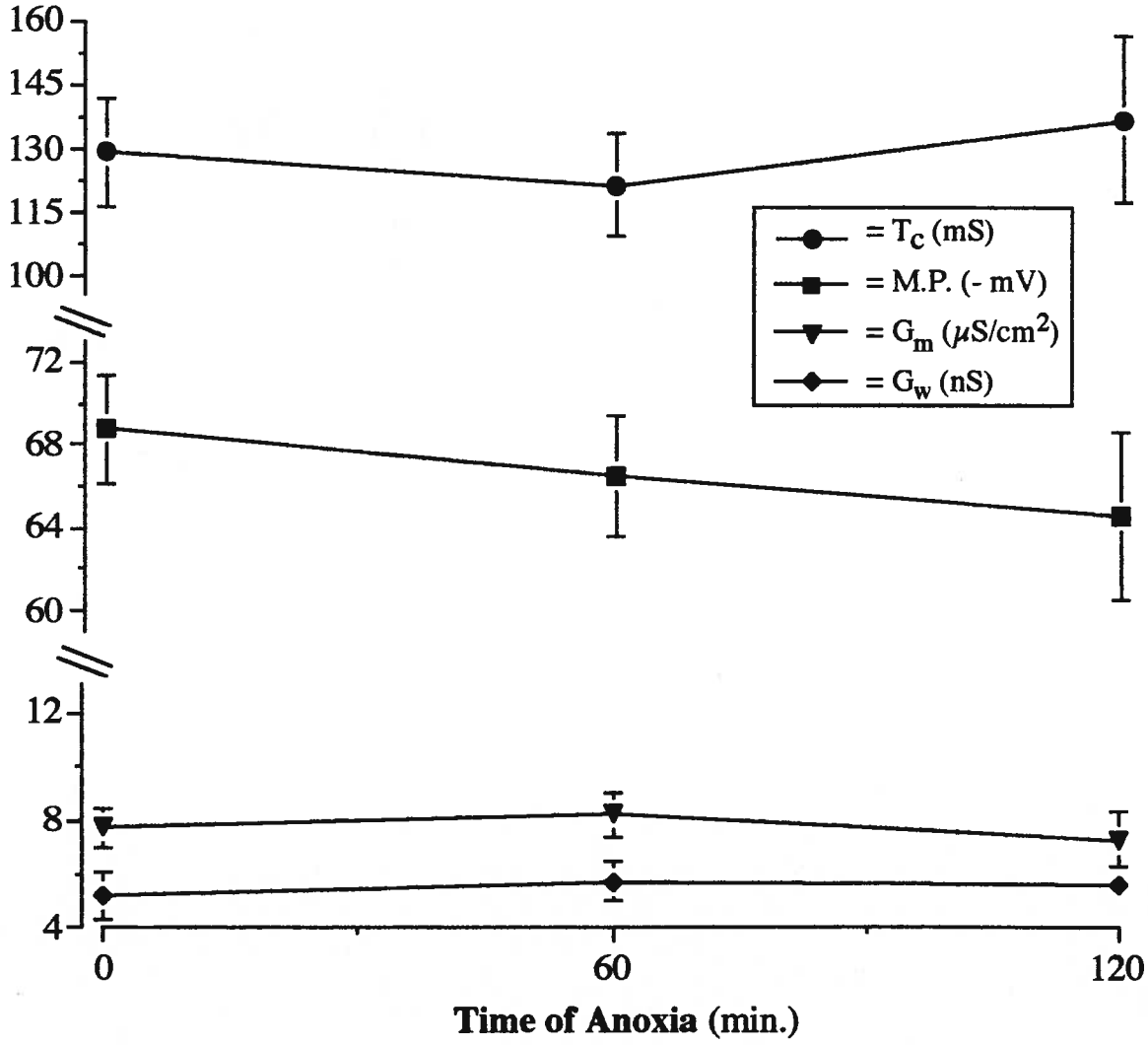

Figure 16. Conductance and membrane potential changes with anoxic exposure. Whole cell conductante (G_W) was calculated from Fig. 17 while specific membrane conductance was calculated from the time constant (T_C) of the membrane charging cureve. Membrane potential (M.P.) was also recorded for the duration of the experiments. See text for further figure details. Data illustrated are means of $n = 8$ pyramidal cortical neurons from turtle. Data are illustrated with SE bars.

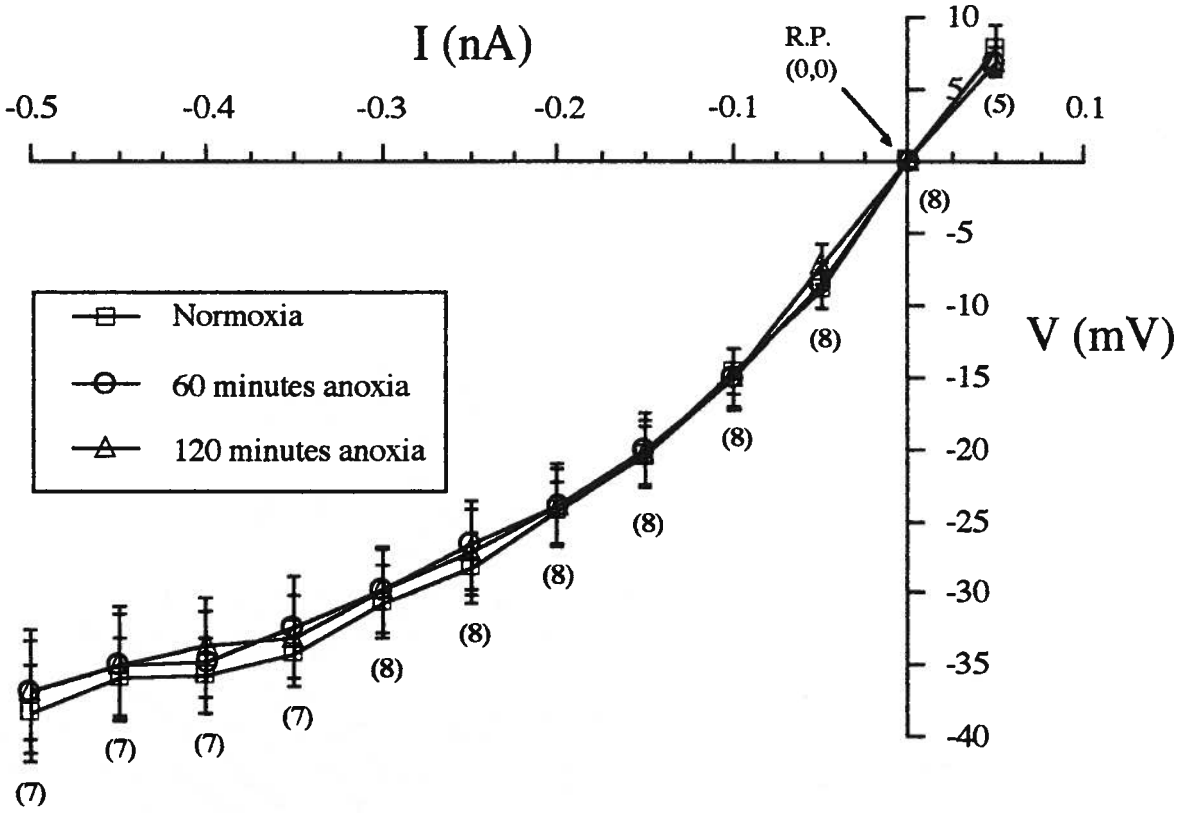

Figure 17. Current (I)-voltage (V) plotfor 8 repeatedly measured turtle pyramidal neurons over a time course of 120 min. of anoxia (0.1 to -0.5 by 0.05 nA steps). Numbers in parentheses are *n* of cells for that point set. Data are illustrated with SE bars. The axies cross at the cell's resting potential (R.P.)

Table 3. Turtle cortical pyramidal cell patch clamp values

	Normoxia		Normoxia		Anoxia[a]	
	n	15 °C ± SE	*n*	25 °C ± SE	*n*	25 °C ± SE
Parameter						
M.P. (mV)	10	-75.0 ± 1.0[d]	10	-72.8 ± 0.5[d]	9	-74.0 ± 2.5[d]
G_W (nS)	10	1.84 ± 0.21[bc]	10	2.73 ± 0.36[c]	10	2.35 ± 0.21[c]
T_C (mS)	10	423.5 ± 28.4[bc]	10	200.7 ± 19.3[c]	10	209.3 ± 23.5[c]
G_m (μS / cm^2)[e]	10	2.46 ± 0.17[bc]	10	5.56 ± 0.67[c]	10	5.37 ± 0.61[c]

[a] Turtle cortical slices were held in an anoxic chamber at ≈ 22 °C for 6 - 9 hrs. prior to recording

[b] Significantly different (P≤ 0.05; Newman - Keuls test) from the control (25 °C) measure.

[c] Significantly different (P ≤ 0.05; Newman - Keuls test) from rat (35 and 25 °C) cortical values (Table 2).

[d] Significantly different (P ≤ 0.05; Tukey HSD test) from rat (35 and 25 °C) cortical values (Table 2).

[e] Assuming a 1 μF / cm2 capacitance.

Refer to text or Table of Abbreviations for an explanation of table abbreviations.

Table 4. Rat cortical pyramidal cell values

	n	25 °C ± SE	*n*	35 °C ± SE
Parameter				
M.P. (mV)	8	-57.5 ± 2.9[d]	10	-55.4 ± 1.3[d]
G_W (nS)	10	4.08 ± 0.57[c]	10	7.56 ± 1.00[bc]
T_C (mS)	10	46.5 ± 4.4[c]	10	25.0 ± 2.0[bc]
G_m (μS / cm^2	10	23.5 ± 2.4[c]	10	42.4 ± 3.5[bc]

[a] Assuming a 1 μF / cm2 capacitance

[b] Significantly different ($P \leq 0.05$; independent t test) from the 25 °C value

[c] Significantly different ($P \leq 0.05$; Newman - Keuls test) from turtle (15 and 25 °C) cortical values (Table 1)

[d] Significantly different ($P \leq 0.05$; Tukey HSD test) from turtle (15 and 25 °C) cortical values (Table 1)

Please refer to Table of Abbreviations or text for an explanation of table abbreviations

Table 5. Effect of temperature on membrane ion leakage

	Turtle 15 - 25 °C	Rat 25 - 35 °C
Measured Q_{10}		
G_m	2.3	1.8
G_w	1.5	1.9
Average	1.9	1.9

Values obtained from Tables 3 and 4

Refer to Table of Abbreviations or text for an explanation of table abbreviations

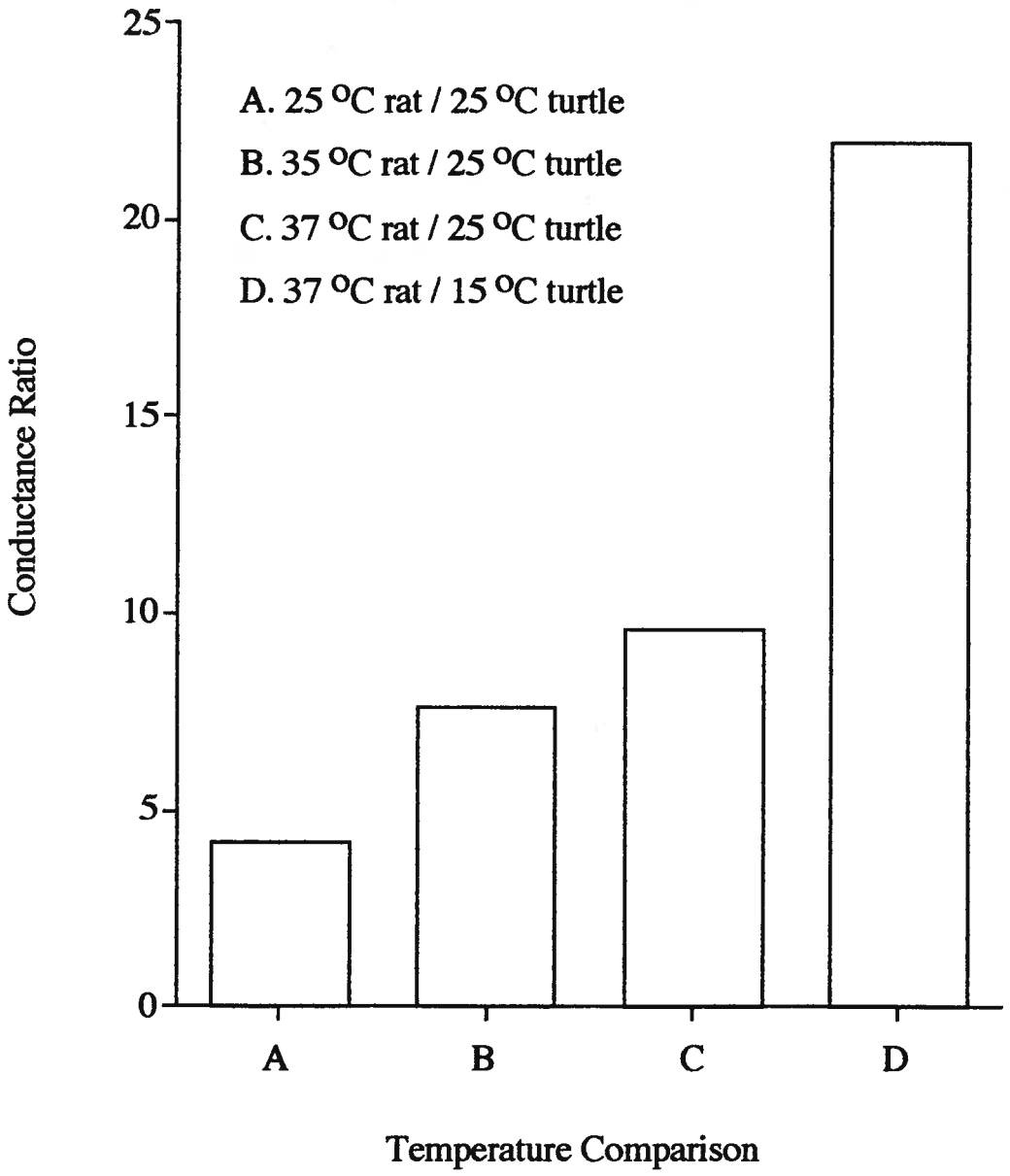

Figure 18. Conductance ratios (G_m) for rat cortical pyramidal neurons vs. turtle cortical pyramidal neurons. Values are obtained from Tables 3 and 4 except for the rat 37 °C value which is calculated fro the rate 35 °C assuming a Q_{10} of 1.9 (Table 5).

Table 6. Na^+-K^+-ATPase activity in Turtle and Rat Cortex

	Turtle μmoles/g/min	Rat μmoles/g/min	Magnitude Difference
Temperature			
25 °C	3.52 ± 0.12	8.03 ± 0.54	2.3[a]
37 °C	----------	19.3[c]	5.5[b]

[a] Rat 25°C / Turtle 25 °C

[b] Rat 37 °C / Turtle 25 °C

[c] Assuming a Q_{10} of 2

patch clamp group. Examples of raw data traces (of which both G_m and G_w were derived) are illustrated by Fig. 15a,b,c.

Intracellular Recording

We tested whether ion channels were down regulated with anoxia (≤ 120 min.) using intracellular recording methods. This method allowed the continuous monitoring of G_m , T_c , and G_w. Results demonstrated that the turtle pyramidal neuron did not significantly change in any measured parameter (T_c, G_m, G_w, M.P.) with anoxia ($P > 0.05$; repeated measures design over time, tested for linear or quadratic fit). Two separate measures of conductance were performed, G_w and G_m (Fig. 16). G_w indicates the conductance of the whole cell. If the area of the cell were known, conductance per unit area could be calculated (G_m). Surface area of the cell is unknown, but G_m can be derived through a simple equation (see methods). The calculation is based on a 1 $\mu F/cm^2$ capacitance of the membrane.

A third observation of anoxic changes in resistance is obtained through the current - voltage plot (Fig. 17). The slope of the line represents voltage - dependent changes in R_w (whole cell resistance; $1/R_W = G_W$). As can be seen in Fig. 17, the voltage dependence of G_w does not significantly change over the course of 120 min. of anoxia ($P > 0.05$, repeated measures design over time, tested for linear or quadratic fits). Thus, neither steady state nor voltage - dependent G_w change during anoxia.

Patch Clamp Results

Intracellular recording methods were used for short term anoxia studies because it allowed the continuous impalement of a cell, and thus, continuous monitoring of G_m or G_w . However, based on previous experiments, we have found that continuous impalement will not yield accurate results after several hours due to eventual electrode clogging or degeneration of the cell. Thus, the use of whole cell patch clamp methods to compare populations was used. The relevant electrophysiological properties of these populations are detailed in Tables 3 and 4. To assess differences in ion leakage between turtle and rat cortical neurons, G_m was calculated for both species at 25 ^oC. Conductance values indicate

a 4.2 fold higher G_m in the rat neuron compared to the turtle. Comparison of conductance at more physiological temperatures (35 °C, rat; 15 °C, turtle) indicated a 17 fold increase in G_m for rat pyramidal neurons. Although not directly measured, G_m for the rat neurons at physiological temperature (37 °C) was inferred from the measured conductance Q_{10} of 1.9 (25 - 35 °C, Table 5). The calculated G_m at 37 °C for the rat neuron was 53.58 μS / cm^2 indicating a 22 fold more conductive membrane for the rat pyramidal neurons compared to turtle pyramidal neurons (15 °C). The conductance ratios between turtle and rat pyramidal neurons are summarized in Fig. 18.

To assess whether ion leakage further decreases with prolonged anoxia, turtle slices were incubated in anoxic aCSF for 6 - 9 hours. Two separate and independent measures of conductance were done (G_w and G_m) for reasons discussed above. The results reported in Table 3 indicate no significant change in G_w or G_m with 6 - 9 hrs. of anoxia supporting and extending intracellular recording results.

Current evidence indicates that anoxic survival of the turtle is highly temperature dependent (Ultsch, 1985). One question which remains unanswered is whether turtle neurons express a large Q_{10} value for ion conductance at lower temperatures. Table 5 summarizes the Q_{10} values for conductance in turtle and rat cortical neurons. Surprisingly, an average Q_{10} of 1.9 was measured for both turtle (15 - 25 °C) and rat (25 - 35 °C). These results indicate that Q_{10} for leakage channels may be conserved across various temperature regimes as well as species.

Interestingly, temperature did not significantly change membrane potential in either the rat or turtle cortical cell populations even though conductance of these cells is changed (Table 1 and 2). Additionally, one might suspect a change in membrane potential if ion channels were down regulated during anoxia. However, there were no significant changes in membrane potential with anoxia, in turtle cortical neurons supporting the findings of no change in either G_m or G_w with anoxia.

Na^+-K^+-ATPase Activity

In order to differently address the concept of lower resting ion leakage in the turtle brain compared to the rat during normoxia, Na^+-K^+-ATPase maximal activity was measured. Because this method uses an artificial substrate (p-nitrophenylphosphate), the results should be interpreted not as absolute values, but values relative to each other. Table 6 illustrates the Na^+-K^+-ATPase activity in cortical homogenates of both the turtle and the rat. The results suggested that there is about a 2.3 fold lower activity in the turtle brain compared to the rat at 25 ^oC. When corrected for temperature (Q_{10} of 2) for the rat brain (37 ^oC), the data indicated a difference of 5.5 fold compared to the turtle cortex (25 ^oC). These results further support the patch clamp recordings of lower ion leakage, and hence, ion pumping requirements in the turtle cortex.

Discussion

The channel arrest hypothesis is based on the premise that as the conductance of a cell (G_m) increases so must the rate of ion pumping if ion homeostasis and membrane potential are to be maintained. This prediction is experimentally supported (Pastuszko *et al.*, 1981; Scott and Nicholls, 1980). The concept can be applied not only to anoxia, but also to normoxia. If one cell is more conductive than another during normoxia, then ion pumping due to this increased conductance may be increased to maintain ion homeostasis (Hochachka and Guppy, 1987). Based on G_m (Fig. 18) and Na^+-K^+-ATPase activity (Table 6), these results support reduced passive ion leakage during normoxia as one mechanism utilized by the turtle neuron to reduce ATP expenditure. The enzymatic V_{max} measures, although supporting a reduced ion leakage in the turtle brain, only support 60% of the observed 4.2 fold difference from G_m ratios suggesting that further down regulation of ion pumping activity may occur *in vivo* in the turtle brain (Fig. 18).

Conductance ratios reported here (25 ^oC) between the turtle and the rat are slightly higher than K^+ conductance ratios reported for similar sized nondiving reptiles (*Amphibolorus vitticeps*) vs. the rat (conductance done at 37 ^oC) using tracer methods (4.2 vs. 3.6 respectively) (Else and Hulbert, 1987). Additionally, oxygen consumption ratios in the

presence of ouabain under the same temperature conditions (37 ^{o}C) suggests ion pumping differences of 4 fold between the rat and *A. vitticeps* (Else and Hulbert, 1987) compared to the 2.3 fold difference reported here in maximal activities of Na^{+}-K^{+}-ATPase (25 ^{o}C). Both the K^{+} conductance studies and the ouabain studies compare well with the G_m ratios reported here for the turtle vs. rat cortex at the same temperature (25 ^{o}C; 4.2) suggesting that the maximal activities of Na^{+}-K^{+}-ATPase may not accurately reflect absolute ion pumping differences because of *in vivo* Na^{+}-K^{+}-ATPase regulation (Rossier *et al.*, 1987). However, the maximal activities of this enzyme do support large pumping capacity differences between the two species.

It is tempting to estimate the energy (ATP) savings achievable based on the lower G_m for the turtle cortex; however, this is not yet possible. First, the specific passive ion conductance contributing to this savings are not yet known. Second, the exact energy expenditure due to ion leakage independent of electrical activity is not well understood. Studies on canine brains *in vivo* suggest that ion pumping due to passive ion leakage consumed more than 40 % of resting ATP turnover (Astrup *et al.*, 1981) suggesting a substantial energy savings. Further speculation on the metabolic energy savings will be discussed in Chapter 5.

The calculations for G_m are based on two assumptions. First, both biological membranes display a 1 $\mu F / cm^2$ capacitance. Careful studies of both ectotherms and endotherms from a variety of cell types yield this value (Brown *et al.*, 1981) suggesting that C_m may be a biophysical constant (Hille, 1992). Since C_m is a function of the membrane composition, and since membrane structure and composition is conserved, it is reasonable that C_m would also be conserved. Secondly, the assumption of a Q_{10} of 1.9 for the rat brain between 35 - 37 ^{o}C is made. We have measured the Q_{10} for membrane conductance in the turtle neuron between the temperatures of 15 - 25 ^{o}C and for the rat neuron between 25 - 35 ^{o}C (Table 3), and have extrapolated the latter values to 37 ^{o}C.

The Q_{10} for both tissues is approximately the same (1.9) (Table 3) which is similar to the whole body metabolic Q_{10} for both species for these temperature ranges (Funk and Milsom, 1987). The conservation of the conductance Q_{10} between animals and temperatures suggests that the Q_{10} for ion channels may be conserved across channel types as well as animals. Single channel studies from a variety of channel types from both ectotherms and endotherms report Q_{10} values ranging from 1.0 to 2.5 with most values between 1.3 - 1.6, close to the aqueous diffusion Q_{10} of 1.3 (Hille, 1992). However, conservation of the conductance Q_{10} may hold true only for leakage channels. The Q_{10} for this study is an average between G_m and G_w. The average is used since these measures although calculated independently of each other should change both qualitatively and quantitatively in parallel with temperature. This parallelism appears to be true for the rat cortical neuron but quantitatively deviates for the turtle neuron. Several reasons could possibly explain this deviation since these two measures are calculated independently of each other. Changes in capacitance, cell size, soma to dendritic conductance and bleb formation (Milton and Calswell, 1990) may all influence G_w differently from G_m with respect to Q_{10}.

In addition to large inherent leakage differences between rat and turtle membranes, the channel arrest hypothesis predicts a decrease in G_w and G_m with anoxia. Results using intracellular recording methods over short term anoxia indicated no change in G_m or G_w (Fig. 16, 17). Data from Chih suggests that K^+ leakage *in vivo* was suppressed by anoxia (Chih *et al.*, 1989). Recent cortical slice data indicated that $[Ca]_i$ accumulation during long term anoxia (180 mins) is slower compared to short term anoxia (5 mins.) after the addition of iodoacetate (glycolytic inhibitor) (Bickler, 1992a). However, specific leakage processes were not measured in either of these papers, and thus, the lowered leakage observed could be caused from a reduction in any leakage process including electrical activity. Due to the above observations as well as limitations of the microelectrode technique, we measured whole cell conductance using patch clamping techniques. The advancement of whole cell patch clamp methods in slices provides a way of easily comparing populations of cells while

ensuring that membrane electrode seals are not significantly contributing to the apparent cell conductance due to the GΩ seal formation between electrode and cell membrane. The values obtained for T_C and G_W were greater than those obtained with intracellular recording techniques. Thus, ion leakage around the microelectrode may significantly contribute to the values of T_C and G_W, masking small conductance changes. However, the results reported here for long term anoxia (6 - 9 hrs.) supported intracellular recording techniques.

Both turtle and rat pyramidal neurons have inwardly rectifying K^+ channel (Connors and Kreigstein, 1986; McCormick, et al., 1985). Thus, one method for changing cell conductance is to change membrane potential. As a result, channel arrest could be achieved by simply depolarizing the cell. However, no noticeable change in membrane potential occurred during anoxia in turtle neurons (Table 1) supporting earlier results with intracellular recording techniques and short term anoxia (Chapter 1).

The energy conservation mechanism predicted by the channel arrest hypothesis is not directly due to ion channels closing, but by a decrease in ATP-dependent ion pump activity resulting from down regulation of ion channels. We have tested one leakage process (leak channels). However, ion leakage can result from a variety of other processes. Current evidence supports both a reduction in ion leakage (Bickler, 1992a; Chih, et al., 1989) and in electrical activity (Feng, et al., 1988; Sick, et al., 1982) in the turtle brain with anoxia. Our results support that the concept that the turtle brain maybe spending less energy on maintaining ion homeostasis in the normoxic state compared to the rat, but that further down regulation with anoxia is not measurable. Accumulating evidence supports down regulation of electrical activity as a more likely scenario for metabolic depression in the turtle brain.

CHAPTER 5: A THEORETICAL APPROACH TO ANOXIA TOLERANCE- A CONCLUSION

Preface

The goals for this final chapter are three fold. First, this chapter serves to unite all of the preceding material into a unified theory of anoxia tolerance. Second, this chapter will serve as a mini review of the preceding material especially that material which relates to this unified theory. Finally, it is hoped, this chapter will serve to generate curiosity and insight which may lead to a better fundamental understanding of the events surrounding both anoxia tolerance and intolerance. Parts of this chapter were excerpted from C. J. Doll (In *Surviving Hypoxia*, CRC Press, pgs. 389-400, 1993).

Introduction

The second law of thermodynamics states that natural processes move towards a state of greater disorder (increasing entropy, $\Delta S > 0$). Living organisms remain in an unchanging state of entropy by consuming energy. In the case of a neuron, glucose is consumed and energy is provided to maintain cellular homeostasis via ion pumping, molecular repair, synthesis etc., thus, $\Delta S \approx 0$ for the organism. However, if the cell cannot provide enough energy to maintain integrity, ΔS will increase. The results may be catastrophic (Chapter 2). Thus, the emphasis of this thesis (the importance in maintaining energy balance for the cell) is really a restatement of the second law of thermodynamics. In this final chapter, two questions will be explored in detail. First, how is the turtle cortical neuron able to maintain membrane integrity during anoxia, and second, why is the rat cortical neuron (a cell which performs similar functions as the turtle neuron) more vulnerable to these same insults?

An Interpretive Model

The results of this thesis in part can be summed up by Fig. 19. This figure represents a unified theory of why the turtle brain is able to survive anoxia and in part why the mammalian brain cannot. It is divided into two parts: the turtle brain (left side) and the mammalian brain (right side).

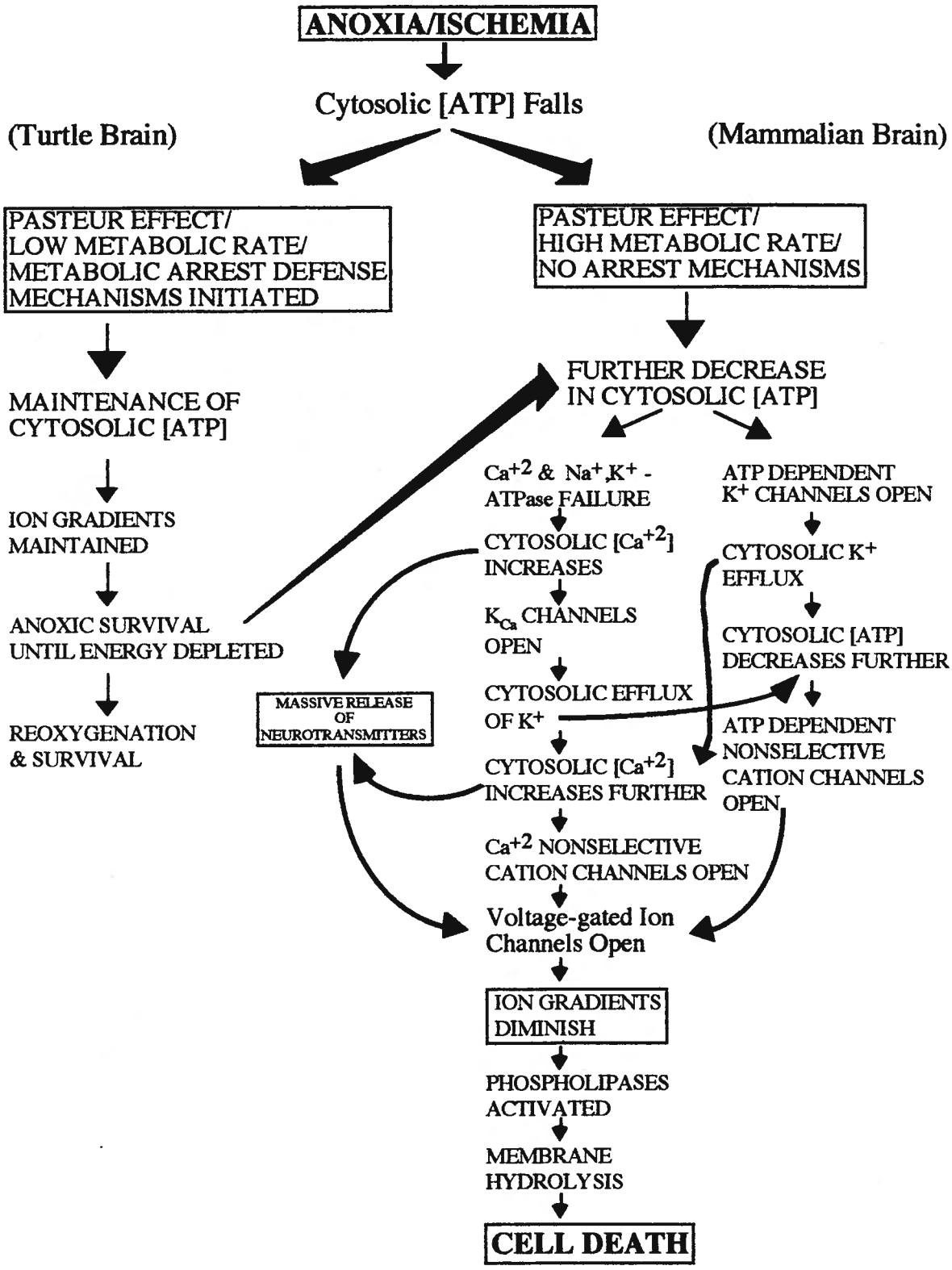

Figure 19. Possible scenario for the degeneration and survival of the turtle and rat neuron. See text for further details.

Mammalian Brain

As discussed in Chapters 1 and 2, a major difference between the turtle and rat brain is in their ability to maintain [ATP] during the anoxic/ischemic insult. I have hypothesized that the declining [ATP] is the trigger which directly or indirectly causes the anoxic/ischemic cascade of events observed in the mammalian brain. There are currently several lines of indirect evidence supporting this position. First the cell's ability to maintain resistance and membrane potential is inversely related to the degree of metabolic inhibition (Reiner, et al., 1990; Chapter 2). Second, temperature plays a direct role in protecting ion gradients suggesting that the lower the metabolic rate (the slower ATP is depleted) the longer ion gradients are maintained (Morris *et al.*, 1991; Okada *et al.*, 1988a; Chapter 2). Third, manipulation of the intracellular or extracellular environment to increase energy rich compounds intracellularly, prolongs the maintenance of ion homeostasis (Caldwell, et al., 1960; Hansen, 1978; Kass and Lipton, 1982; Lipton and Whittingham, 1982; Okada, et al., 1988a). Fourth, there is a direct relationship between loss of electrical activity and [ATP] (Lipton and Whittingham, 1982; Yamamoto and Kurokawa, 1970), as well, bathing mammalian brain slices with creatine to increase intracellular [CrP] (thus, defending $[ATP]_i$) prolongs electrical transmission (Lipton and Whittingham, 1982). Although the fourth point is controversial, with some studies showing changes in synaptic activity before changes in $[ATP]_i$ are detectable (Duffy *et al.*, 1972; Schmahl *et al.*, 1966; Siesjo and Nilsson, 1971), studies in the hippocampus suggest that whole hippocampal slice [ATP] may show little attenuation from control, but when the molecular layer (an area which contains the synapses of the pathway) is examined separately, changes in $[ATP]_i$ are measurable prior to changes in electrical activity (Lipton and Whittingham, 1984 for review). These data would suggest studies which do not detect a substantial fall in [ATP] before electrical changes may not be measuring ATP in appropriate compartmentalized areas (synapses, dendrites, and axon terminals).

Initially, with an anoxic/ischemic insult, there is a large Pasteur effect observed for the mammalian brain (discussed in Chapter 3). Unfortunately, due to the high metabolic rate (9 - 10 fold higher than the turtle brain at 25 ^{o}C; Chapter 3) and the comparatively low amount of glycolytic enzymes (Chapter 3), the mammalian brain is unable to have cellular ATP production meet demand resulting in a loss of $[ATP]_i$ (as discussed in Chapter 2). Fig. 19 depicts the importance of immediate defense mechanisms (see below) to maintain $[ATP]_i$. In the mammalian brain an unsuccessful attempt is made to maintain energy balance despite a large Pasteur effect. Unsuccessful, the mammalian brain enters a cascade of events which leads ultimately to neuronal death (Fig. 19).

(For the next few sections I will refer the reader to review Chapter 2 Introduction where a more complete description and references are given for the discussed material. Additionally, I have referenced Chapter 2 material where the applicable data may be found.)

Both extracellular observations and the hippocampal slice studies (as discussed in Chapter 2), as well as the results from Chapter 2 support the hypothesis that the first visible reaction to anoxia/ischemia is a hyperpolarization and an increase in $[K^+]_O$. Two possible pathways have been hypothesized for this observed increase in $[K^+]_O$ (Krnjevic, 1993; Chapter 2): (i) opening of K_{ATP} channels, or (ii) opening of K_{Ca} channels. With regards to (ii), the activation of these channels by ATP would be indirect. As $[ATP]_i$ decreases, $[Ca^{+2}]_i$ homeostasis mechanisms (ion pumps) fail resulting in an increase in $[Ca^{+2}]_i$ which, in turn, causes activation K_{Ca} channels (Fig. 19).

Talbutamide (K_{ATP} channel blocker) does not inhibit the initial anoxic hyperpolarization in the hippocampal CA1 region (Leblond and Krnjevic, 1989), and several lines of evidence now support K_{Ca} channels involvement in the hyperpolarization in the CA1 region (Krnjevic, 1993, also see Chapter 2). Interestingly, studies in the CA3 hippocampal region where a higher concentration of glibenclamide receptors are found (thus, indicating a greater concentration of K_{ATP} channels) demonstrate that the slow phase of the initial hyperpolarization is blocked by glibenclamide (Mourre *et al.*, 1989); these results imply that

a combination of events cause the anoxic hyperpolarization (as supported by Fig. 19) and that events may vary depending on brain region.

As $[Ca^{+2}]_i$ increases $[ATP]_i$ decreases, three mechanisms for further depolarization and conductance increase are hypothesized. The mechanisms may be synergistic as indicated by crossover arrows in Fig. 19. As previously discussed (Chapter 2), one possible hypothesis for the massive and sudden diminishment of the ion gradients is neurotoxicity . This hypothesis predicts a massive release of excitatory neurotransmitters like glutamate which may cause the sudden diminishment of ion gradients similar to that observed in Fig. 5. This hypothesis has gained support, in part, from observations that excessive application of glutamate does give a similar response to that observed for ischemia and pharmacological ischemia (Choi, 1988a; Rothman, 1985; Wood and Reiner, 1990), and from the observation that there is a sudden release of neurotransmitters corresponding to the ischemic insult (see Chapter 2 for a review). The mechanism for this release is consistent with the hypothesis through an increase in $[Ca^{+2}]_i$. However, two other channel activations may individually or synergistically aid in the anoxic/ischemic neuronal collapse: (i) Ca^{+2} - activated non - selective cation channels (ii) ATP - dependent non - selective cation channels. Both channel types have been identified in neuronal tissue (Ashford, et al., 1988; Partridge and Swandulla, 1988), and therefore, could play a role in the anoxic / ischemic depolarization. Recent studies suggest that preincubation with glibenclamide (K_{ATP} channel antagonists) significantly reduces the amplitude and rate of anoxic $[K^+]_o$ in the hypoglossal nucleus in adult rats. Preliminary observations in hippocampus suggest that glutamate antagonists also reduce the rate of depolarization during pharmacological anoxia in the rat hippocampus, but as in the glibenclamide study above, the neurons still depolarize (Wood and Reiner, 1990) supporting a combination of events being involved in the anoxic/ischemic depolarization. Verification of this hypothesis awaits further detailed studies. Once membrane potential falls below threshold, the activation of voltage-gated ion channels (Na^+, Ca^{+2}, and K^+) can then participate in the observed ion gradient diminishment.

The specific cause of cell death is not well understood. In Fig. 19, I have suggested membrane hydrolysis by the activation of phospholipases as the most likely scenario but permanent damage could also be caused by free radicals (including nitric oxide), pH, cell blebbing, or cytoskeletal destruction (Choi, 1988b; Haddad and Jiang, 1993; Hochachka, 1987 for reviews). Although the actual cause of cellular death is poorly understood, most events up to and including the large conductance and ionic changes leading to the membrane depolarization are reversible, and permanent cellular damage appears to occur after the loss of intracellular ion homeostasis (Hansen *et al.*, 1982; Kirino *et al.*, 1985; Leblond and Krnjevic, 1989; Siemkowicz and Hansen, 1981). It is important to note that an understanding of neuronal functional collapse is considered central for this thesis because it is functional collapse rather than neuronal death *per se* that is ultimately responsible for anoxic death of the whole organism.

Turtle CNS Response

The left half of Fig. 19 is concerned with the turtle brain. There are two important aspects to this figure. First, the ability of the turtle cortical slice to maintain $[ATP]_i$ with anoxia, and second, an arrow linking the turtle to the mammalian side in the event that $[ATP]_i$ is not maintained. However, the turtle cortical slice is capable of maintaining $[ATP]_i$ through a combination of 3 central mechanisms (discussed and supported by studies in Chapter 3): (i) an enhanced glycolytic capacity, (ii) a low normoxic metabolic rate, (iii) the ability to further depress metabolism with anoxia. Support for the linkage of the turtle side to the mammalian side is based on the intracellular observations that the turtle cortical pyramidal neuron could not significantly withstand pharmacological ischemia any better than the rat pyramidal neuron (Fig. 3) with the turtle brain indicating similar conductance and membrane potential changes with pharmacological ischemia (Fig. 5). Additional support for this linkage comes from *in vivo* studies which demonstrate a very rapid rise in $[K^+]_O$ in the turtle brain similar to that observed in the rat brain with ischemia and iodoacetic acid (Sick, et al., 1982; Xia *et al.*, 1992). There is very little information regarding channels, channel

types or densities in the turtle brain; most emphasis is on voltage dependent channels which appear to occur at a lower density in the turtle brain compared to the rat brain (Edwards *et al.*, 1989; Pérez-Pinzón, et al., 1992c; Suarez, et al., 1989; Xia and Haddad, 1993). Identification of K_{ATP} channels in the turtle brain has been confirmed (Jiang, et al., 1992; Xia and Haddad, 1993) with the highest concentration occurring in the turtle cortex. The presence of these channels is consistent with the hypothesis that the mechanisms of pharmacological ischemia depolarization occurs through similar mechanisms in both species.

Metabolic Rate

This thesis has presented the hypothesis that a low metabolic rate is critical for anoxia tolerance. Interestingly, both the turtle and the rat neuron have similar physiological functions (electrical activity, ion pumping, biosynthesis, cellular maintenance, etc.). Chapter 4 was an initial attempt to understand mechanisms which may be down regulated in the turtle cortex during both normoxia and anoxia to conserve ATP utilization. In this section, a theoretical examination of metabolic rate will be explored in an attempt to partially explain the observed brain metabolic rate discrepancies between the turtle and the rat.

Chapter 3 demonstrated a 9 to 10 fold difference in metabolic rate between guinea pig and the turtle cortical slice preparation (Table 7, no. 6 vs. 7). Additionally, deoxyglucose studies have indicated approximately the same difference (Table 7, average of 1 and 2 vs. no. 3). Fig. 20 illustrates an explanation for the metabolic rate differences between the cortical slice preparations of these two species. Because this argument is theoretical, the units on the y axis are arbitrary, and thus, reflect the 10 fold metabolic difference between the tissues (Fig 20a,d).

Because the metabolic rate measures have been performed at physiological temperatures, metabolism must be corrected for temperature. Two studies which examined the effect of temperature on glucose utilization in the mammalian cortex (Table 7, no. 4 and 5) reported a Q_{10} of 2.7 and 4.32 yielding an average Q_{10} of 3.5. Thus in (B) of Fig. 20 the metabolic

Table 7. Glucose consumption measures

*Animal	Preparation	Temperature range (°C)	Glucose μmoles/g/min	Q10	Reference
1 Rat	Whole Brain (*in vivo*)	37	0.45[a]	____	(Hawkins *et al.*, 1974)
2 Rat	Whole Brain (*in vivo*)	37	0.60[a]	____	(Crane *et al.*, 1978)
3 Turtle	Whole Brain (*in vivo*)	25	0.053[a]	____	(Suarez, et al., 1989)
4 Rat	Cortex (*in vivo*)	37.4	1.15[a]		(McCulloch *et al.*, 1982)
		↓ 31.8	0.75[a]	2.7	
5 Mouse	Cortex (*in vivo*)	35.8	0.93[a]		(Ito *et al.*, 1990)
		↓ 27.7	0.27[a]	4.32	
6 Guniea Pig	Cortical Slice	38	0.42[bd]	____	(Rolleston and Newsholme, 1967b)
7 Turtle	Cortical Slice	25	0.048[c]	____	Chapter 3

[a] Technique used was radio labeled glucose or glucose anologue.

[b] Technique used was direct measurement of glucose consumption.

[c] Technique used was calorimetry and then converted to glucose consumption assuming 2820 kJ / mole glucose (Gnaiger and Kemp, 1990).

[d] Corrected for lactate production and glycogen catabolism.

* Numbers superscripted beside animals are for in-text reference

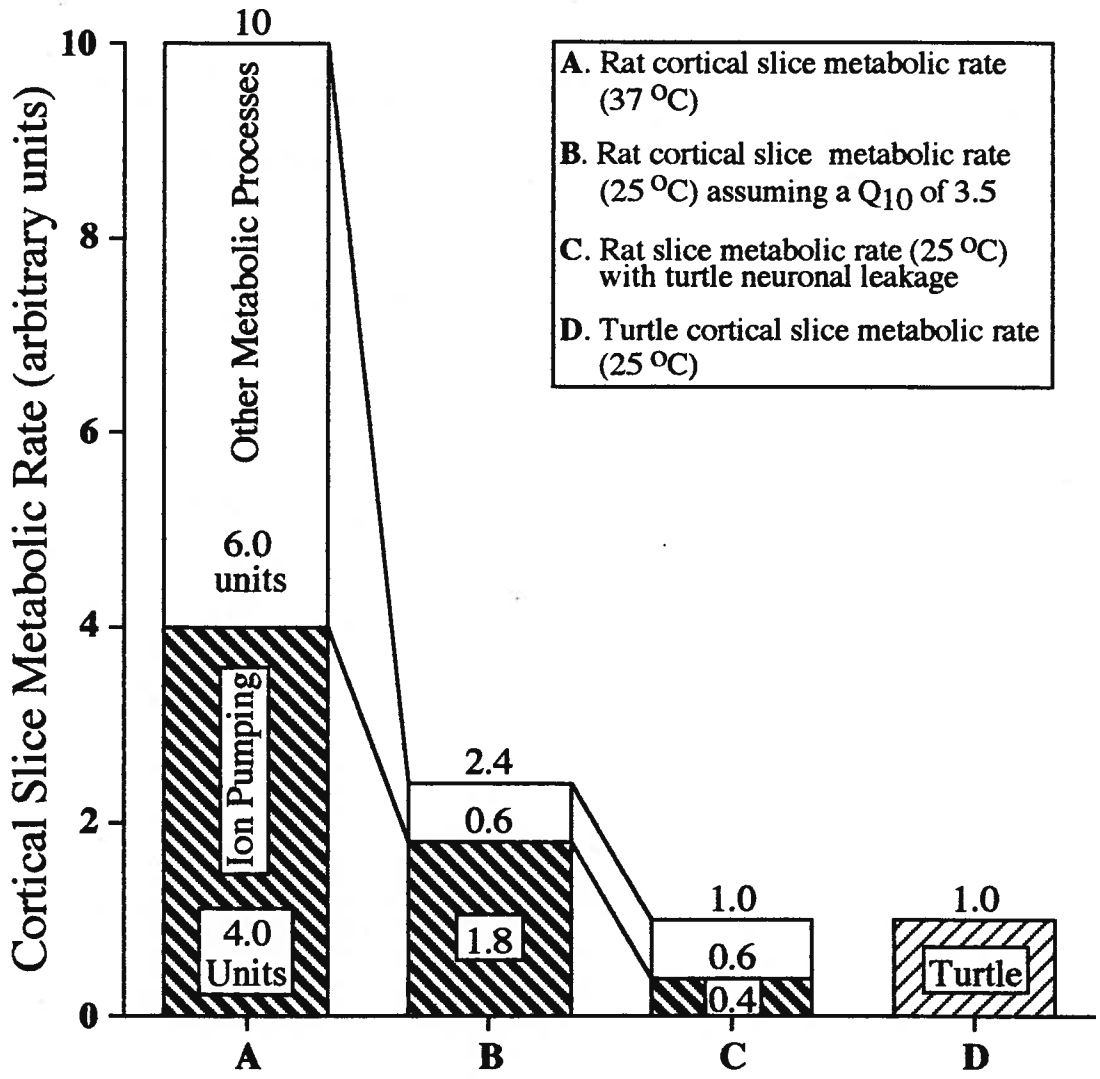

Figure 20. Adjusted metabolic rate for the mammalian cortical slice.

rate of the rat cortical slice has been metabolically adjusted for this temperature based on a Q_{10} of 3.5 yielding a value of 2.4 units (Fig. 20b).

For the rat cortical slice 40% (4 of the 10 units) of the metabolic rate has been allotted to ion pumping (Fig 20a). Two independent studies have suggested this percentage of energy metabolism for ion pumping independent of electrical activity *in vitro* (Whittam, 1962) and *in vivo* (Astrup, et al., 1981). In Chapter 4, the change in conductance with temperature was measured for the rat cortical neuron ($Q_{10_{(35 \rightarrow 25\,^{o}C)}} = 1.9$; Table 5). When the rat neuron is corrected for the 12 ^{o}C temperature change, the adjusted energy allotment for ion pumping is 1.8 units of the total 2.4 units (Fig. 20b). Because the Q_{10} for total energy metabolism (3.5) is larger than the Q_{10} for ion leakage (1.9), the percentage of energy consumed by ion pumping has increased from 40% to 75% of the total allotted energy utilization of the slice, independent of electrical activity (Fig. 20c).

In Chapter 4, the difference in conductance between the turtle and the rat pyramidal neuron at the same temperature (25 ^{o}C) was measured. The turtle neuron expressed 4.2 times less conductance than the rat pyramidal neuron (Fig. 18). Thus, the 1.8 units which has been allotted to the rat neuron for ion pumping at 25 ^{o}C can be divided by 4.2 (= 0.4 units). Thus, both the turtle and the rat now have the same energy allotment for ion pumping. When the 0.4 unit for ion pumping is added to the 0.6 unit (other metabolic processes), the final metabolic rate of the rat cortical slice is identical to the turtle cortical slice (1.0 unit). Since both the total metabolic rate (1.0 unit) and the ion pumping energy allotment (0.4 unit) are the same for both species, then the metabolic rate allotted to other metabolic processes must be the same for both species (0.6 units). Thus, when the rat cortical slice is adjusted to have the same degree of ion pumping as the turtle cortical slice at 25 ^{o}C, the metabolic rate for the two tissues is identical.

These results support four concepts for the turtle and the rat neuron in the absence of electrical activity: (i) the rat neuron, when corrected for both temperature and ion leakage consumes the same amount of ATP as the turtle neuron, (ii) the metabolic rate difference (at

25 °C) between the turtle and the rat cortical slice (2.4 vs. 1.0, Fig 20b vs. d) is due to the amount of ion pumping rather than differences in other metabolic processes; and (iii) the turtle neuron is spending approximately 0.4 of the 1.0 unit on ion pumping (40%) and 0.6 of the 1.0 unit (60%) on other metabolic processes which is identical to the estimated metabolic rate allotted to the rat cortical slice at its physiological temperature (37 °C).

Ectothermy vs. Endothermy

Although the emphasis for anoxia tolerance in this thesis has centered on metabolism and its regulation, a low metabolic rate is not the only component to anoxic survival as has been discussed throughout this section. All three of the components, (i) low metabolic rate, (ii) the ability to further suppress metabolism with anoxia, and (iii) a large glycolytic capacity, must work synergistically. The requirement for such a integrative or collaborative effect may, in part, explain the wide tolerance to anoxia observed among ectotherms, and why being an ectotherm does not necessarily imply being anoxia tolerant. Tolerance among ectothermic vertebrates is highly variable with some amphibians (Penney, 1987; Sick and Kreisman, 1981), and fish (Doudoroff and Shumway, 1970; Randall, 1982; Ultsch, 1989 for reviews)having similar responses as the mammal to anoxia while others such as carp, turtle, alligators, and snakes (Bennett and Dawson, 1969; Ultsch, 1989 for reviews) possess variable anoxic windows. Even among turtle species anoxia tolerance varies (Ultsch, 1985). Ectotherms have lower metabolic rates than similar sized mammals (Schmidt-Nielsen, 1984) and presumable lower brain metabolic rates (Mink, et al., 1981), but a low metabolic rate only in combination with metabolic and glycolytic regulation will provide anoxic protection. Thus, ectothermic species not expressing anoxia tolerance may not fully exhibit one of the three requisite adaptations. Confirmation of this hypothesis awaits further studies of brain metabolism and glycolytic regulation in other ectotherms (anoxia intolerant vs. anoxia tolerant). One study which did examine brain metabolic rates in different ectotherms indicated that the turtle brain (*Pseudemys scripta*) expressed half the metabolic rate compared to the fish (*Carassius auratus*) and frog (*Rana pipiens*) (McDougal, et al., 1968).

Unfortunately, this thesis is written at a time when very little is understood about energy budgets of neurons. Although an attempt has been made at measuring one mechanism for metabolic depression (reduced ion leakage; Chapter 4) we have not identified any metabolic arrest processes in the cortical slice. Experiments with turtle hepatocytes indicate a marked reduction in ion leakage with anoxia (Buck *et al.*, In Press). As discussed in Chapter 4, current evidence supports a marked reduction in electrical activity in the turtle brain. However, studies have demonstrated that O_2 consumption is reduced by only 5 % with the inhibition of voltage dependent Na^+ channels in cortical slices (Okamoto and Quastel, 1972). We have observed a substantial metabolic depression (30-40 %) in the anoxic turtle cortical slice (see chapter 3). Thus, other metabolic process must be depressed in the turtle slice to account for the measured metabolic depression. As a final note, this study focused on the *in vitro* preparation. Changes which occur as a result of the intact tissue have not been determined. It is possible that leakage channel down regulation may occur *in vivo*. Recent studies have demonstrated a reduced Ca^{+2} influx in response to glutamate when the *in vitro* cortex of both turtles and rats was exposed to anoxic turtle plasma in the aCSF (Bickler and Gallego, 1993). Therefore, additional studies may be necessary to determine whether leakage channels are down regulated in response to anoxia in the turtle cortex.

LITERATURE CITED

Ashford, M. L., N. C. Sturgess, N. J. Gardner, and C. N. Hales. Adenosine-5-triphosphate-sensitive ion channels in neonatal rat cultured central neurons. *Pfluegers Arch.* 412: 297-304, 1988.

Astrup, J., P. M. Sorensen, and H. R. Sorensen. Oxygen and glucose consumption related to Na^+-K^+ transport in canine brain. *Stroke* 12: 726-730, 1981.

Aw, T. Y., and D. P. Jones. Cyanide toxicity in hepatocytes under aerobic and anaerobic conditions. *Am. J. Physiol.* 257: C435-C441, 1989.

Beal, M. F. Mechanisms of excitotoxicity in neurologic diseases. *FASEB J.* 6: 3338-3344, 1992.

Ben-Ari, Y. Galanine and glibenclamide modulate the anoxic release of glutamate in rat CA3 hippocampal neurons. *Eur. J. Neurosci* 2: 62-68, 1990.

Bennett, A. F., and W. R. Dawson. Metabolism In: *Biology of the reptilia*, edited by C. Gans. London: Academic Press, 1969, 127-223.

Benveniste, H., J. Drejer, A. Schousboe, and N. H. Diemer. Elevation of the extracellular concentrations of glutamate and aspartate in rat hippocampus during transient cerebral ischemia monitored by intracerebral microdialysis. *J. Neurochem.* 43: 1369-1374, 1984.

Berta, A., C. E. Ray, and A. R. Wyss. Skeleton of the oldest known pinniped *Enaliactos mealsi. Science Wash. D. C.* 244: 60-63, 1989.

Beyersdorf, F., A. Unger, A. Wildhirt, U. Kretzer, N. Deutschlander, S. Kruger, G. Matheis, A. Hanselmann, G. Zimmer, and P. Satter. Studies of reperfusion injury in skeletal muscle: preserved cellular viability after extended periods of warm ischemia. *J. Cardiovasc. Surg.* 32: 664-676, 1991.

Bickler, P. E. Cerebral anoxia tolerance in turtles: regulation of intracellular calcium. *Am. J. Physiol.* 263: R1298-R1302, 1992a.

Bickler, P. E. Effects of temperature and anoxia on regional cerebral blood flow in turtles. *Am. J. Physiol.* 262: R538-R541, 1992b.

Bickler, P. E., and S. M. Gallego. Inhibition of brain calcium channels by plasma proteins from anoxic turtles. *Am. J. Physiol.* 265: R277-R281, 1993.

Blanton, M. G., J. J. Lo, and A. R. Kreigstein. Whole cell recording from neurons in slices of reptilian and mammalian cerebral cortex. *J. Neurosci. Meth.* 30: 203-210, 1989.

Block, B. A. The billfish brain and eye heater: a new look at non-shivering thermogenesis. *News Physiol. Sci.* 2: 208-213, 1987.

Borgström, L., K. Norberg, and B. K. Siesjö. Glucose consumption in rat cerebral cortex in normoxia, hypoxia and hypercapnia. *Acta Physiol. Scand.* 96: 569-574, 1976.

Boyle, R. New pneumatical experiments about respiration. *Trans. R. Soc. Lond. B Biol.* 5: 2011-2031, 1670.

Brooks, S. P. J., and K. B. Storey. Regulation of glycolytic enzymes during anoxia in the turtle *Pseudemys scripta*. *Am. J. Physiol.* 257: R278-R283, 1989.

Brown, T. H., D. H. Perkel, J. C. Norris, and J. H. Peacock. Electronic structure and specific membrane properties of mouse dorsal root ganglion neurons. *J. Neurophysiol.* 45: 1-15, 1981.

Buck, L. T., and P. W. Hochachka. An assessment of the importance of succinate as an anaerobic endproduct in the diving turtle (*Chrysemys picta bellii*). *J. Exp. Biol.* , In Press.

Buck, L. T., P. W. Hochachka, and E. Gniager. Microcalorimetric measurement of reversible metabolic suppression induced by anoxia in isolated hepatocytes. *J. Exp. Biol.* , In Press.

Caldwell, P. C., A. L. Hodgkin, R. D. Keynes, and T. I. Shaw. The effects of injecting energy-rich phosphate compounds on the active transport of ions in the active transport of ions in the giant axons of *Loligo*. *J. Physiol. Lond.* 152: 561-590, 1960.

Castellini, M. A., G. N. Somero, and G. L. Kooyman. Glycolytic enzyme activities in tissues of marine and terrestrial mammals. *Physiol. Zool* 54: 242-252, 1980.

Chih, C. P., M. Rosenthal, and T. J. Sick. Ion leakage is reduced during anoxia in turtle brain: a potential survival strategy. *Am. J. Physiol* 257: R1562-R1564, 1989.

Choi, D. W. Calcium-mediated neurotoxicity: relationship to specific channel types and role in ischemic damage. *TINS* 11: 465-469, 1988a.

Choi, D. W. Glutamate neurotoxicity and diseases of the nervous system. *Neuron* 1: 623-634, 1988b.

Clark, G. D., and S. M. Rothman. Blockage of excitatory amino acid receptors protects anoxic hippocampal slices. *Neuroscience* 21: 665-?, 1987.

Clark, V. M., and A. T. Miller Jr. Studies on anaerobic metabolism in the fresh-water turtle (*Pseudemys Scripta Elegans*). *Comp. Biochem. Physiol.* 44A: 55-62, 1973.

Connors, B. W., and A. R. Kreigstein. Cellular physiology of the turtle visual cortex: distinctive properties of pyramidal and stellate neurons. *J. Neurosci.* 6: 164-177, 1986.

Crane, P. D., L. D. Braun, E. M Cornford, J. E. Cremer, J. M. Glass, and W. H. Oldendorf. Dose dependent reduction of glucose utilization by pentobarbital in rat brain. *Stroke* 9: 12-18, 1978.

Cserr, H. F., M. DePasquale, and D. C. Jackson. Brain and cerebrospinal fluid ion composition after long-term anoxia in diving turtles. *Am. J. Physiol.* 255: R338-R343, 1988.

Cummins, T. R., D. F. Donnelly, and G. G. Haddad. Effect of metabolic inhibition on the excitability of isolated hippocampal CA1 neurons: developmental aspects. *J. Neurophysiol.* 66: 1471-?, 1991.

Daves, D. G. Distribution of systemic blood flow during anoxia in the turtle, *Chrysemys scripta. Resp. Physiol.* 78: 383-390, 1989.

Daw, J. C., D. P. Wenger, and R. M. Berne. Relationship between cardiac glycogen and tolerance to anoxia in the western painted turtle, *Chrysemys picta bellii*. *Comp. Biochem. Physiol.* 22: 69-73, 1967.

DeLong, R. L. Diving patterns of northern elephant seal bulls. *Mar. Mamm. Sci* 7: 369-384, 1991.

Dessauer, H. C. Blood chemistry of reptiles: physiological and evolutionary aspects In: *Biology of the Reptilia*, edited by C. Gans and T. S. Parsons. London: Acedemic Press, 1970, 1-72.

Dessauer, H. C., and W. Fox. Changes in ovarian follicle composition with plasma levels of snakes during estrus. *Am. J. Physiol.* 197: 360-366, 1959.

Doudoroff, P., and D. L. Shumway. Dissolved oxygen requirements of freshwater fishes. *F.A.O. Fisheries Technical Paper*, No. 86: 1970.

Drewes, L. R., and D. D. Gilboe. Glycolysis and the permeation of glucose and lactate in the isolated perfused dog brain during anoxia and postanoxic recovery. *J. Biol. Chem.* 218: 2489-2496, 1973.

Duffy, T. E., S. R. Nelson, and O. H. Lowry. Cerebral carbohydrate metabolism during acute hypoxia recovery. *J. Neurochem.* 19: 959-977, 1972.

Duncan, J. A., and K. B. Storey. Subcellular enzyme binding and the regulation of glycolysis in anoxic turtle brain. *Am. J. Physiol.* 262: R517-R523, 1992.

Edelman, I. S. Transition from the poikilotherm to the homeotherm: possible role of sodium transport and thyroid hormone. *Fed. Proc.* 35: 2180-2184, 1976.

Edwards, A. R., P. L. Lutz, and D. G. Baden. Relationship between energy expenditure and ion channel density in the turtle and rat brain. *Am. J. Physiol.* 257: R1354-R1358, 1989.

Else, P. L., and A. J. Hulbert. Evolution of mammalian endothermic metabolism: "leaky" membranes as a source of heat. *Am. J. Physiol.* 253: R1-R7, 1987.

Elsner, R., and B. Gooden. *Diving and Asphyxia.* Cambridge: Cambridge University Press, 1983, 168.

Feng, Z., M. Rosenthal, and T. J. Sick. Suppression of evoked potentials with continued ion transport during anoxia in turtle brain. *Am. J. Physiol.* 255: R478-R484, 1988.

Feng, Z. -C., M. Rosenthal, and T. J. Sick. Extracellular pH and suppression of electrical activity during anoxia in turtle and rat brain. *Am. J. Physiol.* 258: R205-R210, 1990.

Feng, Z.-C., T. J. Sick, and M. Rosenthal. Orthodromic field potentials and recurrent inhibition durin anoxia in turtle brain. *Am. J. Physiol* 255: R485-R491, 1988.

Fry, F. E. J., and J. S. Hart. The relation of temperature to oxygen consumption in the goldfish. *Biol. Bull.* 94: 66-77, 1948.

Fujiwara, N., H. Higashi, K. Shimoji, and M. Yoshimura. Effect of hypoxia on rat hippocampal neurons *in vitro*. *J. Physiol* 384: 131-151, 1987.

Funk, G. D., and W. K. Milsom. Changes in ventilation and breathing pattern produced by changing body temperature and inspired CO_2 concentration in turtles. *Respir. Physiol* 67: 37-51, 1987.

Furler, S. M., A. B. Jenkins, L. H. Storlien, and E. W. Kraegen. In vivo location of the rate-limiting step of hexose uptake in muscle and brain tissue of rats. *Am. J. Physiol.* 261: E337-E347, 1991.

Gatten, R. E., Jr. Anaerobic Metabolism in freely diving painted turtles (*Chrysemys picta*). *J. Exp. Zool.* 216: 377-385, 1981.

Gingerich, P. D., and D. E. Russell. Dentition of early eocene Pakicetus (Mammalia, *Cetacea*). *Contrib. Mus. Paleontol. Univ. Mich.* 28: 1-20, 1991.

Glass, M. L., R. B. Boutilier, and N. Heisler. Ventilatory control of arterial Po_2 in the turtle *Chrysemys picta bellii*: effects of temperature and hypoxia. *J. Comp. Physiol.* 151: 145-153, 1983.

Globus, M. Y.-T., R. Busto, W. D. Dietrich, E. Martinez, I. Valdes, and M. D. Ginsberg. Effect of ischemia on the in vivo release of striatal dopamine, glutamate, and γ-aminobutyric acid studied by intracerebral microdialysis. *J. Neurochem.* 51: 1455-1456, 1988.

Gnaiger, E. Energetics of invertebrate anoxibiosis: direct calorimetry in aquatic oligochaetes. *FEBS Lett.* 112: 239-242, 1980.

Gnaiger, E., and R. B. Kemp. Anaerobic metabolism in aerobic mammalian cells: information from the ratio of calorimetric heat flux and respirometric oxygen flux. *Biochim Biophys Acta* 1016: 328-332, 1990.

Haas, H. L., B. Schaerer, and M. Vosmansky. A simple perfusion chamber for the study of nervous tissue slices in vitro. *Nerurosci. Methods* 1: 323-325, 1979.

Haddad, G. G., and C. Jiang. Oxygen Deprivation in the CNS. *Prog. Neurobiol.* 40: 278-318, 1993.

Hammerstedt, R. H., and H. A. Lardy. The effect of substrate cycling ion the ATP yield of sperm glycolysis. *J. Biol. Chem.* 258: 8759-8765, 1983.

Hand, S. C., and E. Gniager. Anaerobic dormancy quantified in *Artemia* embryos: a calorimetric test of the control mechanism. *Science Wash. D.C.* 239: 1425-1427, 1988.

Hansen, A. J. The extracellular potassium concentration in brain cortex following ischemia in hypo- and hyperglycemic rats. *Acta Physiol. Scand.* 402: 324-329, 1978.

Hansen, A. J. Ion and membrane changes in brain anoxia In: *Protection of tissues against hypoxia*, edited by A. Wauquier, M. Borgers and W. K. Amery. Amsterdam: Elsevier Biomedical Press, 1982, 199-209.

Hansen, A. J. Effect of anoxia on ion distribution in the brain. *Physiol. Rev.* 65: 101-148, 1985.

Hansen, A. J., J. Hounsgaard, and H. Jahnsen. Anoxia increases potassium conductance in hippocampal nerve cells. *Acta Physiol. Scand.* 115: 301-310, 1982.

Hansen, A. J., and T. Zeuthen. Extracellular ion concentrations during spreading depression and ischemia in the rat brain cortex. *Acta Physiol. Scand.* 113: 437-445, 1981.

Hardewig, I., A. D. F. Addink, M. K. Grieshaber, H. O. Portner, and G. van den Thillart. Metabolic rates at different oxygen levels determined by direct and indirect calorimetry in the oxyconformer *Sipunculus nudus. J. Exp. Biol.* 157: 143-160, 1991.

Hawkins, R. Cerebral Energy Metabolism In: *Cerebral Energy Metabolism and Encephalopathy*, edited by D. W. McCandless. New York: Plenum Press, 1985, 3-23.

Hawkins, R. A., A. L. Miller, J. E. Cremer, and R. L. Veech. Measurement of the rate of glucose utilization by rat brain in vivo. *J. Neurochem.* 23: 917-923, 1974.

Herbert, C. V., and D. C. Jackson. Temperature effects on the responses to prolonged submergence in the turtle Chrysemys picta bellii. I. Blood acid-acid base and ionic changes during the following anoxic submergence. *Physiol. Zool.* 58: 655-669, 1985.

Herreid, C. F., II. Hypoxia in invertebrates. *Comp. Biochem. Physiol.* 67A: 311-320, 1980.

Higashi, H., S. Sugita, S. Nishi, and K. Shimoji. The effect of hypoxia on hippocampal neurons and its prevention by Ca^{+2} antagonists In: *Mechanisms of Cerebral Hypoxia and Stroke*, edited by G. Somjen. New York: Plenum Press, 1988, 205-218.

Hille, B. *Ionic Channels of Excitable Membranes.* Sunderland: Sinauer Ass. Inc, 1992, 607.

Hindell, M. A., D. J. Slip, and H. R. Burton. The diving behavior of adult male and female southern elephant seals *Mitounga leonina* (Pinnipedia: Phocidae). *Aust. J. Zool.* 39: 595-619, 1991.

Hitzig, B. M., M. P. Kneussl, V. Shih, R. D. Brandstgetter, and H. Kazemi. Brain amino acid concentrations during diving and acid-base stress in turtles. *J. Appl. Physiol.* 58: 1751-1754, 1985.

Hochachka, P. W. *Living Without Oxygen.* Harvard University Press, 1980, 181.

Hochachka, P. W. Defense strategies against hypoxia and hypothermia. *Science Wash. D.C.* 231: 234-241, 1986.

Hochachka, P. W. Metabolic Arrest. *Intensive Care Med.* 12: 127-133, 1987.

Hochachka, P. W., and M. Guppy. *Metabolic Arrest and the Control of Biological Time.* Cambridge: Harvard University Press, 1987, 227.

Hochachka, P. W., T. G. Owen, J. F. Allen, and G. C. Whittow. Multiple end products of anaerobiosis in diving vertebrates. *Comp. Biochem. Physiol.* 50B: 17-22, 1975.

Hochachka, P. W., and G. N. Somero. *Biochemical Adaptation.* Princeton: Princeton University Press, 1984, 538.

Ismail-Beigi, F., and I. S. Edelman. Mechanism of thyroid calorigenesis: Role of active sodium transport. *Proc. Natl. Acad. Sci. U.S.A.* 67: 1071-1078, 1970.

Ito, K., Y. Sawada, H. Ishizuka, Y. Sugiyama, H. Suzuki, T. Iga, and M. Hanano. Measurement of cerebral glucose utilization from brain uptake of [^{14}C]-deoxyglucose and [^{3}H]3-O-methylglucose in the mouse. *Pharmacol. Methods* 23: 129-140, 1990.

Jackson, D. C. Metabolic depression and oxygen depletion in the diving turtle. *J. App. Physiol.* 24: 503-509, 1968.

Jackson, D. C. Long-term submergence at 3 oC of the turtle, Chrysemys picta bellii, in normoxia and severely hypoxic water. II. Extracellular ionic responses to extreme lactate acidosis. *J. Exp. Biol.* 96: 29-43, 1982a.

Jackson, D. C. Plasma ion balance of submerged anoxic turtles at 3 ^{o}C: the role of calcium lactate formation. *Respir. Physiol.* 49: 159-174, 1982b.

Jackson, D. C., and K. Schmidt-Neilsen. Heat production during diving in the freshwater turtle, Pseudemys scripta. *J. Cell. Physiol.* 67: 225-231, 1966.

Jiang, C., Y. Xia, and G. G. Haddad. Role of ATP-sensitive K^{+} channels during anoxia: major differences between rat (newborn and adult) and turtle neurons. *J. Physiol* 448: 599-612, 1992.

Jones, M. D., Jr., and R. J. Trystman. Cerebral oxygenation of the fetus, newborn, and adult. *Seminars Perinatology* 8: 205-216, 1984.

Kass, I. S., and P. Lipton. Mechanisms involved in irreversible anoxic damage to the *in vitro* rat hippocampal slice. *J. Physiol.* 332: 459-472, 1982.

Kauppinen, R. A., and D. G. Nicholls. Synaptosomal bioenergetics. The role of glycolysis, pyruvate oxidation and responses to hypoglycemia. *Eur. J. Biochem.* 158: 159-165, 1986.

Kauppinen, R. A., and D. G. Nichols. Failure to maintain glycolysis in anoxic nerve terminals. *J. Neurochem.* 47: 1864-1869, 1986.

Keiver, K. M., and P. W. Hochachka. Catecholamine stimulation of hepatic glycogenolysis during anoxia in the turtle *Chrysemys picta. Am. J. Physiol.* 261: R1341-R1345, 1991.

Keiver, K. M., J. Weinberg, and P. W. Hochachka. The effect of anoxic submergence and recovery on circulating levels of catecholamines and corticosterone in the turtle, *Chrysemys picta. Gen. Comp. Endocrinol.* 85: 308-315, 1992.

Kelly, D. A., and K. B. Storey. Organ-specific control of glycolysis in anoxic turtles. *Am. J. Physiol.* 255: R774-R779, 1988.

Kerem, D., and R. Elsner. Cerebral tolerance to asphyxial hypoxia in the dog. *Am. J. Physiol* 225: 593-600, 1973a.

Kerem, D., and R. Elsner. Cerebral tolerance to asphyxial hypoxia in the harbor seal. *Respir. Physiol.* 19: , 1973b.

Kirino, T., A. Tamura, and K. Sano. Selective vulnerability of the hippocampus to ischemia-reversible and irreversible types of ischemic cell damage. *Prog. Brain Res* 63: 39-58, 1985.

Kitner, D., J. H. Fitzpatrick Jr., J. A. Louie, and D. D. Gilboe. Cerebral oxygen and energy metabolism during and after 30 minutes of moderate hypoxia. *Am. J. Physiol.* 247: E475-E482, 1984.

Kooyman, G. L. *Diverse Divers.* Berlin: Springer-Verlag, 1989, 200.

Kraig, R. P., and C. Nicholson. Extracellular ionic variations during spreading depression. *Neurosci* 3: 1045-1059, 1978.

Krnjevic, K. Membrane current activation and inactivation during hypoxia in hippocampal neurons In: *Cellular Defense Strategies to hypoxia*, edited by P. W. Hochachka, P. Lutz, A. Wauquier, M. Rosenthal and G. van den Thillart. Boca Raton: CRC Press, 1993,

Krnjevic, K., and J. Leblond. Changes in membrane currents of hippocampal neurons evoked by brief anoxia. *J. Neurophysiol.* 62: 15-30, 1989.

Krnjevic, K., and Y. Xu. Mechanisms underlying anoxic hyperpolarization of hippocampal neurons. *Can. J. Physiol. Pharmacol.* 68: 1609-?, 1990.

Krnjevic, K., and Y. Z. Xu. Dantrolene suppresses the hyperpolarization or outward current observed during anoxia in hippocampal neurons. *Can J. Physiol. Pharmacol.* 67: 1602-1604, 1989.

Ksiezak, H. J., and G. E. Gibson. Oxygen dependence of glucose and acetycholine metabolism in slices and synaptosomes from rat brain. *J. Neurochem.* 37: 305-314, 1981.

Leblond, J., and K. Krnjevic. Hypoxic changes in hippocampal neurons. *J. Neurophysiol.* 62: 1-15, 1989.

Leivestad, H. The effect of prolonged submersion on the metabolism and the heart rate of the toad (*Bufo bufo*). *Univ. Bergen Arbok Naturvitenskap Rekke* 5: 1-15, 1960.

Lipton, P., and T.S. Whittingham. Reduced ATP concentration as a basis for synaptic transmission failure during hypoxia in the in vitro guinea -pig hippocampus. *J. Physiol.* 325: 51-65, 1982.

Lipton, P., and T. S. Whittingham. Energy metabolism and brain slice function In: *Brain Slices*, edited by R. Dingledine. New York: Plenum Press, 1984,

Lowry, O. H., J. V. Passonneau, F. X. Hasselberg, and D. W. Schulz. Effect of ischemia on known substrates and cofactors of the glycolytic pathway in brain. *J. Biol. Chem.* 239: 18-30, 1964.

Lutz, P. L. Mechanisms for anoxic survival in the vertebrate brain. *Annu. Rev. Physiol.* 54: 619-637, 1992.

Lutz, P. L., and P. M. McMahon. γ-Aminobutyric acid concentrations are maintained in anoxic turtle brain. *Am. J. Physiol.* 249: R372-R374, 1985.

Lutz, P. L., P. M. McMahon, M. Rosenthal, and T. J. Sick. Relationship between aerobic and anaerobic energy production in turtle brain in situ. *Am. J. Physiol.* 247: R740-R744, 1984.

Lutz, P. L., M. Rosenthal, and T. J. Sick. Living without oxygen: turtle brain as a model of anaerobic metabolism. *Mol. Physiol.* 8: 411-425, 1985.

Lynch, R. M., and R. J. Paul. Compartmentation of glycolytic and glycogenolyic metabolism in vascular smooth muscle. *Science Wash. D.C.* 222: 1344-1346, 1983.

Macmillan, V., and B. K. Siesjö. Cerebral energy metabolism In: *Scientific Foundations of Neurology*, edited by M. Critchley, J. O'leary and B. Jennett. London: William Heinemann Medical Books Ltd, 1972, 21-32.

Mangum, C., and W. Van Winkle. Response of aquatic invertebrates to declining oxygen conditions. *Amer. Zool.* 13: 529-541, 1973.

McBride, B. W., and L. P. Milligan. Magnitude of ouabain-sensitive respiration of lamb hepatocytes (*Ovis aries*). *Int. J. Biochem.* 17: 43-49, 1985.

McCormick, D. A., B. W Connors, J. W. Lighthall, and D. A. Prince. Comparative electrophysiology of pyramidal and sparsely spiny stellate neurons of the neocortex. *J. Neurophysiol.* 54: 783-806, 1985.

McCulloch, J., H. E. Savaki, J. Jehle, and L. Sokoloff. Local cerebral glucose utilization in hypothermic and hyperthermic rats. *J. Neurochem.* 39: 255-258, 1982.

McDougal, D. B., Jr., J. Holowach, M. C. Howe, E. M. Jones, and C. A. Thomas. The effects of anoxia upon energy sources and selected metabolic intermediates in the brains of fish, frog, and turtle. *J. Neurochem.* 15: 577-588, 1968.

McIlwain, H., and H. S. Bachelard. *Biochemistry and the Central Nervous System.* Edinburgh: Chruchill Livingston, 1971, 616.

Milton, R. L., and J. H. Calswell. How do patch clamp seals form. *Pflugers Arch.* 416: 758-765, 1990.

Mink, J. W., R. J. Blumenschine, and D. B. Adams. Ratio of central nervous system to body metabolism in vertebrates: its constancy and functional basis. *Am. J. Physiol* 241: R203-R212, 1981.

Morris, M. E., J. Leblond, N. Agopyan, and K. Krnjevic. Temperature dependence of extracellular ionic changes evoked by anoxia in hippocampal slices. *J. Neurophysiol.* 65: 157-167, 1991.

Mourre, C., Y. Ben Ari, H. Bernardi, M. Fosset, and M. Lazdunski. Antidiabetic sulfonylureas: localization of binding sites in the brain and effects on the hyperpolarization induced by anoxia in hippocampal slices. *Brain Res.* 486: 159-164, 1989.

Musacchia, X. J. The viability of *Chrysemys picta* submerged at various temperatures. *Physiol. Zool.* 32: 47-50, 1959.

Nilsson, G., A. A. Alfaro, and P. L. Lutz. Changes in turtle brain neurotransmitters and related substances during anoxia. *Am. J. Physiol.* 259: R376-R384, 1990.

Nilsson, G. E., and P. L. Lutz. Release of inhibitory neurotransmitters in response to anoxia in turtle brain. *Am. J. Physiol.* 261: R32-R37, 1991.

Nilsson, G. E., P. L. Lutz, and T. L. Jackson. Neurotransmitters and anoxic survival of the brain: a comparison of anoxia-tolerant and anoxia-intolerant vertebrates. *Physiol. Zool.* 64: 638-652, 1991.

Okada, Y., M. Tanimoto, and K. Yoneda. The protective effect of hypothermia on reversibility in the neuronal function of the hippocampal slice during long lasting anoxia. *Neurosci. Lett.* 84: 277-282, 1988a.

Okada, Y., M. Tanimoto, and K. Yoneda. The protective effect of hypothermia on reversibility in the neuronal function of the hippocampal slice during long lasting anoxia. *Neurosci. Lett.* 84: 277-282, 1988b.

Okamoto, K., and J. H. Quastel. Tetrodotoxin-sensitive uptake of ions and water by slices of rat brain *in vitro. Biochem. J.* 120: 37-47, 1972.

Partridge, L. D., and D. Swandulla. Calcium-activated non-specific cation channels. *TINS* 11: 69-72, 1988.

Pasteur, L. Experiences et vues nouvelles sur la nature des fermentations. *C.R. Acad. Sci* 52: 1260-1264, 1861.

Pastuszko, A., D. F. Wilson, M. Erencinska, and I. A. Silver. Effects of in vitro hypoxia and lowered pH on potassium fluxes and energy metabolism in rat brain synaptosomes. *J. Neurochem* 36: 116-123, 1981.

Penney, D. G. Effects of prolonged diving anoxia on the turtle, *Pseudemys scripta elegans. Comp. Biochem. Physiol.* 47A: 933-941, 1974.

Penney, D. G. Frogs and turtles: different ectotherm overwintering strategies. *Comp. Biochem. Physiol.* 86A: 609-615, 1987.

Pérez-Pinzón, M. A., C. Y. Chan, M. Rosenthal, and T. J. Sick. Membrane and synaptic activity during anoxia in the isolated turtle cerebellum. *Am. J. Physiol.* 263: R1057-R1063, 1992a.

Pérez-Pinzón, M. A., M. Rosenthal, P. L. Lutz, and T. J. Sick. Anoxic survival of the isolated cerebellum of the turtle *Pseudemis scripta elegans. J. Comp. Physiol. B* 162: 68-73, 1992b.

Pérez-Pinzón, M. A., M. Rosenthal, T. J. Sick, P. L. Lutz, J. Pablo, and D. Mash. Downregulation of sodium channels during anoxia: a putative survival strategy of turtle brain. *Am. J. Physiol.* 262: R712-R715, 1992c.

Processer, C. L., L. M. Barr, R. D. Pinc, and C. Y. Lauer. Acclimation of goldfish to low concentrations of oxygen. *Physiol. Zool.* 30: 137-141, 1957.

Prosser, C. L. *Adaptational Biology: Molecules to Organisms.* New York: Wiley & Sons, 1986, 1-784.

Randall, D. The control of respiration and circulation in fish during exercise and hypoxia. *J. Exp. Biol.* 100: 275-288, 1982.

Reiner, P. B., A. G. Laycock, and C. J. Doll. A pharmacological model of ischemia in hippocampal slice. *Neurosci. Lett.* 119: 175-178, 1990.

Ridge, J. W. Hypoxia and the energy charge of the cerebral adenylate pool. *Biochem. J.* 127: 351-355, 1972.

Robin, E. D., N. Lewiston, A. Newman, L. M. Simon, and J. Theodore. Bioenergetic pattern of turtle brain and resistance to profound loss of mitochondrial ATP generation. *Proc. Natl. Acad. Sci. USA* 76: 3922-3926, 1979.

Robin, E. D., D. A. Robin, R. Ackerman, N. Lewiston, A. J. Hance, M. Caligiuri, and J. Theodore. Prolonged diving and recovery in the freshwater turtle, Pseudemys scripta-I. lunge and blood gasses, pH, lactate concentrations and "cation gap". *Comp. Biochem. Physiol.* 70A: 359-364, 1981.

Rolleston, F. S., and E. A. Newsholme. Control of glycolysis in cerebral cortex slices. *Biochem. J.* 104: 524-533, 1967a.

Rolleston, R. S., and E. A. Newsholme. Effects of fatty acids, ketone bodies, lactate and pyruvate on glucose utilization by guinea - pig cerebral cortex slices. *Biochem. J.* 104: 519-523, 1967b.

Rossier, B. C., K. Geering, and J. P. Kraehenbuhl. Regulation of the sodium pump: how and why? *TIBS* 12: 483-487, 1987.

Rothman, S. The neurotoxicity of excitatory amino acids is produced by passive chloride influx. *J. Neurosci.* 5: 1483-1489, 1985.

Sánchez-Prieto, J., and P. González. Occurrence of large Ca^{2+}-independent Release of glutameate during anoxia in isolated nerve terminals (synaptosomes). *J. Neurochem.* 50: 1322-1324, 1988.

Schmahl, F. W., E. Betz, E. Dettinger, and H. Hohorst. Energiestoffwechs der grosshirnrinde und elektroencephalogram bie sauerstoffmangel. *Plug. Arch. Gesamte Physiol.* 292: 46-59, 1966.

Schmidt-Nielsen, K. *Animal physiology: Adaptation and environment.* Cambridge: Cambridge University Press, 1979, 1-560.

Schmidt-Nielsen, K. *Scaling, why is animal size so important.* Cambridge: Cambridge Univ. Press, 1984,

Schulte, P. M., C. D. Moyes, and P. W. Hochachka. Integrating metabolic pathways in post-exercise recovery of white muscle. *J. Exp. Biol.* 166: 181-195, 1992.

Schurr, A.., C. A. West, and B. M. Rigor. Lactate-supported synaptic function in the rat hippocampus slice preparation. *Science Wash. D. C.* 240: 1326-1328, 1988.

Scott, I. D., and D. G. Nicholls. Energy transduction in intact synaptosomes. *Biochem. J.* 186: 21-33, 1980.

Shick, J. M., A. De Zwaan, and A. M. T. De Bont. Anoxic metabolic rate in the mussel *Mytilus edulis l.* estimated by simultaneous direct calorimetry and biochemical analysis. *Physiol. Zool.* 56: 56-63, 1983.

Shoubridge, E. A., R. W. Briggs, and G. K. Radda. ^{31}P NMR saturation transfer measurements of the steady state rates of creatine kinase and ATP synthetase in the rat brain. *FEBS Lett.* 140: 288-292, 1982.

Shoubridge, E. A., and P. W. Hochachka. The origin and significance of metabolic carbon dioxide production in the anoxic goldfish. *Mol. Physiol.* 1: 315-338, 1981.

Sick, T. J., E. P. Chasnoff, and M. Rosenthal. Potassium ion homeostasis and mitochondrial redox status of turtle brain during and after ischemia. *Am. J. Physiol* 248: R531-R540, 1985.

Sick, T. J., and N. R. Kreisman. Potassium ion homeostasis in amphibian brain: contribution of active transport and oxidative metabolism. *J. Neurophysiol.* 45: 998-1012, 1981.

Sick, T. J., M. Perez-Pinzon, P. L. Lutz, and M. Rosenthal. Maintaining coupled metabolism and membrane function in anoxic brain: a comparison between the turtle and rat In: *Surviving Hypoxia*, edited by P. W. Hochachka, P. L. Lutz, T. J. Sick and G. van den Thillart. Boca Raton: CRC Press, 1993, 351-364.

Sick, T. J., M. Rosenthal, J. C. LaManna, and P. L. Lutz. Brain potassium ion homeostasis during anoxia and metabolic inhibition in the turtles and rats. *Am. J. Physiol.* 243: R281-R288, 1982.

Sick, T. J., E. L. Solow, and E. L. Roberts Jr. Extracellular potassium ion activity and electrophysiology in the hippocampal slice: paradoxical recovery of synaptic transmission during anoxia. *Brain Res.* 418: 227-234, 1987.

Siemkowicz, E., and A. J. Hansen. brain extracellular ion composition and EEG activity following 10 minutes ischemia in normo- and hyperglycemic rats. *Stroke* 12: 236-240, 1981.

Siesjo, B. K. *Brain Energy Metabolism.* New York: Wiley, 1978, 607.

Siesjo, B. K., and L. Nilsson. The influence of arterial hypoxemia upon labile phosphates and upon extracellular and intracellular lactate and pyruvate concentrations in the rat brain. *Scand. J. Clin. Invest.* 27: 83-96, 1971.

Suarez, R. K. Thinking with and without oxygen: energy metabolism in vertebrate brains. *Can. J. Zool.* 66: 1041-1045, 1987.

Suarez, R. K., C. J. Doll, A. E. Buie, T. G. West, G. D. Funk, and P. W. Hochachka. Turtles and rats: a biochemical comparison of anoxia-tolerant and anoxia -sensitive brains. *Am. J. Physiol.* 257: R1083-R1088, 1989.

Suzuki, R., T. Yamguchi, Y. Inaba, and H. G. Wagner. Microphysiology of selectively vulnerable neurons. *Prog. Brain Res.* 63: 59-68, 1985.

Swann, A. C., and R. W. Albers. Sodium+photassium-activated ATPase of mammalian brain regulation of phosphatase activity. *Biochim et Biophys Acta* 382: 437-456, 1975.

Ultsch, G. The Viability of nearctic freshwater turtles submerged in anoxia and normoxia at 3 and 10 ^{o}C. *Comp. Biochem. Physiol.* 81A: 607-611, 1985.

Ultsch, G. R. Ecology and physiology of hibernation and overwintering among freshwater fishes, turtles and snakes. *Biol. Rev.* 64: 435-516, 1989.

Ultsch, G. R., and D. C. Jackson. Long-term submergence at 3 ^{o}C of the turtle, *Chrysemys picta bellii*, in normoxic and severely hypoxic water. I. Survival, gas exchange, and acid-base balance. *J. Exp. Biol.* 96: 11-28, 1982.

van Waversveld, J., A. D. F. Addink, G. van den Thillart, and H. Smit. Direct calorimetry on free swimming goldfish at different oxygen levels. *J. Therm. Anal.* 33: 1019-1026, 1988.

Wegener, G. Insect brain metabolism under normoxic and hypoxic conditions In: *Arthropod Brain: Its Evolution, Development, Structrue and Functions*, edited by A. P. Gupta. New York: John Wiley & Sons, Inc., 1987, 369-397.

Wegener, G., R. Michel, S. Kieffer, and M. Thuy. Different metabolic reactions to anoxia in the central nervous system of lower vertebrates and adult insects and their possible significance for postanoxic revival. *Mol. Physiol* 8: 653-655, 1987.

Whalen, W. J., D. Buerk, and C. A. Thuning. Blood flow-limited oxygen consumption in resting cat skeletal muscle. *Am. J. Physiol.* 224: 763-768, 1973.

Whittam, R. The dependence of the respiration of brain cortex on active cation transport. *Biochem. J.* 82: 205-212, 1962.

Whittam, R., and D. M. Blond. Respriatory control by an adenosine triphosphatase involved in active transport in brain cortex. *Biochem. J.* 92: 147-157, 1964.

Wood, E. H., and P. B. Reiner. Glutamate plays a minor role in the membrane events leading to neuronal death in a pharmacological model of ischemia *in vitro*. *Soc. Neurosci. Abstr.* 16: 274, 1990.

Xia, Y., and G. G. Haddad. Neuroanatomical distribution and binding properties of saxitoxin sites in the rat and turtle CNS. *J. Compar. Neurol.* 330: 381-404, 1993.

Xia, Y., C. Jiang, and G. G. Haddad. Oxidative and glycolytic pathways in rat (newborn and adult) and turtle brain: role during anoxia. *Am. J. Physiol.* 262: R595-R603, 1992.

Yamamoto, C., and M. Kurokawa. Synaptic potentials recorded in brain slices and their modification by changes in the level of tissue ATP. *Exp. Brain Res.* 10: 159-170, 1970.

Yellen, G. Single Ca^{2+} -activated nonselective cation channels in neuroblastoma. *Nature* 296: 357-359, 1982.

APPENDIX A: TECHNIQUES

Because a large part of this thesis focuses on electrophysiological techniques which are not familiar to a large portion of the scientific community, this section is devoted to describing these methods in a more general detail. However, I refer the reader to the methods of individual chapters for technique specifics.

The two most common methods of electrophysiological recording are the sharp electrode (intracellular) recording technique and the patch clamp technique. The intracellular recording technique uses a very fine piece of glass tubing which is pulled (simultaneously heating) to a sharp point $\leq .1\ \mu M$ in diameter. The electrode is then filled with a current carrying solution usually KCl $\approx$ 2M and connected to a headstage giving it direct hookup to an amplifier. The electrode is then lowered on to the surface of the cell membrane. Penetration of the electrode through the membrane is accomplished via a current pulse. Once the electrode penetrates the cell membrane, a seal forms due to the attraction of the charged lipids of the membrane and the glass (Fig. 21).

Two subcategories of intracellular recording technique are current clamping and voltage clamping. Current clamping is a method in which the experimenter controls the current which is injected into the cell and recording the resulting voltage deflection for that given amount of current (I). Voltage clamping is a method in which the experimenter controls the voltage potential (V_m) of a cell and records the resulting I. Both techniques are suited to particular applications. For this thesis, current clamping methods are exclusively used.

The second major technique is patch clamping (Fig. 21). The setup for patch clamping is similar to intracellular recording techniques. Instead of breaking through the cell membrane, the electrode is lowered to the surface of the cell, where, through the use of negative pressure, a high resistance seal ($\geq$ 1GΩ) is created. This technique involves the use of a much larger electrode tip (tip diameter $\approx$ 1 - 5 μM). Once the seal has formed, several configurations can be attained (Fig. 22). Note that with intracellular recording, the electrode solution does not immediately equilibrate with the intracellular contents, but with the whole

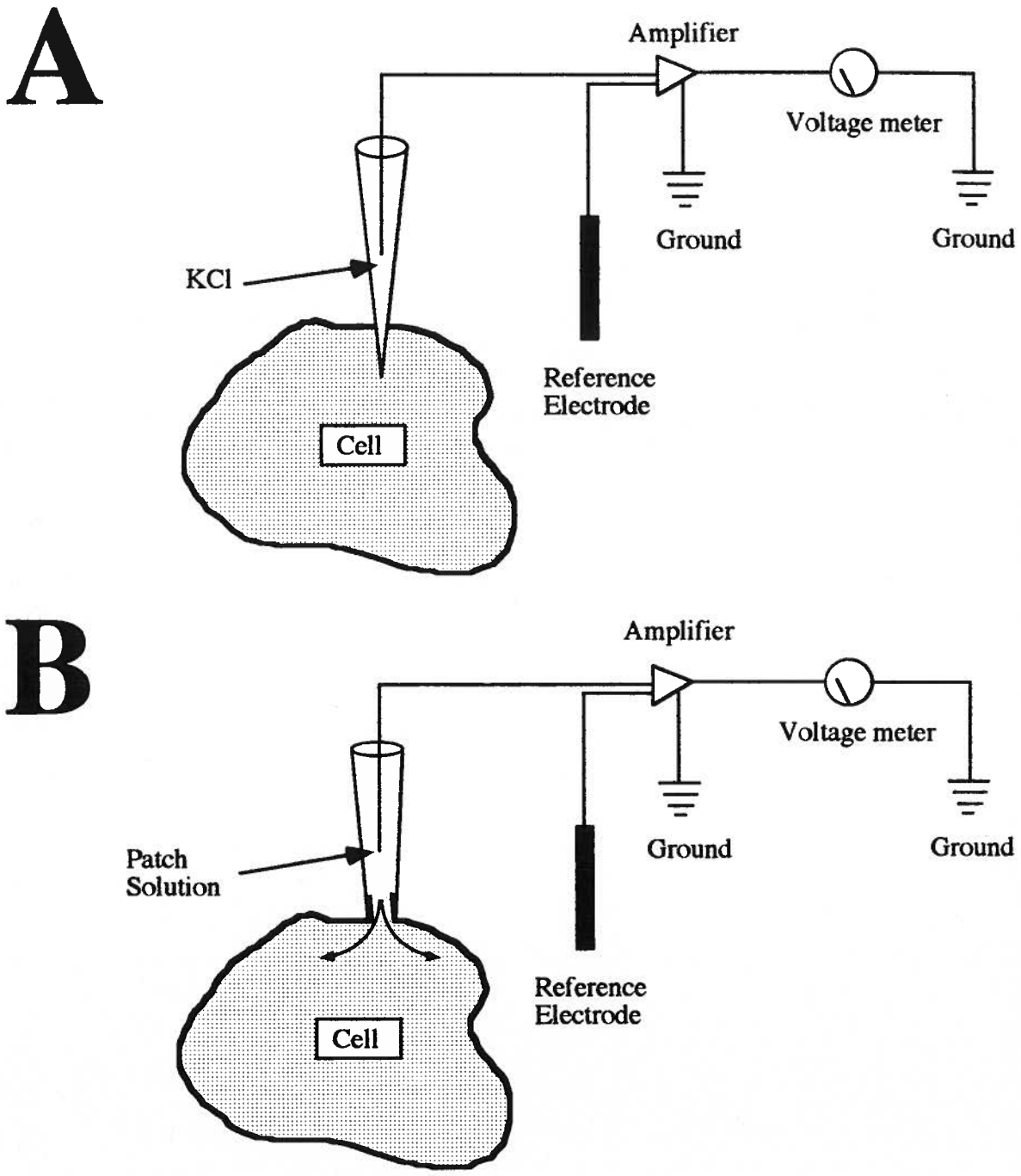

Figure 21. Electrophysiological recording techniques. (A) represents intracellular recording techniques using sharp electrodes. A method commonly used with both voltage and current clamp techniques. (B) represents patch clamping. Note that the electrode does not penetrate the cell membrane, rather it is bonded to the outside membrane (see text for further details)

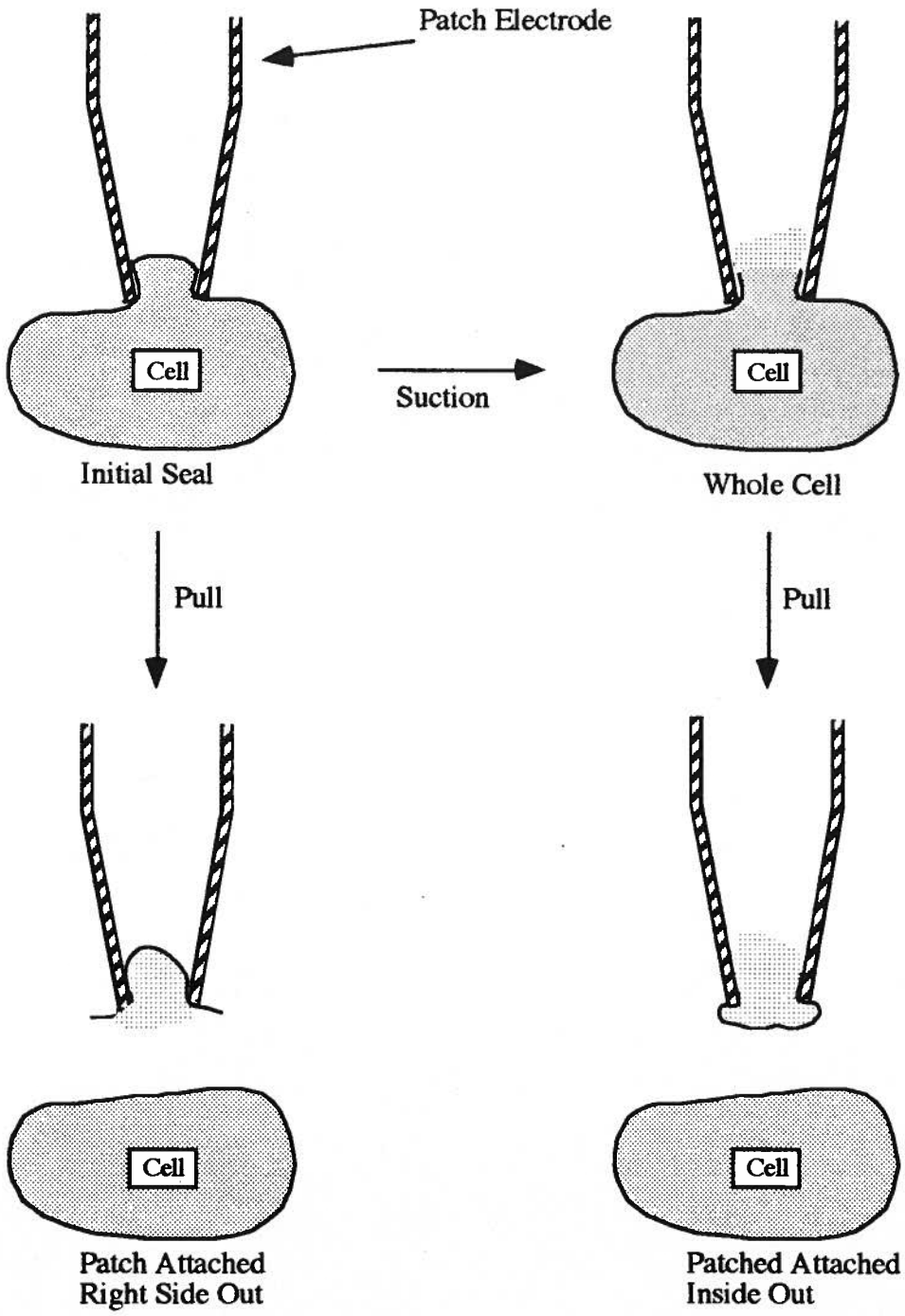

Figure 22. The four configurations of patch clamping. All methods start with the on-cell configuration and are subsequently modified by pulling or sucking once attached to the cell. All configurations result in the formation of a GΩ seal being formed between the electrode and cell membrane.

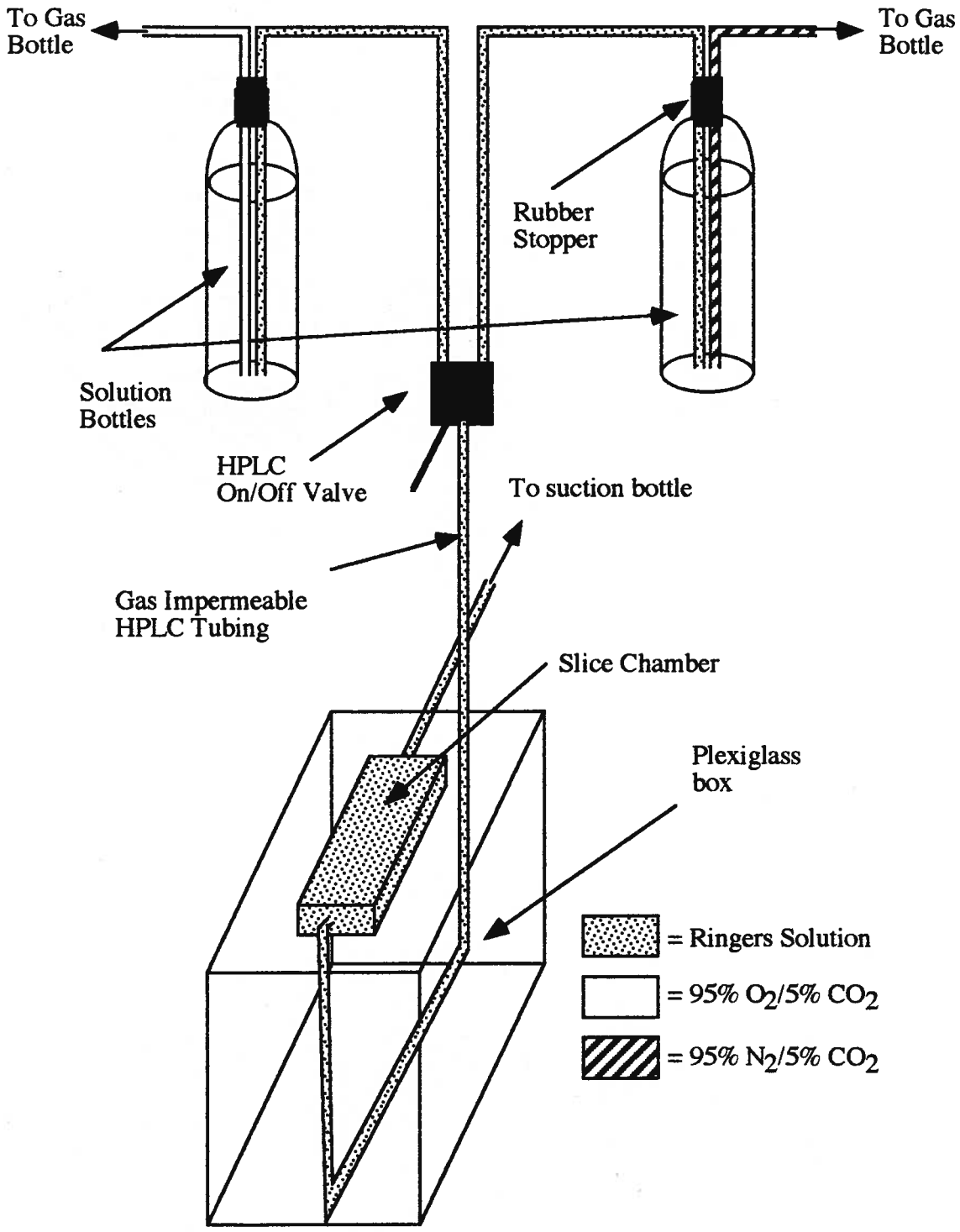

Figure 23. The slice chamber recording set-up and perfusion system for both patch clamping and intracellular recording techniques.

cell patch clamp configuration, the electrode content equilibrates rapidly with the cell cytoplasm.

Both electrophysiological recording techniques used in this study involved a flow through slice chamber (Fig. 23). This chamber was simple a Plexiglas box in which the top had a channel cut. Fluid entered the chamber in the front via gravity. Excess fluid was suctioned off at the opposite end drawing fluid across the slice. Slices were encapsulated in a mesh on both the top and bottom which was weighted down with platinum wire. This configuration allowed aCSF to flow both above and below the slice ensuring viability of the tissue. Mixture bottles were switched via a low volume HPLC valve. Fluid flow across the slice was approximately 1.5 ml/min.

APPENDIX B: TERMONOLOGY

With regards to the techniques used, there are several common terms which are used in the electrophysiology field, but are not well understood by the non-electrophysiologists. This thesis focuses considerably on resistance and conductance of cells. Because electrical currents in solution are carried by ions in that solution, solution electricity is really the study of how ions move in solution. Thus, when the term resistance or conductance is used in reference to a cell parameter, this is not in reference to how an electric current is moving per se, but how ions are moving across the cell membrane. Perhaps the simplest term is whole cell resistance (R_W). This term refers to the resistance of the whole cell (impedance to the flow of ions across the cell membrane). It is generally determined by injecting a current pulse across the cell membrane using either whole cell patch clamping or intracellular recording techniques in the current clamp mode and measuring the resulting change membrane potential (V_m). Since the current was preselected and the resulting V_m is measured, the resistance (R_W) can be calculated by Ohms law:

$$\mathbf{V_m = I \; X \; R_W}$$

This simple equation will indicate the resistance that the ions in a solution encounter when going from the current generating electrode to the bath ground. Since the electrode is in the cell (or on the cell membrane in the case of patch clamping), and the resistance through the solution is negligible, the resulting resistance measure is due primarily to the cell membrane. Since the current can potentially leave the cell anywhere on the membrane, this term is an average over the whole cell. The reverse is true when considering whole cell conductance (G_W). That is:

$$\mathbf{G_W = 1/R_W}$$

Conductance is a measure of how easily ions flow across the membrane. A cell with a high resistance will have a low conductance and vise versa. Once again, this is in reference to the whole cell which is attached to the electrode.

This terminology is not to be confused with specific membrane resistance (R_m) or specific membrane conductance (G_m). This terminology refers to the resistance or conductance for a given area of membrane and is calculated totally independent of the whole cell measures discussed above. G_m is generally calculated from the membrane charging curve of the cell. As a current is injected into a cell, part of the current goes to charge the capacitance of the cell membrane, and part of the current escapes through the ion channels. As the membrane reaches its maximum charging potential, more and more current escapes through ion channels. The resulting curve is termed a membrane charging curve (for an example see Fig. 15, Chapter 4). The time at which it takes a membrane to become 63% charged of its maximum charging potential is termed the time constant (T_c). This term by itself does not yield a considerable amount of information, but in conjunction with the following equation, it yields the cell G_m:

$$T_c = C_m / G_m$$

where C_m is equal to the specific capacitance of the membrane. Given that C_m is known, this equation then allows the calculation of G_m or R_m. Specific limitations to this equation will be discussed in Chapter 3. Also, one could calculate the G_m and R_m by dividing G_w or R_w by the total cell membrane surface area respectively. However, this is a considerable more difficult task since each cell area would have to be measured.

Specific membrane resistance/conductance and whole cell membrane resistance / conductance may look similar, but the information which is provided is not interchangeable. Because R_w and G_w are averaged over the whole cell, they are dependent on cell size as well as G_m and R_m. Thus, it is appropriate to compare the R_w and G_w from a single cell across an insult, it is not correct to compare R_w and G_w to different cells or species. In contrast, G_m and R_m can be used for both comparison from a single cell across an insult, or between different cells in a group, or across species since it does not have the limitations of being dependent on cell size. However, both of these parameters are easily measured, and in

some cases the results appear redundant; however, because these measures are calculated independently of each other, the provide a very useful validation of results.

Throughout this thesis, several terms are used in regards to various tissue insults. A basic understanding of this terminology will aid the reader in better understanding these insults. The terms anoxia/hypoxia can refer to several different states. Anoxia indicates a situation of no O_2, and hypoxia indicates low oxygen tension. However these terms can be complicated by such additives as pharmacological anoxia, environmental anoxia, and physiological anoxia. Physiological anoxia refers to the blood P_{O_2} of zero. For example, since a seal can not extract oxygen from the water it encounters environmental anoxia, yet it does not encounter physiological anoxia as discussed above. For the experiments in this thesis which deal with anoxia, they will be considered physiological anoxia since the tissue is bathed in aCSF equilibrated with 95% N_2 / 5% CO_2. Anoxia is similar to pharmacological anoxia which denotes a situation in which anoxia is present, but also NaCN (cytochrome P-450 inhibitor) to eliminate the possibility of any residual O_2 metabolism.

The third term ischemia denotes a situation in which the tissue receives no blood flow. In this case, the tissue is rapidly confronted with anoxia and once endogenous stores of glucose and glycogen are used, a situation of no energy production occurs because exogenous substrate (glucose) is not delivered. The experiments dealing with electrophysiology utilize a flow through slice chamber (as discussed previously). The flow through design of this chamber makes true ischemia impossible to mimic. However, the development of a pharmacological mimic of this insult (pharmacological ischemia) allows a reasonable facsimile of this insult (Reiner, et al., 1990). Pharmacological ischemia subjects the cortical slice to a perfusing solution of pharmacological anoxia and iodoacetic acid (IAA). Iodoacetic acid blocks glycolysis by inhibiting glyceraldehyde-3-phosphate dehydrogenase (glycolytic enzyme). Pharmacological ischemia is considered more severe compared to ischemia because of its rapid block of the glycolytic pathway.